

In compliance with the
Canadian Privacy Legislation
some supporting forms
may have been removed from
this dissertation.

While these forms may be included
in the document page count,
their removal does not represent
any loss of content from the dissertation.

**HYDROLOGICAL AND ENERGY BUDGET PROCESSES
OF THE
SUBARCTIC CANADIAN SHIELD**

By

CHRISTOPHER SPENCE, B.A. (Hons.), M.Sc.

A Thesis

Submitted to the School of Graduate Studies

in Partial Fulfillment of the Requirements

for the Degree of

Doctor of Philosophy

McMaster University

©Copyright by Christopher Spence, 2003

CANADIAN SHIELD ENERGY BUDGETS AND HYDROLOGICAL PROCESSES

Ph.D. (2003)
(Geography and Geology)

McMaster University
Hamilton, Ontario

**TITLE: Hydrological and Energy Budget Processes of the Subarctic
Canadian Shield**

AUTHOR: Christopher Spence, B.A. (Hons.), M.Sc. (University of Regina)

SUPERVISORS: Dr. Ming-ko Woo and Dr. Wayne R. Rouse

NUMBER OF PAGES: xiv, 104

ABSTRACT

There has been only infrequent research of the hydrology and energy budget of the subarctic Canadian Shield even though it is the third largest ecozone in Canada. In order to investigate important and largely unknown processes, two study sites near Yellowknife, Northwest Territories were instrumented to measure the components of the energy and water budgets. This was done to determine the predominant water and energy flux processes acting on subarctic Canadian Shield hillslopes and to understand runoff generation processes in the region. Results indicate that the magnitude of the spring snowmelt and its potential to flood exposed bedrock portions of the landscape controls the energy budget in the early part of the summer. In wet years high latent heat fluxes early in the summer deplete moisture storage by the end of July, after which latent heat fluxes decrease until the end of the growing season. In drier years, sensible heat dominates the early summer energy budget to a much larger degree than observed elsewhere in the subarctic. It then becomes a very arid landscape. High evaporation to precipitation ratios throughout the summer are an important feature of the western Canadian Shield subarctic region and this is important to its hydrology. Soil offers high available storage relative to adjacent exposed bedrock because evapotranspiration exceeds precipitation and soil filled areas dry. These differences in available storage result in a spatially heterogeneous runoff response within the basin because landscape elements spill runoff only where available storage is filled. Lateral inflows can be the primary source for filling soil zones to

their storage capacity. The dependence of downslope landscape units on lateral inflows from upslope results in a cascading pattern of surface runoff generation. This is significantly different enough from the variable source area concept to indicate that another process must be operating. The element threshold concept is presented to generalize the suite of hydrological processes acting on subarctic Canadian Shield headwater basins. The new concept has the following attributes. It more accurately defines the important processes contributing to variable headwater subarctic Canadian Shield landscape runoff. It accounts for the different hydrological processes that occur in headwater basins. It recognizes that saturation thresholds vary extensively across headwater basins and that this affects subsequent runoff generation, such creates a disjointed contributing area that expands downslope depending on slope, soils, and vegetation. This thesis shows that hydrological and soil-vegetation-atmosphere modeling must account for dynamic small scale landscape elements and hydrological linkages in order to accurately represent the runoff generation processes on the subarctic Canadian Shield.

ACKNOWLEDGEMENTS

I would like to thank Dr.'s Ming-ko Woo and Wayne Rouse for their assistance, guidance, patience and perseverance. I greatly appreciate their faith in my abilities and the opportunity they have provided me. Funding for this research was provided by the Mackenzie GEWEX Study, Indian and Northern Affairs Canada via the Northern Student Training Program, McMaster University and Environment Canada. Access to the Pocket Lake site was kindly provided by Miramar Mining. Thanks go to Jesse Jasper and Shauna Sigurdson for supporting this work. There were many people who provided field assistance throughout this project, including Jennifer Dougherty, Bob Reid, Shawne Kokelj, Mark Dahl, Claire Oswald, Andrea Czarnecki, Chris Clarke, Kerry Walsh, Devon Worth and Derek Steadman, who all deserve my gratitude. Of special note is Iain Stewart who withstood one of the most evil blizzards it has been my displeasure to experience. Thank you to my family and friends who encouraged me to pursue this work. Bob Reid, without knowing it, was there with some very inspirational words when they were most needed. Thank you to Lauren and Katherine who are a sanctuary from the world and provide a perspective on what is truly most important in life. My greatest thanks must go to my wife, Raycine, who has supported me throughout this endeavour in every way that one person can support another.

TABLE OF CONTENTS

Title Page	i
Descriptive Note	ii
Abstract	iii
Acknowledgements	v
Table of Contents	vi
List of Figures	viii
List of Tables	xii
Symbols	xiv
CHAPTER 1: INTRODUCTION	1
1.1 The Shield Environment	1
1.2 Past Work on Shield Hydrometeorology and Hydrology	2
1.3 Statements of Objectives	5
1.4 Presentation of Thesis	6
CHAPTER 2: STUDY AREAS	7
CHAPTER 3: METHODS	14
3.1 Skeeter Lake	14
3.2 Pocket Lake	18
CHAPTER 4: ENERGY BUDGETS OF THE SUBARCTIC SHIELD LANDSCAPE	27
4.1 Interannual differences	34
4.2 Site hydrology and energy budget feedbacks	37
CHAPTER 5: HYDROLOGICAL PROCESSES OVER EXPOSED BEDROCK	39
5.1 Hydrological Processes	39
5.1.1 Rainfall	39
5.1.2 Snow ablation	39
5.1.3 Storage	40
5.1.4 Evaporation	45
5.1.5 Infiltration	47
5.1.6 Runoff	50
5.2 Seasonal water balance	52
5.3 Rainfall-runoff curves	54

CHAPTER 6: HYDROLOGICAL PROCESSES IN A SOIL FILLED VALLEY	56
6.1 Hydrological Processes	56
6.1.1 Ground frost	56
6.1.2 Snowmelt	57
6.1.3 Rainfall	57
6.1.4 Infiltration	58
6.1.5 Inflow from exposed bedrock upland	59
6.1.6 Evapotranspiration	60
6.1.7 Storage	61
6.1.8 Subsurface runoff	65
6.1.9 Surface runoff	65
6.2 Hydrological linkages between upland and valley	69
6.3 The fill and spill flow mechanism	70
CHAPTER 7: HYDROLOGICAL PROCESSES IN HEADWATER BASINS	74
7.1 Runoff events	75
7.1.1. Summer season with dry conditions and low rainfall	75
7.1.2 Summer season with dry conditions and high rainfall	77
7.1.3 Spring season with dry conditions and high rainfall and melt	80
7.2 Contributing areas	84
7.3 Hydrological elements and the Element Threshold Concept	86
CHAPTER 8: CONCLUSIONS	93
REFERENCES	97

LIST OF FIGURES

Figure 1	Photo of Skeeter Lake upland with a location map. The arrow points to the climate tower. The lightest gray tones are exposed bedrock, B. The wetland, PW, is located behind the tower. Black spruce, BS, and mixed stands, MW, are scattered throughout the site. White arrows denote direction of surface water flow. The distance across the picture is approximately 500 m.	10
Figure 2	Instrumentation at the Pocket Lake site with location map and photo. Pocket Lake can be seen as the dark shades at the bottom of the photo. The basin is outlined in black and the soil filled valley in gray in both the map and photo.	13
Figure 3	Frequency distribution of fracture width, b, in each plot.	20
Figure 4	Monthly air temperature and precipitation. The white circles represent 1999 observations and the white boxes, 2000 observations at Skeeter Lake. The black squares are Environment Canada 1961-1990 averages for Yellowknife with the bars representing \pm one standard deviation.	28
Figure 5	a) Cumulative precipitation and b) cumulative change in soil moisture storage on the Skeeter Lake upland during 1999 and 2000.	29
Figure 6	Cumulative spring snowmelt and runoff at Skeeter Lake in 1999 and 2000.	30
Figure 7	The Skeeter Lake upland seasonal energy budget pattern for 1999 and 2000. The values presented are 5 day running means.	32
Figure 8	Skeeter Lake upland average diurnal energy budgets for common months in 1999 and 2000.	33
Figure 9	The seasonal pattern of evaporation, surface resistance and vapour pressure deficit. Values shown are 5 day running means.	36

Figure 10	Rainfall time series measured at Pocket Lake in a) 1999 and b) 2000.	41
Figure 11	Spring of 2000 a) snow ablation, b) evaporation and c) snowmelt for three of the four plots at Pocket Lake. Ablation rates are illustrated at the top, evaporation in the middle and snowmelt at the bottom.	42
Figure 12	Frequency and areal distributions of depressions in each bedrock runoff plot.	43
Figure 13	a) 1999 rainfall time series and b) storage in individual depression class sizes in plot 5.	44
Figure 14	a) 1999 rainfall and b) 1999 cumulative evaporation from plot 7 and individual depression class sizes within plot 7.	46
Figure 15	Hyetographs and hydrographs from two storms as as measured in Plot 5 during the summer of 2000.	48
Figure 16	Ground temperatures adjacent to plot 6 in April and August 2000.	49
Figure 17	Infiltration – melt ratios versus average daily melt rates at three bedrock runoff plots.	49
Figure 18	Individual rainfall and runoff measurements for each plot for the period of study.	51
Figure 19	Conceptual rainfall runoff curves illustrating the effects of a) physiographic and b) climatic factors on runoff at the bedrock plot scale. The factors are i) increasing fracture width at the bedrock plot scale, ii) increasing storage capacity, iii) storage capacity further downslope, iv) decreasing precipitation intensity, v) increasing event duration and vi) increasing evaporative demand.	55
Figure 20	Cumulative rainfall measured at Pocket Lake from 10 May to 25 September 2000.	58

Figure 21	Daily lateral inflow from exposed bedrock to the soil filled valley.	60
Figure 22	Cumulative daily evapotranspiration and change in storage during a dry period (18 July to 11 August) in the middle of the 2000 growing season.	61
Figure 23	Daily soil moisture measurements at different locations and depths in the soil filled valley, summer 2000.	62
Figure 24	The water table across and along the soil filled valley during wet (27 August 2000) and dry (16 August 2000) conditions. The locations of other transects are referenced on each cross section. Information on transect H only covers the western 16 m of its length. The white circles denote locations of piezometers or wells. Refer to Figure 1 for locations of transects.	63
Figure 25	Half hourly measurements of soil moisture storage at the soil edge and the water table at transect H.	64
Figure 26	Inflow from exposed bedrock, the response of soil moisture at the center of the soil filled valley at Transect G and runoff during the 23 August rainfall event.	67
Figure 27	Cumulative water budget in a soil filled valley in the spring of 2001.	68
Figure 28	Cumulative water budget in a soil filled valley in the summer of 2000.	70
Figure 29	An illustration of conceptualized fill-and-spill runoff generation. a is a longitudinal profile of the valley and b is a cross section. P is precipitation, t is time at step 1, 2 or 3. SSSF is subsurface stormflow and SOF is saturation overland flow. A is the contributing area at t_2 or t_3 .	73
Figure 30	Characteristics of the 23 June 2000 rainfall- runoff event at the Pocket Lake site.	76
Figure 31	Characteristics of the 23 August 2000 rainfall-runoff event at the Pocket Lake site.	78

Figure 32	Contributing areas (left) and surface runoff linkages (right) during the August 2000 event. The shading represents a cumulative expansion of the contributing area.	80
Figure 33	Frequency distributions of snow depth and snow water equivalent from the 2001 spring snow survey.	81
Figure 34	Snow depletion curves for three ablation lines.	81
Figure 35	Characteristics of the 2001 spring melt runoff event.	83
Figure 36	Contributing areas (left) and surface runoff linkages (right) during the 2001 spring melt. Unlike Figure 32, the shading represents the contributing locations only on those particular days.	84
Figure 37	Variation in land cover, fraction of the basin wide contributing area and runoff ratio at the Pocket Lake catchment. The upland runoff includes that measured at the valley inflow weir sites plus that estimated using eq. 9.	85
Figure 38	Skeeter Lake upland with one longitudinal drainage profile. Initials in the photograph denote land cover types shown in Figure 1. Numbers in the bottom frame denote hydrological elements. Arrows denote surface runoff and those elements with active contributing functions. Sequentially wider arrows imply surface runoff under wetter conditions.	90

LIST OF TABLES

Table 1	Hydrological characteristics of the soil layers in the headwater valley.	13
Table 2	Physical characteristics of runoff plots.	20
Table 3	Skeeter Lake upland monthly energy budget ratios, average Bowen ratios, evaporation rates and precipitation during 1999 and 2000.	33
Table 4	Average β and Q/Q^* results from the Canadian Shield and other subarctic locations for comparable periods. Table lists wettest locales and conditions first, then drier examples with each subsequent row down the table.	37
Table 5	Monthly mean evaporation from lysimeters.	45
Table 6	Water budget measurements of two rainfall runoff events at Plot 5. Water budget terms are expressed in millimeters. E/P is the evaporation ratio and I/P the infiltration ratio.	49
Table 7	Characteristics of selected events showing rainfall (P), plot evaporation (E) and runoff ratio (R_b/P).	50
Table 8	Water balance totals and ratios. The 1999 summer measurements from Plot 6 began on July 13 and from Plot 7 on July 8.	52
Table 9	Average values of selected chemical characteristics of water from the Pocket basin site from 1995 to 2000. Stable isotope values are presented in standard δ notation as deviations per mille from Vienna-SMOW (standard mean ocean water) such that $\delta_{\text{sample}} = 1000 \{ (R_{\text{sample}}/R_{\text{SMOW}}) - 1 \}$ where R is $^2\text{H}/\text{H}$ and $^{18}\text{O}/^{16}\text{O}$.	69
Table 10	Water budgets of the growing season in 2000 and spring melt in 2001. All units are in mm. N/A denotes not available because of flooding in the trenches.	70

Table 11	Cumulative change in storage from May 10, 2000 until the occurrence of three events in the study basin. All units are in m^3 .	75
Table 12	Runoff ratios for the three events at different scales.	79
Table 13	Characteristics of several runoff events at Pocket Lake catchment. L_p is the lag time between peak rainfall and peak runoff. t^* is the recession coefficient defined by Carey and Woo (2001). f_{ca} is the fraction of the basin contributing to surface runoff.	79
Table 14	Contributions to the basin water budget during the 2000 growing season and 2001 spring melt. All units are in m^3 .	85
Table 15	Features of the variable source area concept and element threshold concept.	91
Table 16	Characteristics of Canadian Shield headwater basins and slopes demonstrating the element threshold concept compared with small basins exhibiting the variable source concept.	91

SYMBOLS

α	Priestley-Taylor coefficient (dimensionless)	K_s	soil hydraulic conductivity (m/d)
β	Bowen ratio	L_p	lag between peak rainfall and peak surface runoff (days or hours)
Δ	slope of the saturation vapour pressure temperature curve	M	snowmelt rate (mm/d)
ΔS	rate of change in storage (mm/d)	P	rainfall rate (mm/d)
ΔS_s	rate of change in saturated soil storage (mm/d)	P_f	fraction of the fractured bedrock plot area occupied by an individual fracture
ΔS_u	rate of change in unsaturated soil storage (mm/d)	Q^*	net radiation flux density (W/m^2)
$\Delta \theta$	rate of change in unsaturated soil moisture content (%)	Q_e	latent heat flux density (W/m^2)
ϕ	porosity (dimensionless)	Q_g	ground heat flux density (W/m^2)
γ	psychrometric constant ($kPa/^\circ C$)	Q_h	sensible heat flux density (W/m^2)
λ	latent heat of vapourization (J/kg)	r_a	aerodynamic resistance (s/m)
μ	viscosity of water (m^2/s)	r_s	surface resistance (s/m)
ρ_a	air density (kg/m^3)	R	rate of bedrock plot runoff (mm/d)
ρ_f	bedrock fracture density (%)	R_b	rate of runoff from bare bedrock plots (mm/d)
ρ_w	water density (kg/m^3)	R_{sc}	rate of runoff from soil covered bedrock plots (mm/d)
A	area (m^2)	R_{bss}	rate of runoff from bedrock side slopes to valley
b	fracture aperture width (m)	R_g	subsurface runoff rate (mm/d)
C	electrical conductivity (mS/cm)	R_s	surface runoff rate (mm/d)
c_p	heat capacity of air ($J/kg^\circ C$)	S	storage (mm)
D	vapour pressure deficit (kPa)	S_c	storage capacity (mm)
E	bedrock plot evaporation rate (mm/d)	SWE	snow water equivalent (mm)
E_l	lysimeter evaporation rate (mm/d)	S_y	specific yield (dimensionless)
ET	evapotranspiration rate (mm/d)	t	present time step
f_a	fraction of air in soil column	t^*	recession coefficient
f_i	fraction of ice in soil column	T	time (days)
f_s	fraction of soil in soil column	T_g	ground temperature ($^\circ C$)
f_w	fraction of water in soil column	z	soil thickness (m)
F	bedrock infiltration (mm)		
g	gravity (m/s^2)		
I	bedrock plot infiltration rate (mm/d)		
I_b	rate of lateral inflow from bedrock upland (mm/d)		
I_{bw}	rate of lateral inflow measured at weirs (mm/d)		
I_{bss}	rate of lateral inflow estimated from bedrock side slopes (mm/d)		
K_T	ground thermal conductivity ($W/m^\circ C$)		
K_f	fracture hydraulic conductivity (m/s)		

CHAPTER 1

INTRODUCTION

1.1 The Shield Environment

The Canadian Shield occupies about one-third of Canada's land area, extending from the humid temperate latitudes of southern Ontario and southern Quebec to the eastern Queen Elizabeth Islands of the High Arctic. The Shield is underlain by Precambrian bedrock and has been subjected to Pleistocene glaciation that removed and reworked much of the overburden. Very often, glaciation left a rolling topography with exposed bedrock upland, soil mantled slopes and soil-filled valleys that may be occupied by wetlands and lakes.

One third of Canada's freshwater area is contained within or on the edge of the Shield, including very large lakes (e.g. Lake Superior and Great Slave Lake) and major rivers, several of which (e.g. Churchill in Labrador, la Grande in Quebec, Churchill and Nelson in Manitoba) have been harnessed to produce hydroelectricity. On a local scale, Shield terrain is considered to be a favourable repository site for mining and nuclear wastes because of its restricted groundwater flow. Mining and industrial development of the Shield has now extended into the subarctic. However, this area is considered

to be prone to climatic warming induced by enhanced greenhouse gas emissions (Maxwell, 1997). There is therefore a growing need to better understand the energy and water budgets of northern Shield basins in order to predict human and climatic impacts on the environment. Recent attempts to model the hydrology of small to meso-scale northern basins have produced mixed results (Pietroniro et al. 1998; Spence, 2001). Spence (2001) suggested that the available models do not adequately simulate the pertinent hydrological processes operating in the subarctic Canadian Shield as many of the processes that affect the exchanges of energy and water remain insufficiently known. Individual water budget components and integrated basin processes are often poorly studied or often give contradictory results.

1.2 Previous Work on Shield Hydrometeorology and Hydrology

Energy budget studies in the subarctic Canadian Shield have been pursued mainly in the wetter environment of the eastern parts of the Shield in Québec and Labrador. Singh and Taillifer (1986) identified the existence of regional scale advection on the energy balance of subarctic forest. Lafleur and Adams (1986) examined the effect of the open canopy on the radiation budget. Fitzjarrald and Moore (1994) presented results from Schefferville, Québec, which showed notably high Bowen ratios. Wight (1973) calculated very low landscape evaporation rates near Yellowknife that differ substantially from those found in the close-crowned boreal forest and in non-Shield subarctic open woodland regions (Sellers et al.,

1997 and Rouse et al., 1997) which implies that the presence of exposed Precambrian bedrock in the subarctic Canadian Shield may result in restricted water availability. Amiro and Wuschke (1987) speculated that exposed bedrock, with its high thermal conductivity, higher net radiation and little to no latent heat flux, should have a large ground heat flux, but as exposed bedrock tends to occupy small portions of the landscape, basin wide values of ground heat flux remain relatively small. There have been no studies into how these distinctive characteristics of the subarctic Canadian Shield energy balance may affect the hydrology.

Evaporation rates influence antecedent moisture conditions, which is known to influence the magnitude of runoff from Shield headwater basins (Branfireun and Roulet, 1998). Little is known of the mechanisms of runoff generation from exposed bedrock or bedrock covered by very shallow soil. Allan and Roulet (1994) identified Hortonian overland flow processes as the predominant process on exposed bedrock. Buttle and Peters (1997) assumed that the water not lost to runoff evaporates, but Thorne et al. (1994) found that exposed bedrock ridges are groundwater recharge zones which indicated that infiltration can be significant. Besides the observation that wetter conditions produce higher runoff volumes and ratios (Peters et al., 1995; Allan and Roulet, 1994), water fluxes from exposed bedrock surfaces during and between individual storms have not been studied in detail.

Surface runoff from exposed bedrock enters soil covered areas along the bedrock surface (Peters et al., 1995). Upon reaching the soil zone, runoff produced on exposed bedrock uplands is modified by the storage and flow delivery mechanisms in the soil-filled zone (Allan and Roulet, 1994). Runoff generation studies in southern areas of the Canadian Shield (Buttle and Sami, 1992) have identified that saturation overland flow is the primary runoff generation process acting in soil zones. Many factors will influence saturation overland flow in Canadian Shield soil zones and, in turn, headwater basin runoff ratios, including ground frost and antecedent moisture. Metcalfe and Buttle (2001) found that ground frost near Thompson, Manitoba prevented infiltration of snowmelt and increased runoff production. In contrast, Landals and Gill (1972) researching near Yellowknife observed that ground frost alone does not change runoff ratios. The magnitude of the runoff response to summer rainfall events in soil filled valleys is strongly controlled by the dryness of the soil (Branfireun and Roulet, 1998).

The diversity of land cover configurations, the differences in hydrological behaviour of land cover types, and the interactions among land cover types on the subarctic Canadian Shield may also be responsible for the large headwater basin runoff ratio variability. There remains insufficient understanding of the relationship between catchment water balance, soil-zone storage, ground frost and hydrological linkages within and between land cover types in controlling intra-seasonal runoff response from Canadian Shield headwater basins. Furthermore, there have been

no inter-annual studies that attempt to explain year to year variability in runoff response at the headwater basin scale. What is truly lacking and is necessary to explain runoff response variability is an understanding of unified energy and hydrological dynamics in the Canadian Shield.

1.3 Statement of Objectives

The goal of this study is to understand how the principle water and energy flux processes operating in the subarctic Canadian Shield landscape interact to produce runoff from headwater basins. This goal embraces the following research objectives:

- (1) to investigate the microclimatic and hydrological processes that influence the partitioning of the energy budget, and to identify feedbacks between these processes in a subarctic Shield basin;
- (2) to investigate the major hydrological processes occurring on two principal land cover types found in a headwater catchment, including (a) exposed bedrock upland and (b) soil-filled valley;
- (3) to understand how these land cover types combine and interact in a headwater basin in terms of runoff production, using the results from (1) and (2) above.

The analysis of field results and the synthesis of the findings are used to formulate a conceptual model of runoff generation from small subarctic Shield basins.

1.4 Presentation of Thesis

This thesis is organized as follows. Chapter 2 describes the northwestern portion of the Canadian Shield and the two study sites. Chapter 3 details the field methods. Chapter 4 addresses the first objective of this research by summarizing Shield energy budget processes. Chapters 5 and 6 explain runoff generation processes from exposed bedrock and soil filled zones, respectively. Chapter 7 addresses the last objective of this research by showing how the processes from individual land cover types interact in order to produce basin runoff and presents a conceptual model of Canadian Shield runoff generation. Chapter 8 provides conclusions. Several chapters have been presented individually as journal articles (articles based on Chapters 4 and 5 are published and that from Chapter 6 has been submitted).

CHAPTER 2

STUDY AREAS

The study areas lie within the Slave Geological Province of the Canadian Shield. The bedrock is composed of volcanic, and sedimentary rocks intruded by Archean batholiths and plutons creating a granitic-metamorphic terrane. The oldest rocks are gneiss and granitoid rocks that range from 2.8 to 4 billion years of age. Most of the region includes the Yellowknife Supergroup which close to Great Slave Lake is characterized by interbedded greywacke siltstones and mudstones. The youngest assemblage is comprised of granitoid rock about 2.58 to 2.62 billion years of age (Fyson and Padgham, 1993). Glacial action has scoured the region repeatedly during the Quaternary exposing much of the bedrock described above. As such, the landscape exhibits much evidence of glacial action. Glaciofluvial deposits in the form of eskers and deltas appear throughout the region. Glacial erratics are found on upland areas. Dystric Brunisols are the dominant soils. Turbic and Organic Cryosols are found in poorly drained frozen peat filled depressions. The area is underlain by discontinuous permafrost (Brown, 1978).

Watersheds and drainage courses are controlled by the bedrock structure with a resulting trellis drainage pattern. Hummocky rock surfaces formed by glacial erosion result in a large number of lakes, which account for roughly 25% of the land area. The annual hydrologic regime is dominated by the spring freshet and can be characterized as subarctic-nival. Large individual lakes and a large number of small lakes can attenuate the annual hydrograph so that it resembles a muskeg large river regime (Church, 1974).

Arboreal vegetation in the subarctic Shield is predominantly open black spruce (*Picea mariana*) forest with periodic stands of white spruce (*Picea glauca*), jack pine (*Pinus banksiana*), birch (*Betula spp.*) and aspen (*Populus tremuloides*). Lichen and moss covered bedrock and boulders dominate the ground cover. Peat wetlands are common in low lying areas. Vegetation in these areas is mostly moss (*Sphagnum spp.*) with shrubs such as Labrador tea (*Ledum groenlandicum*) and willow (*Salix spp.*) with a thin black spruce overstory. Forest fires create vegetation communities that vary widely in composition and age.

The climate of the region as indicated by the meteorological record at Yellowknife indicates short cool summers with a July average daily temperature of 16°C and long cold winters with a January average daily temperature of -29°C (Phillips, 1990). The region averages about 300 mm of precipitation with approximately 55% of that falling as snow. Convective storms produce much of the summer precipitation and as a result summer rainfall is quite variable from year

to year. As the jet stream moves south over the region in September, conditions are often cool and damp. If this shift begins earlier in late August, the annual precipitation will tend to be higher than normal because of the extended period during which rainfall occurs before freeze up.

Two sites were studied. The first is located 100 km north of Yellowknife, Northwest Territories, Canada at $63^{\circ} 35.5'N$ $113^{\circ} 53.5'W$ (Figure 1). It is an upland with an average 2% slope that is the main source area for a small headwater lake, unofficially known as Skeeter Lake. Skeeter Lake drains intermittently to the Yellowknife River at Lower Carp Lake 500 m to the east. Exposed bedrock ridges to the north, east and west surround a shallow valley 700m wide by 1200m long. Most of the 20m of relief at the site is due to the bedrock ridges.

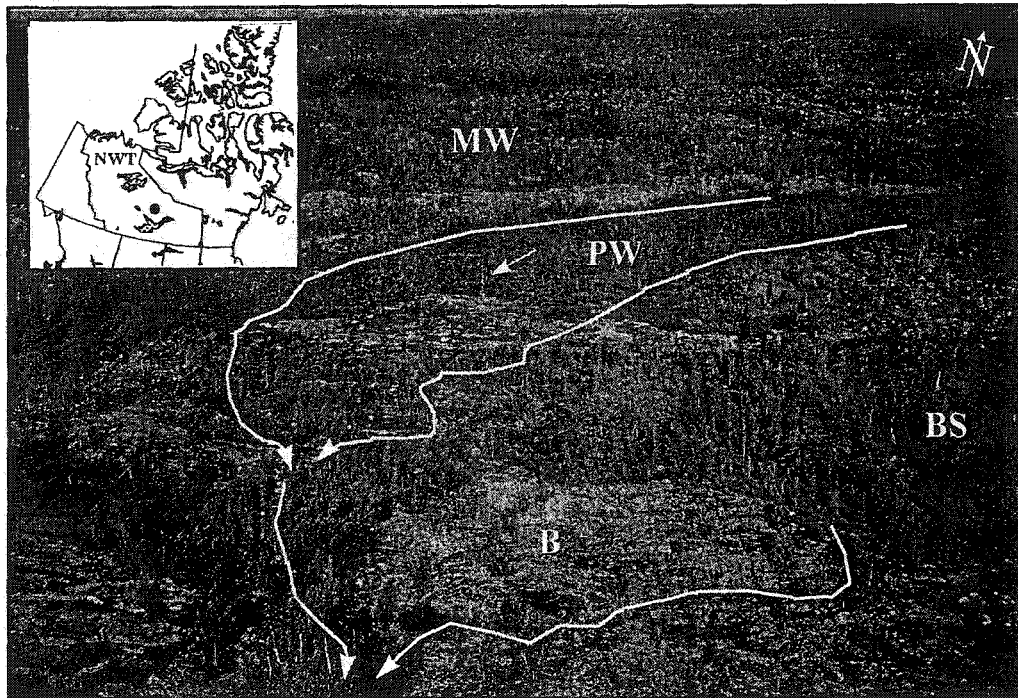


Figure 1: Photo of Skeeter Lake upland with a location map. The arrow points to the climate tower. The lightest gray tones are exposed bedrock, B. The wetland, PW, is located behind the tower. Black spruce, BS, and mixed woods stands, MW, are scattered throughout the site. White arrows denote direction of surface water flow. The distance across the picture is approximately 500 m.

Vegetation is typical of the subarctic Shield. The surface cover at the site is heterogeneous and includes stands of black spruce (26%), mixed stands of spruce and aspen (26%), a peat wetland (20%) and exposed bedrock (28%). Black spruce dominates the arboreal vegetation, but there is a significant portion of trembling aspen. Maximum tree heights are less than 4 m with an average height of 3 m. The tree canopy is open with average tree spacing estimated at about 4 m. This allows for a significant understory dominated by dwarf birch (*Betula glandulosa*), Labrador tea (*Ledum groenlandicum*) and blueberry (*Vaccinium angustifolium*). Exposed bedrock is scattered throughout, with much of it in the

eastern portions of the upland. Lichens (fruticose, foliose and crustose forms including *Cladina* spp. and *Cladonia* spp.) dominate the sparse vegetation cover on exposed bedrock. Soils occupy some shallow (<20 cm) depressions in the exposed bedrock. There are two patches of sandy and cobbly soils derived from glaciofluvial deposits in the southern reaches of the upland. The depth of these deposits is not known but given the bedrock slope in the area it could be up to 10 m. The soils in the wetland include a moss mat up to 30 cm deep above organic soils with an estimated average depth of 1 m. There have been no mineral soils observed below the organic soils, which are underlain by granitic bedrock. Observations suggest the soils in the wetland completely thaw every year but permafrost may occur in the two patches of sandy soils because of their greater depth.

The annual snow cover begins in October and disappears near the end of April or beginning of May when a quick and intense spring thaw normally occurs (Wedel et al., 1990). Snowmelt water passes from the ridges through the upland along two channels at the edges of the wetland. These become poorly defined in places of bedrock outcrops which promote swathes of sheetflow. Near the south side of the upland the runoff is confined into one outlet which follows a steep channel exiting into Skeeter Lake (Figure 1). No runoff occurs from the upland during the summer months, but some may occur during wet autumns.

The second study site is a 4.9 ha basin with an exposed bedrock upland 3.8 ha in size and a lower soil filled valley 1.1 ha in size draining towards Pocket Lake, located 4 km north of the City of Yellowknife in Canada's Northwest Territories (Figure 2). The upland occupies 78% of the basin and the valley, 22%. The Pocket Lake Basin has been used intermittently as a hydrologic study site since the early 1970's when it was designated as an experimental basin under Canada's contribution to the International Hydrological Decade. The basin physiography and climate have been previously described in Landals and Gill (1972), Wight (1973), Reid (1997) and Spence and Stephens (1997).

The bedrock outcrops are moderately to highly fissured with joints and exfoliation fractures. Lichens (fruticose, foliose and crustose forms incl. *Cladina* spp. and *Cladonia* spp.) sparsely cover the outcrops. Individual stands of dwarf birch (*Betula glandulosa*) and jack pine occur sporadically. Moss can be found in some depressions and in fracture apertures. Silty sandy soils derived from erosion of the bedrock face fill some bedrock depressions.

Black spruce grow at the edge of the valley along the soil/bedrock border. Understory vegetation includes willow (*Salix* spp.), Labrador tea and rose (*Rosa* spp.) bushes. Ground cover includes moss (*Sphagnum* spp.), lichen (*Cladonia* spp.) grass (*Eriophorum* spp.) and sedges (*Carex* spp.). The upper part of the

valley has a gradient of 1%, while the lower section descends at 9%. The substrate consists of three distinct layers each composed of organic soils, silty sands and a basal layer of cobbles and boulders (Table 1) which pinches out towards the valley sides. The bedrock hillslopes rise abruptly from the soil-filled valley floor.

Beneath the soil, a bedrock sill stretches across the lower reach of the valley.

Down valley from the sill the bedrock and soil surfaces have similar gradients.

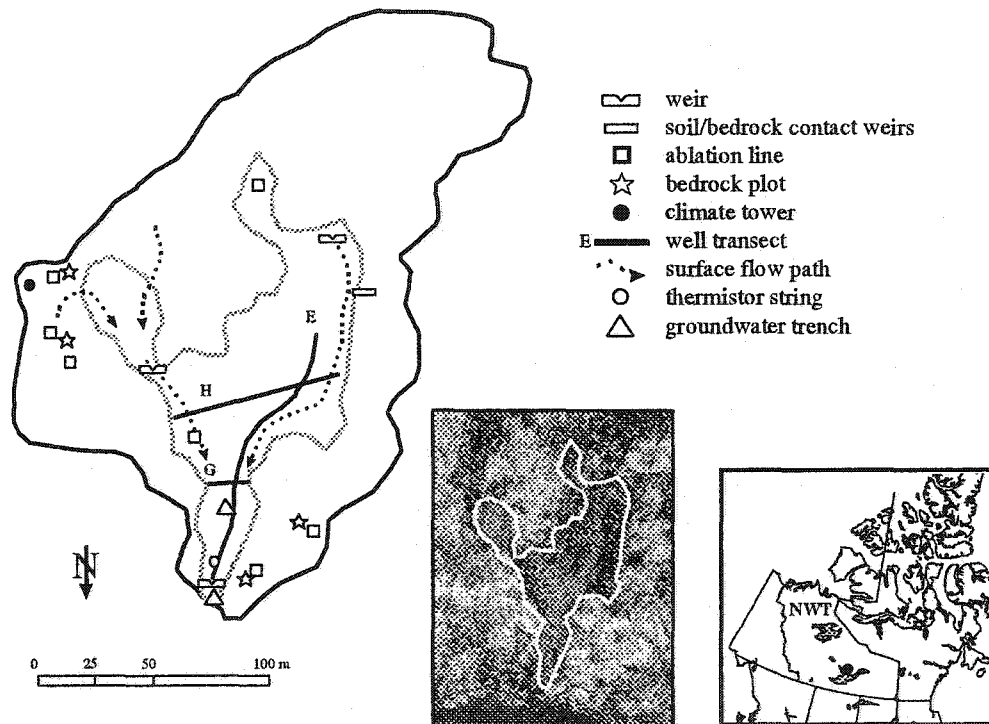


Figure 2: Instrumentation at the Pocket Lake site with location map and photo. Pocket Lake can be seen as the dark shades at the bottom of the photo. The basin is outlined in black and the soil filled valley in gray in both the map and photo.

Table 1: Hydrological characteristics of the soil layers in the headwater valley.

Soil type	Depths (m)	Porosity (ϕ)	Hydraulic conductivity (K) (m/d)
organic	0 - 0.35	0.75	10
silty sands	0.35 - 1.5	0.5	1
cobbles and boulders	1.5 - 1.75	0.35	10

CHAPTER 3

METHODS

3.1 Skeeter Lake

A 6 m meteorological tower was employed at the Skeeter Lake upland to measure the atmospheric variables of air temperature, relative humidity and wind speed (all at 2 m height) and soil moisture at three depths (0.02 m, 0.1 m and 0.2 m) using Campbell Scientific time domain reflectometry (TDR) sensors. These measurements were continuous and were integrated over half hour periods.

Gravimetric soil moisture measurements were used to calibrate the TDR probes and determine physical properties of the soil. Wind direction was measured hourly at an Environment Canada remote climate station on an island in Lower Carp Lake 2 km from the study site. Wind directions are rarely different between the island tower and the study site. Rainfall volume, P , across the site was measured using 3 Meteorological Service of Canada Type B rain gauges. Rainfall intensity was recorded hourly using a tipping bucket wired to a data logger (Campbell Scientific CR10X). The snow water equivalent of the spring snowpack was calculated using snow density measurements with an Eastern Snow Conference snow survey kit and snow depth with an aluminum rod along snow surveys as described in Pomeroy and Gray (1995). Daily snowmelt, M , was calculated by

measuring the lowering of the snowpack and the snow density at the top of the snowpack as described in Heron and Woo (1978). Surface runoff, R_s , was calculated from continuous stage measurements at a 90° V notch weir at the outlet of the upland.

The energy budget at the terrestrial surface is:

$$Q^* = Q_h + Q_e + Q_g \quad (1)$$

where Q^* is net radiation, Q_h is the sensible heat flux and Q_g is the ground heat flux. The latent heat flux (Q_e) can be estimated by rearranging the energy budget equation to:

$$Q_e = Q^* - Q_h - Q_g \quad (2)$$

Q^* , Q_h and Q_g were measured continuously and integrated for half hourly periods. The sensible heat flux was measured using a robust eddy correlation system at 6.5 m height similar to that described by Amiro and Wuschke (1987). A 25 μ m copper-constantan unshielded single junction thermocouple was used to measure temperature and an R.M. Young vertical propeller anemometer to measure vertical wind speed. Because a propeller anemometer underestimates higher frequency eddies (Garratt, 1975), the corrections of Moore (1986) and Blanford and Gay (1992) were applied to estimates of sensible heat flux, which resulted in a +31% correction to Q_h . This is of similar magnitude to the necessary corrections in

previous studies by Blanford and Gay (1992), Amiro and Wuschke (1987) and Petrone et al. (2000).

Q^* was measured with a Kipp and Zonen NR Lite net radiometer mounted 6 m above the surface on the meteorological tower. Immediately prior to field use, the net radiometer was factory calibrated and is expected to have an accuracy of $\pm 10\%$. As the sensible heat measurements are a composite value from the tower footprint which changes with wind speed and direction and the net radiometer measures a disc beneath the tower, the two cannot be used together to solve for latent heat flux as they are measuring two different areas. To address this problem, coincident net radiation measurements using another factory calibrated Kipp and Zonen NR Lite were made at 6 m over each land cover type for 24 hour periods. Spatial differences in Q^* are very small. The root mean differences between daily values of tower and mobile measurements over the different terrain types was 8.3%. Correlation coefficients between each land cover's net radiation flux and the tower measurement were determined. The hourly footprint of the tower was estimated using the methods described in Schuepp *et al.* (1990). The proportion of each land cover type along the footprint was determined using a classified Landsat TM image (30 m resolution) of the Skeeter Lake upland from the NWT Centre for Remote Sensing. Using the hourly footprint and the correlations between the main tower and each land cover type, hourly land cover weighted net radiation values were calculated for a period of twenty one weeks

from May to October, 1999. Hourly weighted and tower values were compared and an empirical equation derived that was used to determine weighted Q^* values beyond the original comparison period.

Ground temperatures were measured half hourly using thermistor strings to 1 m depth in both soil covered and exposed bedrock areas. Bedrock thermistors were inserted into a 2.5 cm hole drilled with a Pjonjar rock drill backfilled with sawdust. Ground heat flux was calculated for each segment within the thermistor string using the Fourier heat flow equation:

$$Q_g = K_T \frac{(T_{g2} - T_{g1})}{(z_2 - z_1)} \quad (3)$$

and totaled to determine Q_g for the entire one meter depth. In eq. (3), K_T is the thermal conductivity and T_g is the ground temperature ($^{\circ}\text{C}$) at the specified depth z (m). The thermal conductivity of the bedrock is treated as constant at $3.4 \text{ W/m}^{\circ}\text{C}$ (Drury and Lewis, 1981) while the thermal conductivity of the soil is a function of the proportions of soil, air, water and ice given by (Farouki, 1981) as:

$$K_T = .025^{f_a} \cdot 0.57^{f_w} \cdot 2.2^{f_i} \cdot 0.25^{f_s} \quad (4)$$

where f is the fraction of a , air; w , water; i , ice and s , solids, in the soil column.

The water content was determined using the TDR measurements. Ice content was determined by the difference in soil moisture values immediately prior to freeze up in the fall and the measured TDR value during the following spring. Soil and exposed bedrock ground heat flux measurements were weighted by the percentage

coverage of each, to estimate the ground heat flux within the tower footprint. The potential measurement error of $\pm 30\%$ in the soil moisture measurement results in an estimated error of $\pm 11\%$ in the ground heat flux. The maximum error of the latent heat flux, calculated as a residual, is $\pm 21\%$ as the sum of the error in the other energy flux measurements.

To provide some insight as to the processes that control evapotranspiration, ET , at this site, the evapotranspiration rate can be compared to the surface resistance, r_s , (s/m). Surface resistance can be calculated using the Penman Monteith equation (Jarvis and McNaughton, 1986):

$$ET = \frac{1}{\lambda} \cdot \left[\frac{\Delta(Q^* - Q_g) + \rho_a \cdot c_p \cdot D / r_a}{\Delta + \gamma(1 + r_s / r_a)} \right] \quad (5)$$

where λ is the latent heat of vapourization (J/kg), γ is the psychrometric constant (kPa/°C), Δ is the slope of the saturation vapour pressure temperature curve (kPa/°C), ρ_a is air density (kg/m³), c_p is the heat capacity of air (J/kg°C), D is the vapour pressure deficit (kPa), and r_a is the aerodynamic resistance (s/m).

3.2 Pocket Lake

A meteorological tower on the bedrock upland above the valley was equipped with a Meteorological Service of Canada Type B rain gauge to measure rainfall volume. Rainfall intensity was measured at the same tower using a tipping-

bucket rain gauge with signals recorded by a Campbell Scientific CR10X datalogger. The snow water equivalent and snow density of the spring snowpack were calculated using the same methods as at Skeeter Lake. The snow survey was stratified into exposed ridge and valley terrain, both crossed by five random survey lines each of which includes at least five snow density and twenty snow depth samples. Daily snowmelt was calculated along four ablation lines on the bedrock ridge and two in the valley using the same methods as at Skeeter Lake.

Table 2 lists the characteristics of the experimental bedrock plots constructed and monitored between May 1999 and May 2001 in the Pocket Lake Basin. Periodic leakage at Plot 6 prevented the 2001 summer water budget from being completed. Plot 4 contains several soil filled depressions covered by a growth of moss and lichen (~50 mm). The largest and deepest depression (85 mm), located immediately above the weir, has a high storage capacity which influences the effective storage for the entire plot. Plot 5 has the same proportion of vegetation and soil cover as Plot 4, but it is mostly located at the upper end of the plot. Storage capacity in both plots was filled at the beginning of the period of record. Plots 6 and 7 are mostly exposed bedrock surfaces with little storage capacity. Prior to 30 June 1999, 22 days without rainfall left both Plots 6 and 7 dry. Most fractures in the plots tend to be narrow (surface aperture < 5 mm) and short (0.5 m) and this agrees with previous measurements of aperture size in boreholes and mine drifts in granitic bedrock (Gale, 1982). Only two large

fractures, one each in Plots 4 and 6 have lengths over 2 m and apertures close to 30 mm while Plot 7 is devoid of large fractures (Figure 3).

Table 2: Physical characteristics of runoff plots

Plot	Area (m ²)	Aspect	Soil cover (%)	Storage capacity S_c (mm)	Infiltration rate I (mm/day)	Fracture density ρ_f (%)
4	38	E	25	43	2.8	0.52
5	30	E	25	18	1.6	0.63
6	12	SW	3	1.2	2.4	0.97
7	6	SW	Bare	1.4	1.3	0.11

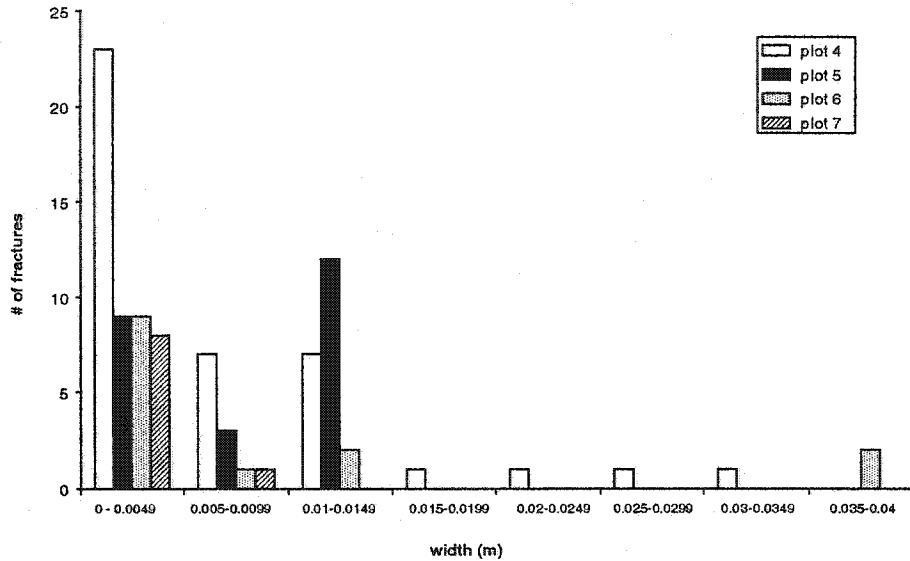


Figure 3: Frequency distribution of fracture width, b , in each plot.

Water on each plot is stored on the bedrock surface, in depressions and in soil patches on the rock. Storage was calculated as the residual of the water budget. To provide a check on the estimated value, storage capacities of the bedrock surface and depressions were measured by pouring water onto the rock and noting the volume added before runoff would commence. Soil samples were

taken for field capacity determination in the laboratory. The plot storage capacity, S_c , was calculated by weighting the storage capacity of each component of the plot by its fractional areal coverage. A conservative $\pm 25\%$ was used as the error estimate for the storage measurement.

Snow lysimeters 300 mm in diameter were installed at each plot to estimate evaporation and sublimation, E_l , during the melt season by measuring their daily change in weight. To estimate evaporation losses in the summer, weekly evaporation was obtained using lysimeters 120 mm in diameter deployed after 1 August 1999 in soil filled depressions in one of the plots. The summer evaporation values allowed an estimate of the average α value of the Priestley-Taylor (1972) equation:

$$\alpha = \frac{E_l \cdot (\lambda \rho_w)}{(\frac{\Delta}{\Delta + \gamma}) \cdot (Q^* - Q_g)} \quad (6)$$

where ρ_w is water density (kg/m^3). Daily evaporation estimates were calculated using the average value of α . Instrumentation for the measurement of these meteorological terms was deployed at a climate tower on a bedrock ridge (Figure 2) that was instrumented in a similar fashion as the Skeeter Lake tower described above. Bedrock plot evaporation, E , is a pro-rated value of E_l depending on the extent of wet portions in the plots as determined by rainfall and storage capacity measurements.

The groundwater flow system in granitic rock can be viewed as impermeable blocks dissected by fractures, the latter being the only effective conduits of flow (Davison, 1984). A parallel plate analogue was used to calculate hydraulic conductivity within individual fractures, K_f , (m/s) (Domenico and Schwartz, 1998):

$$K_f = \frac{b^2 g}{12\mu} \quad (7)$$

where b is the aperture width (m), g is acceleration due to gravity (m/s^2) and μ is the kinematic viscosity of water (m^2/s). Fracture mapping at the bedrock surface was performed to determine b . Field studies by Raven et al. (1985) show that (7) represents fluid velocity at shallow depths so this equation is appropriate for estimating the infiltration rate for each fracture. The infiltration rate for each plot is:

$$I = \rho_f \cdot \left[\sum_n (K_f \cdot P_f) \right] \quad (8)$$

where P_f is the fraction of the fractured area occupied by an individual fracture.

Witherspoon et al. (1980) estimated the accuracy of the cubic law in granite at $\pm 25\%$. Water was poured into depressions above fracture apertures in Plot 6 and covered to prevent evaporation in order to determine if infiltration was affected by ground frost on 11 April 2000 when the rock was frozen and 30 August 2000 when the rock was thawed.

Bedrock plot runoff, R , was measured by cementing aluminum sheet metal into the rock to block the outlet of a natural bedrock catchment from which a hose was run to an 80L bucket. After each runoff event, the volume in the bucket was noted and converted to a runoff depth. At two plots, runoff rates were also recorded by measuring the change in water level in the bucket with a float recorder wired to a Campbell Scientific CR10X data logger. To test the accuracy of the runoff instrumentation, known volumes of water were applied to the bottom of each plot immediately above the weir and the volume in the collection bucket was measured. The instrumentation underestimated runoff by an average of 7%. This correction factor was applied to all runoff measurements.

Geophysical surveys were conducted to define the surface and bedrock topography of the soil filled valley. The bedrock surface beneath the soil-filled valley was mapped using a combination of probing by hammering a steel rod into the sediment until encountering the bedrock and a pulseEKKO IV ground penetrating radar with a 400V transmitter and an antenna centre frequency of 100 MHz (Spence, 1996). Soil temperature was recorded at half hourly intervals using a thermistor string located at the foot of the hillslope (Figure 1). A steel rod was used to probe for the depth of the frost table during the spring and early summer.

Soil infiltration rates were determined under different ground frost conditions using double-ring infiltrometers. Evapotranspiration from the soil filled valley was estimated using the eddy correlation-energy budget techniques described for Skeeter Lake and the instrumentation at the tower on the bedrock upland. Lateral inflow from upslope exposed bedrock to the valley (I_b) was measured with volumetric measurements and velocity-area flow calculations at the upslope weir sites (Figure 2), with velocity obtained using a Price type pygmy current meter. It was assumed that additional inflow from bedrock side slopes outside areas captured by the weirs could be estimated using runoff data from the bedrock runoff plots because of their similar drainage areas and physiography. The extent of bare and soil covered areas on the bedrock side slopes was delineated from air photos and side slope inflow calculated as a portion of total lateral inflow following:

$$R_{bss} = \frac{(R_{br} \cdot a_{br}) + (R_{sc} \cdot a_{sc})}{a_{bss}} \quad (9)$$

where a_{br} and a_{sc} are areas of the bare and soil covered portions of the total bedrock side slopes area, a_{bss} . R_{br} and R_{sc} represent average runoff from the bare and soil covered plots, respectively, which was measured as described earlier. R_{bss} , runoff from the side slopes, was converted into millimetres over the area of the valley, v , using:

$$I_{bss} = \frac{R_{bss} \cdot a_{bss}}{a_v} \quad (10)$$

and added to I_{bw} , inflow measured at the weirs to produce total lateral inflow, I_b .

$$I_b = I_{bw} + I_{bss} \quad (11)$$

Peters et al. (1995) identified that runoff from exposed bedrock enters the soil zone along the bedrock surface. At the bottom of a bedrock hillslope, daily volumetric measurements were made at a runoff plot that consisted of paired weirs, one at the soil-bedrock contact and the other at the soil surface. The partitioning of runoff into surface flow and flow along the bedrock surface during both frozen and unfrozen conditions at this location was assumed to occur everywhere along the soil-filled valley bedrock contact. At the outlet of the basin, stage recorded continuously at a 90° V-notch weir was converted into surface outflow (R_s) by a rating curve obtained from periodic discharge measurements using the velocity-area method. Subsurface flow (R_g) was collected in two trenches. They were operative only in the summer as flooding prevented their usage during the spring. Areas contributing to surface runoff were mapped based on visual observations. Runoff volumes and depths from each land cover component or runoff plot were calculated by multiplying runoff depths by the respective contributing drainage area.

A network of piezometers along three transects enabled the determination of the direction of groundwater movement within the soil-filled valley. Hydraulic

conductivity was calculated using pump tests as described in Freeze and Cherry (1979). The water table was measured continuously at two wells, one at the edge and the other in the center of the valley along transect H (Figure 2). Six additional wells along transect G, three along transect H and two along transect E were measured opportunistically. Field calibrated Campbell Scientific CS615 time domain reflectometry (TDR) soil moisture sensors were installed at 0.05 and 0.3 m depths within the middle of the soil-filled valley (196.45 and 196.2 masl, respectively) and to 0.3 m depth at the valley edge (197.05 masl). Daily change in storage, ΔS , was calculated as:

$$\Delta S = \Delta S_u + \Delta S_s = \Delta \theta [z - z_w(t)] + S_y [z_w(t) - z_w(t-1)] \quad (12)$$

where ΔS_u and ΔS_s are the changes in storage in the unsaturated and saturated zones; $\Delta \theta$ is the spatial average change in moisture content in the unsaturated zone; S_y is the specific yield of soil, measured here to be 0.13; z is total soil thickness, $z_w(t)$ and $z_w(t-1)$ are height of the water table (measured from the bedrock upward) for the present (t) and the previous ($t-1$) time periods. The valley edge was delineated using the strip of trees visible in Figure 2. The average valley change in storage was a prorated calculation based on the relative areas of valley edge and centre.

CHAPTER 4

ENERGY BUDGETS OF THE SUBARCTIC SHIELD LANDSCAPE

The period of record is from 1 May to 1 October 1999 and 12 May to 2 August 2000 and is uninterrupted, except for 7 - 13 June and 21 June - 13 July 1999 when air temperature and relative humidity data were not logged because caribou chewed through those sensors' wires. Figure 4 compares the precipitation and temperature record against normal conditions for the city of Yellowknife for the period of record. May, June and July precipitation and temperature in the region is normally 84 mm and 11°C. Rainfall was below normal at 50 mm and 64 mm in 1999 and 2000, respectively. Average temperatures for the same three month period were 9°C and 11°C in 1999 and 2000, respectively. Prolonged dry periods at the beginning of both summers resulted in a decline in soil moisture that slowed at the end of July (Figure 5). Rain at the end of the summer of 1999 and the snowmelt of 2000 replenished some of the water lost, but over the entire study period, there was a net soil moisture loss of 73 mm.

In 1999, snow meltwater flooded into the bedrock depressions because there was little available soil storage at the site after a wet fall in 1998. Despite a

similar volume of snowmelt in 2000 (Figure 6), much of the water went to replenishing soil moisture storage (Figure 5b) reducing the fraction of snow meltwater that ran off from 0.76 in 1999 to 0.58 in 2000. The ponding on the bedrock associated with the larger runoff in 1999 was subdued in 2000, so much of the exposed bedrock began the summer dry.

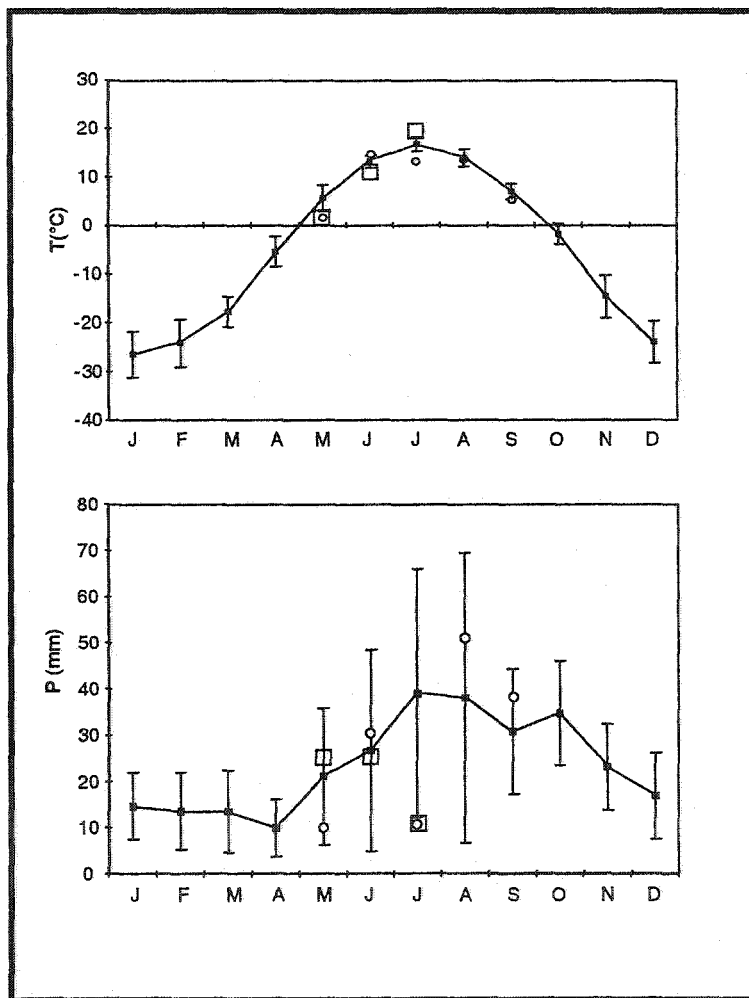


Figure 4: Monthly air temperature and precipitation. The white circles represent 1999 observations and the white boxes, 2000 observations at Skeeter Lake. The black squares are Environment Canada 1961-1990 averages for Yellowknife with the bars representing \pm one standard deviation.

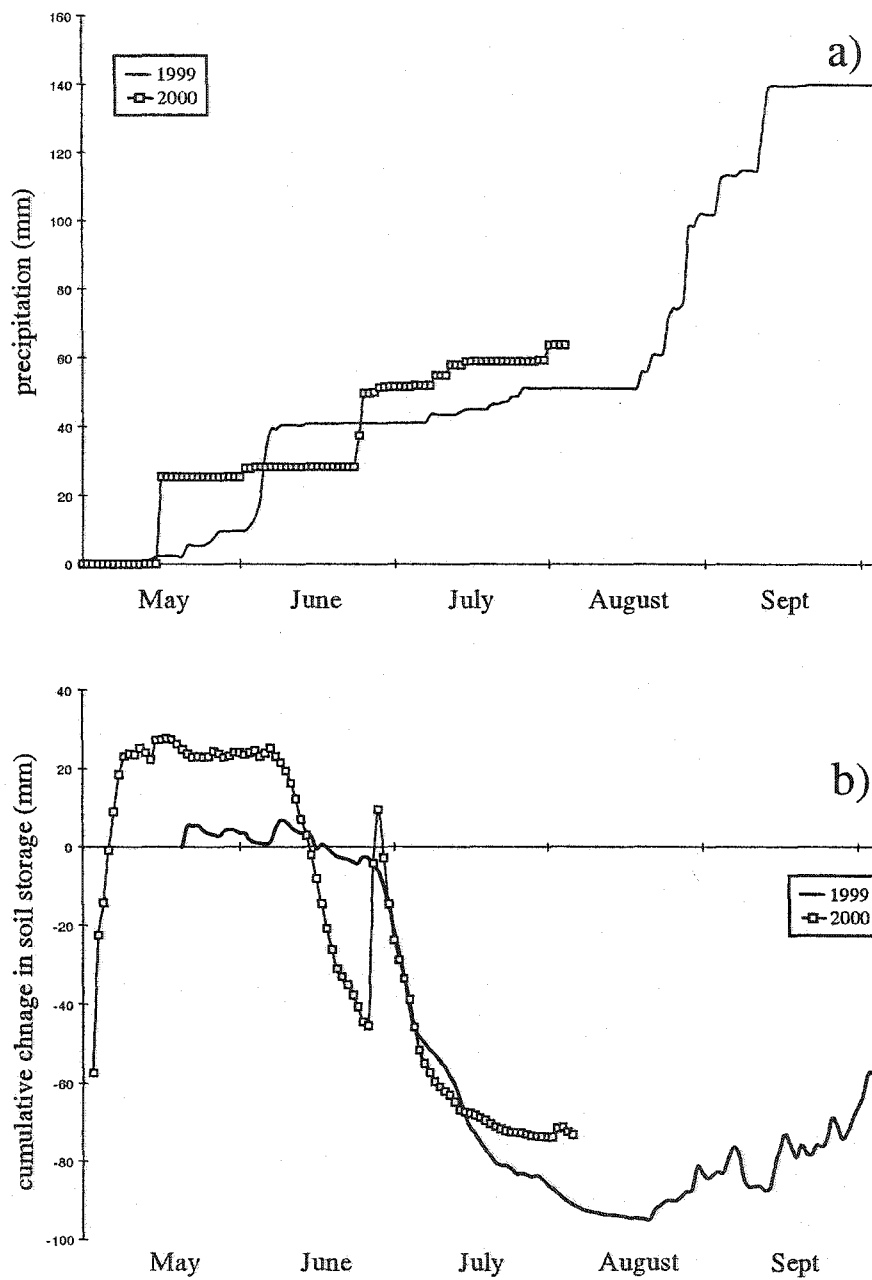


Figure 5: a) Cumulative precipitation and b) cumulative change in soil moisture storage on the Skeeter Lake upland during 1999 and 2000.

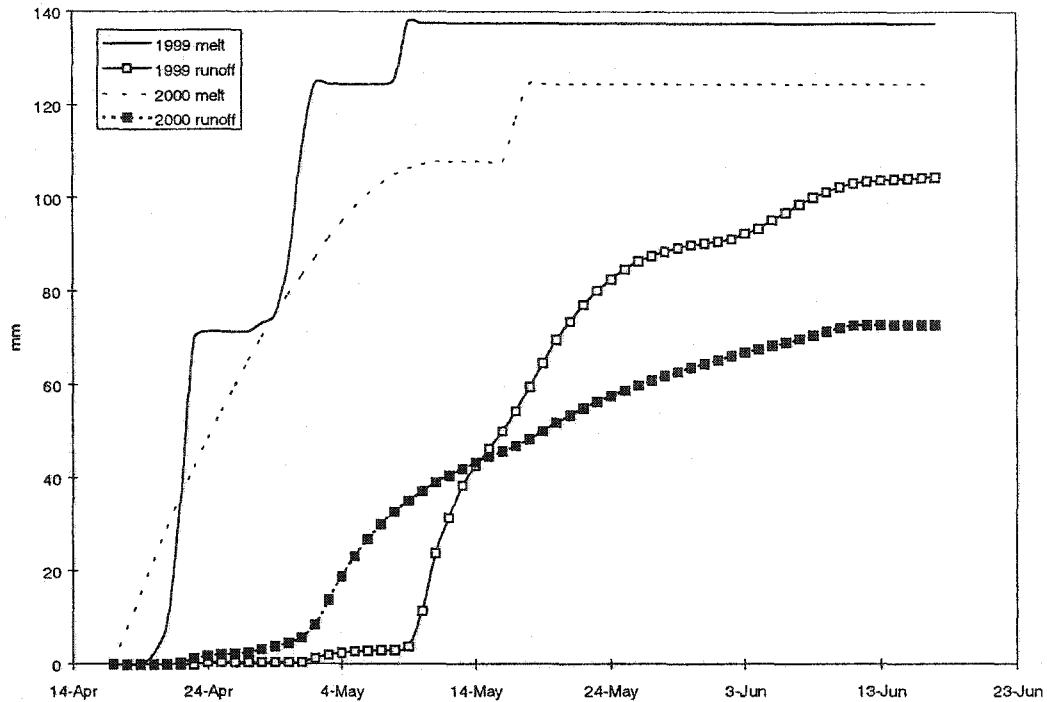


Figure 6: Cumulative spring snowmelt and runoff at Skeeter Lake in 1999 and 2000.

In 1999, Q^* and Q_e increased from 1 May to a maximum on 20 June (Figure 7). After the summer solstice, daily Q^* declined gradually until the end of September when it approached zero. Q_e declined after the summer solstice to the end of July, remained steady through the month of August and declined further in September due to low radiation input and cool and wet conditions. Q_h remained relatively steady throughout the season and exceeded Q_e from mid July to the end of September. Positive Q_g was significant early in the summer but values were small once the ground had warmed by the end of June. Negative Q_g in September augmented Q_h so that it equaled or exceeded Q^* through the second half of the

month. While Q^* in 2000 had a similar pattern to that observed in 1999, Q_e remained low until the end of the study period (Figure 7). Q_h was much larger and Q_g slightly larger than in 1999.

Net radiation peaked near mid day (1130 to 1400 MST) during every month in the study period (Figure 8). There was a slight delay until the sensible heat peaked in the afternoon (1400 MST). Latent heat rose quickly in the morning to a maximum from 1000 to noon MST and then receded slowly through sunset. The ground warmed during the day (1200 to 1500 MST) and released a small amount of heat overnight.

Q^* was larger in May 2000 than May 1999, but the situation was reversed in June. Net radiation was similar in July of both years (Figures 7 and 8). Monthly Bowen, Q_h/Q^* and Q_g/Q^* ratios differed significantly between 1999 and 2000 (Table 3). Bowen ratios were less than unity through the early summer of 1999 and increased to the end of September. Monthly average Bowen ratios in 2000 were consistently greater than unity. May and June Q_h/Q^* ratios also suggest that more energy was directed to evaporation in 1999 than in 2000. May Q_g/Q^* values were similar in 1999 and 2000, but June and July values were larger in 2000.

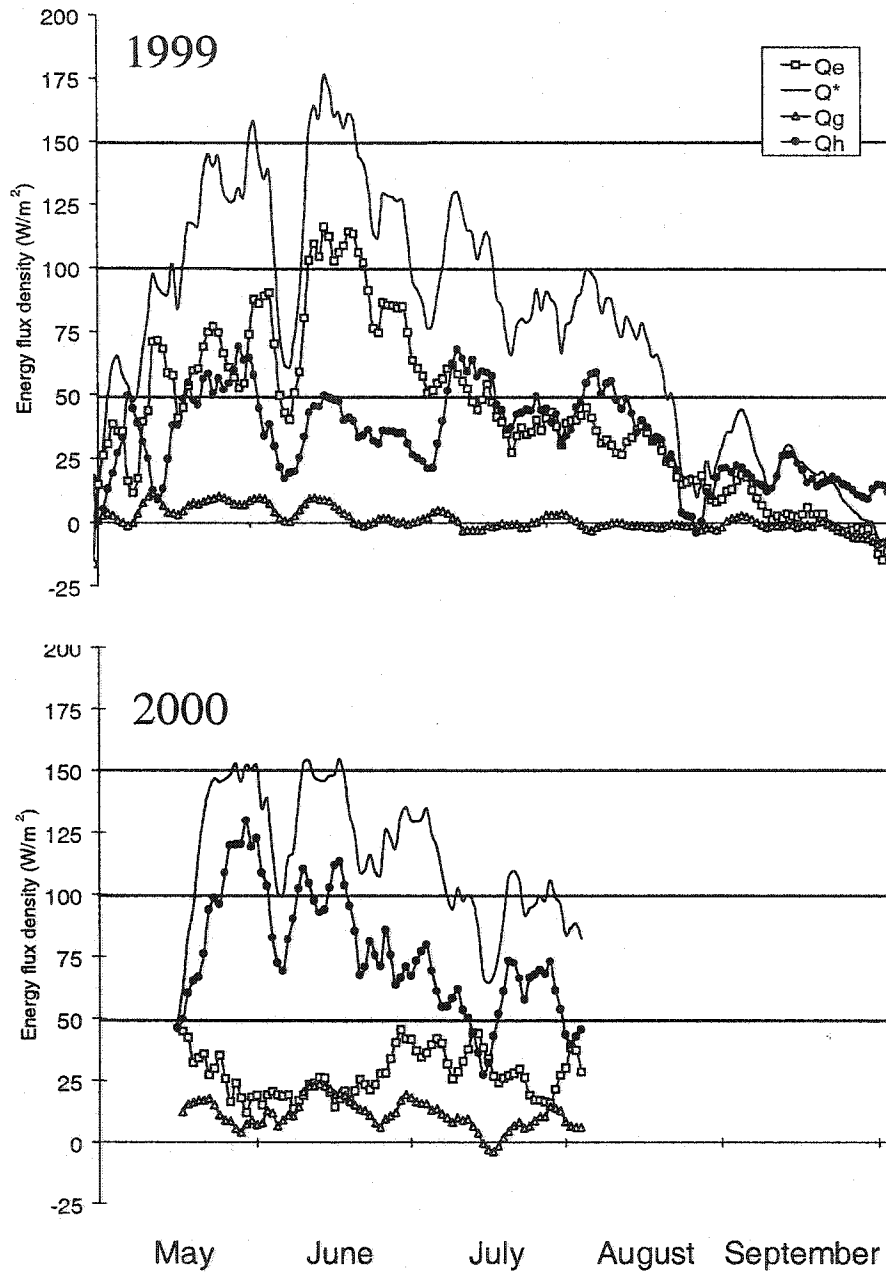


Figure 7: The Skeeter Lake upland seasonal energy budget pattern for 1999 and 2000. The values presented are 5 day running means.

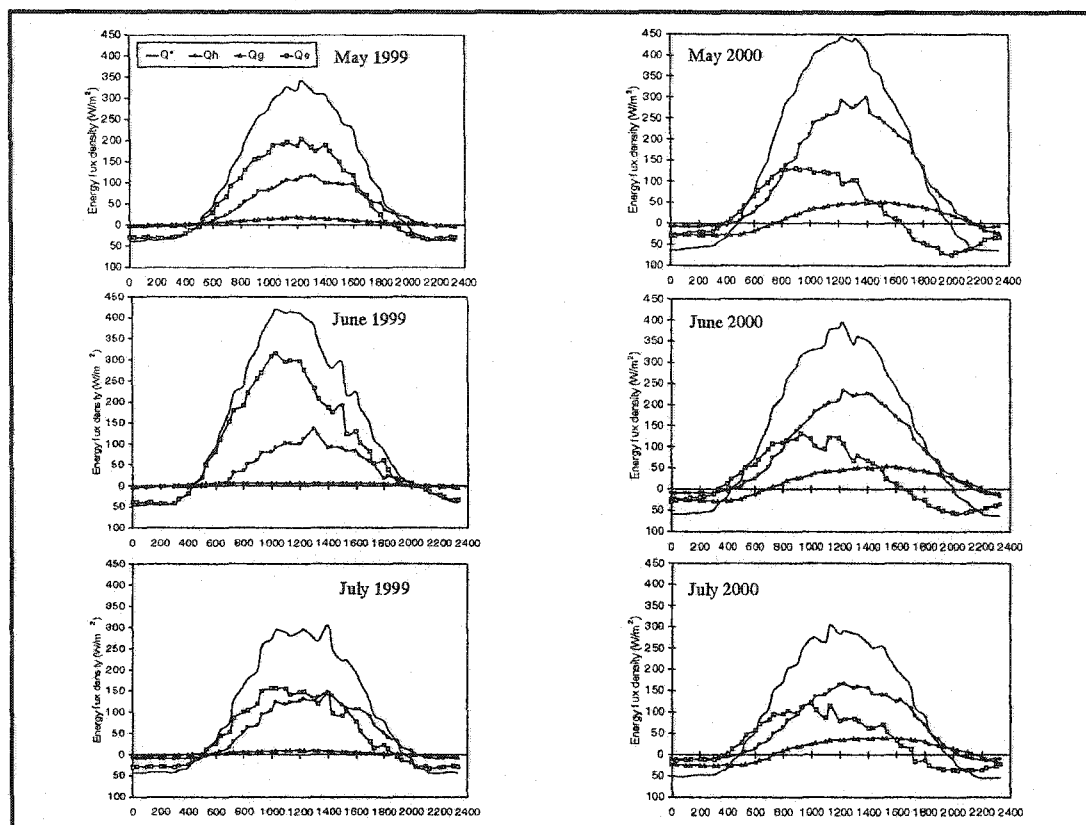


Figure 8: Skeeter Lake upland average diurnal energy budgets for common months in 1999 and 2000.

Table 3: Skeeter Lake upland monthly energy budget ratios, average Bowen ratios, evaporation rates and precipitation during 1999 and 2000.

Month	Q_h/Q^*	Q_g/Q^*	Q_e/Q^*	Daily β	ET (mm/day)	P (mm)
1999						
May	0.52	0.40	0.08	0.78	1.95	7.4
June	0.75	0.20	0.05	0.42	3.02	31.4
July	0.45	0.52	0.03	1.20	1.65	10.1
August	0.34	0.63	0.03	1.10	0.98	51.1
September	0.11	0.96	-0.07	2.30	0.16	37.8
2000						
May	0.18	0.78	0.07	3.10	0.83	25.5 * (snow)
June	0.22	0.65	0.11	3.50	0.89	26.2
July	0.36	0.56	0.06	2.00	1.10	12.2

4.1 Interannual differences

In 1999, after all of the snowpack, except for late lying drifts, had melted, meltwater remained flowing through the upland until mid June (Figure 6). As water levels receded some areas became detached from the runoff, which left much water ponded in depressions created by the bedrock microtopography. As a result, initial evapotranspiration rates were high and there was a general decrease in rates and increase in Bowen ratios during the long dry period beginning after the summer solstice in June and persisting through July. At the beginning of this period surface resistances were lower than observed by Lafleur (1992) and vapour pressure deficits were high (Figure 9) so that evaporation rates exceeded those observed at other subarctic sites (Jarvis et al., 1997; Lafleur, 1992; Wright, 1981). It was not until the bedrock surfaces dried that a loss in soil moisture was observed (Figure 5). As the soil dried, latent heat flux decreased while vapour pressure deficits remained high but surface resistance increased, suggesting there was some physiological response by the vegetation or a physical barrier in the soil that prevented a loss of moisture. Sphagnum peat and black spruce vegetation do not have a large degree of physiological control on evaporation (Baldochi et al., 1997) so it is expected there was a physical control on evaporation from the lichen and moss cover as Bello and Arama (1989) and Lafleur and Schreder (1994) have observed high evaporation rates over wet lichen and moss while Kershaw and

Rouse (1971) note that dry lichen and moss cover is an effective mulch in preventing evapotranspiration from the soil.

In 2000, the original snowpack was almost gone before the mid May snowstorm. Runoff ceased early and there was less ponding and fewer soil covered areas filled with water, so the site began the summer much drier than in 1999. Despite high vapour pressure deficits, surface resistance was high because of the dry conditions so evapotranspiration rates in the early summer were low (Figure 9). These rates increased and Bowen ratios decreased after significant rainfall in late June.

For comparable periods, Q_e/Q^* values and evapotranspiration rates in 1999 were much higher than in 2000 and indeed higher than for most other subarctic terrain types (Table 4) (Lafleur, 1992; Jarvis et al., 1997; Lafleur et al., 1997; Wright, 1981). Low β and high Q_e/Q^* in 1999 at first suggest the Skeeter Lake upland is a relatively wet subarctic environment, but high β and low Q_e/Q^* in 2000 imply the site is a more arid environment than has previously been observed in subarctic Canada. The differences between 1999 and 2000 were substantially greater than annual differences found by Lafleur (1992) in wetland open canopy black spruce tamarack forest, for comparable precipitation amounts. Most of the studies of subarctic energy budgets have been performed in wetter climates (eg., Schefferville, Quebec [Wright, 1981; Fitzjarrald and Moore, 1994])

or in terrain with deeper soils (eg., Churchill, Manitoba [Lafleur et al., 1992]) or a combination of both (eg., Thompson, Manitoba [Lafleur et al., 1997]). This provides a moisture buffer in most subarctic environments that is not present in the northwestern subarctic Canadian Shield. The lack of a buffer creates a situation where the landscape has the potential for much larger interannual variability in the energy budget than do other subarctic landscapes.

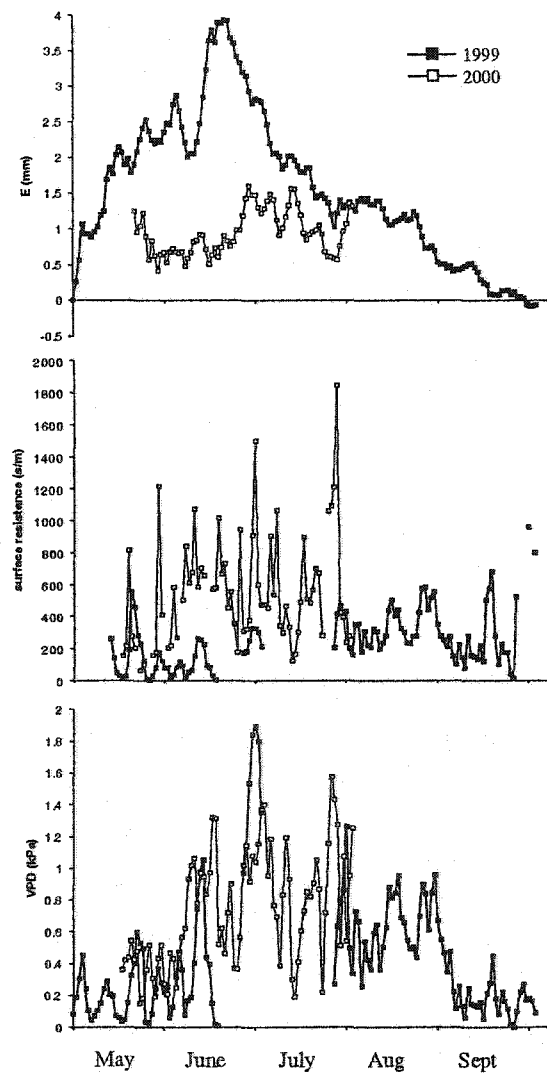


Figure 9: The seasonal pattern of evaporation, surface resistance and vapour pressure deficit. Values shown are 5 day running means.

Table 4: Average β and Q/Q^* results from the Canadian Shield and other subarctic locations for comparable periods. Table lists wettest locales and conditions first, then drier examples with each subsequent row down the table.

Reference	β	Q/Q^*	land cover	location
Moore et al., 1994	0.2 - 0.8	0.63	wetland	Schefferville, PQ
Lafleur et al., 1997	~ 0.6	n/a	wetland	Thompson, MN
<i>this study's 1999 results</i>	0.8	0.6	<i>mixed</i>	<i>Lower Carp Lake, NT</i>
Rouse and Bello, 1985	1.3 - 1.9	n/a	black spruce	Churchill, MN
McCaughey et al., 1997	2	n/a	jack pine	Thompson, MN
Moore et al., 2000	2.5	0.25	jack pine	Thompson, MN
Fitzjarrald and Moore, 1994	2.5	n/a	black spruce	Schefferville, PQ
<i>this study's 2000 results</i>	2.8	0.25	<i>mixed</i>	<i>Lower Carp Lake, NT</i>

4.2 Site hydrology and energy budget feedbacks

The magnitude of the spring freshet controls the summer energy budget.

When the snowmelt magnitude is large, as in 1999, the subarctic Shield landscape is prone to flooding in flat lying areas like the Skeeter Lake study site. Soil depths are shallow and much water can spill onto surrounding exposed bedrock. When conditions are wet as they were in June 1999, latent heat fluxes are large as much of the net radiation goes to evaporating the water ponded on the exposed bedrock. The 2000 snowmelt was more subdued and created conditions where the bedrock and soils remained dry and heated more, augmenting ground and sensible heat fluxes. The low storage capacity of the soil cover does not allow much water to remain in the landscape from year to year, so that the early summer energy budget is highly variable and dependent on the magnitude of the snowmelt.

It is expected that a storage deficit will develop every year on subarctic Shield terrain. In Schefferville where the climate is much wetter, Moore et al.

(1994) observed a summer storage deficit. Much of the summer rainfall in the Yellowknife region is re-circulated water from convective storms (Szeto, 1998) so a positive feedback system may exist where wet conditions (i.e., heavy ponding) enhance summer rainfall, which reduces summer storage deficits. The effect of climate variability will be to determine the magnitude of the deficit. Wet years may see a small deficit which will increase the likelihood of runoff events in the fall. During a normal year, the storage deficit may prevent a runoff response from fall rains. The large moisture deficit in a dry year may have implications for snowmelt the following spring, as meltwater will be directed to replenishing storage, hence lowering the size of the spring freshet. Spence (2000) illustrated that headwater lake storage deficits are important in controlling the magnitude of the spring freshet at the basin scale, the results from this study imply that storage deficits are important at the hillslope scale.

CHAPTER 5

HYDROLOGICAL PROCESSES OVER EXPOSED BEDROCK

5.1 Hydrological Processes

The following section described hydrological processes observed at the Pocket Lake bedrock plots from 9 May to 9 September 1999 and 30 March to 26 September 2000.

5.1.1 Rainfall

Figure 10 shows the rainfall time series for 1999 and 2000 with individual events ranging from 0.6 mm to 36.2 mm. In 1999, the large events were associated with prolonged rainfall in the autumn, but in 2000 the largest events were summer thunderstorms of short duration.

5.1.2 Snow ablation

Snow drifting into bedrock depressions resulted in high variability in snow depth, snow water equivalent and snowmelt patterns between the plots. After a short period of limited melting, when maximum daytime temperature rose above freezing at the end of March, snow ablation ceased until 14 April. Snow ablation peaked between 20 and 22 April reaching 63, 24 and 15 mm/day in plots 4, 5 and

7, respectively (Figure 11). This event removed much of the residual snow in plots 5 and 7 but snow remained in plot 4 until 30 April. Evaporation accounted for most or all of ablation after melt rates peaked.

5.1.3 Storage

Storage capacity varied significantly among the plots (Table 2) because of their uneven microtopography. Observations suggest that only depressions over 50 mm in depth contained soil. The smallest depressions (<10 mm) existed only on the bedrock face. Between these depths, depressions often contained fracture apertures. The frequency distributions of mean depth and areal extent of depressions (Figure 12) were both highly skewed, indicating a dominance of the smaller depressions.

Storage in deeper depressions remained longer after rainfall than in smaller depressions (Figure 13), presumably because the deeper depressions could hold more water. Deep depressions reached their capacity more slowly and less often than the shallow ones. The daily time step in Figure 13 cannot reveal the attainment of capacity in the shallow depressions because much moisture was lost to evaporation within one day. Only those days with low evaporation during the late summer and fall, or intense rain in the mid summer, exhibited storage in the shallow depressions that remain longer than a day.

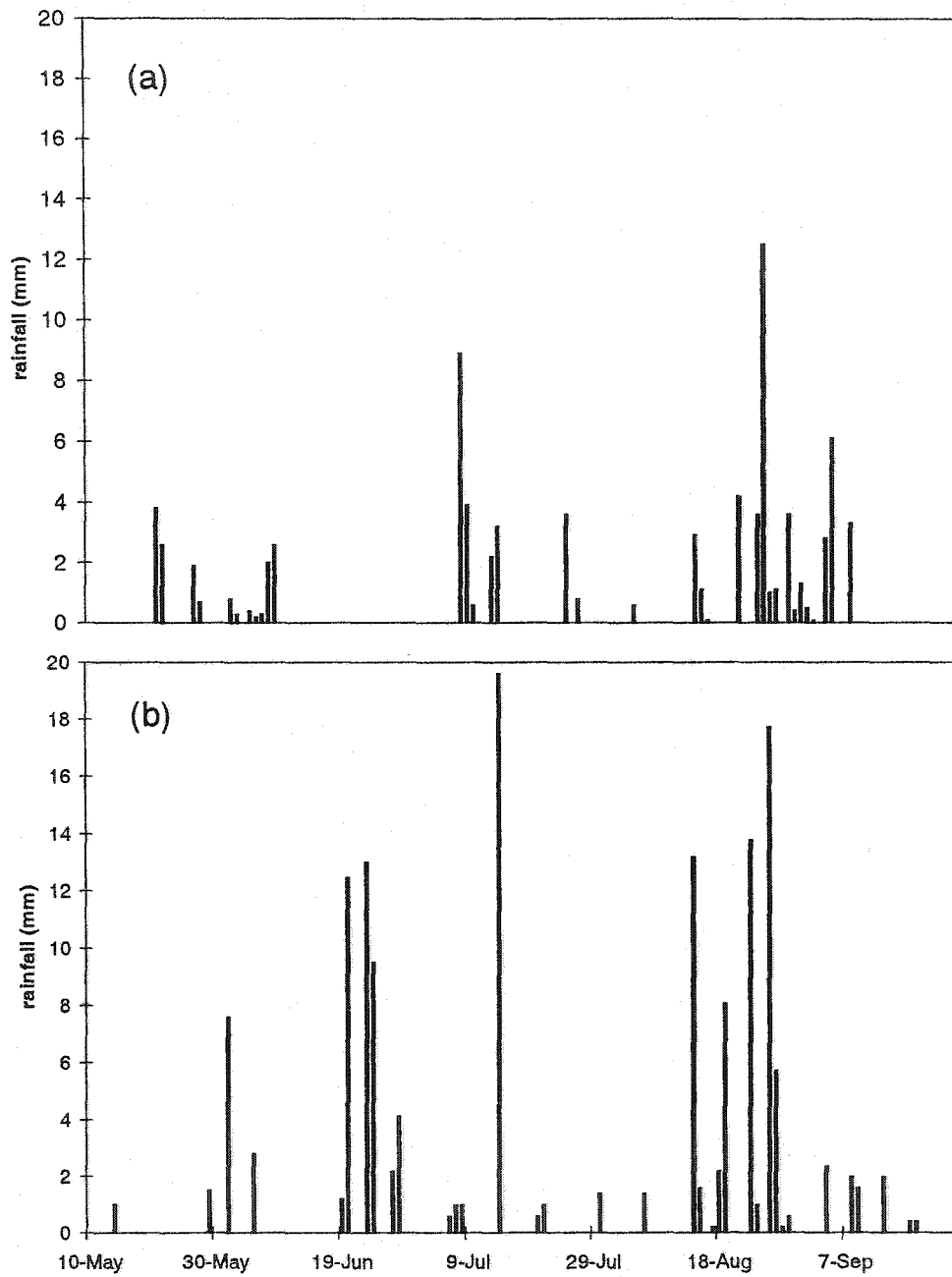


Figure 10: Rainfall time series measured at Pocket Lake in a) 1999 and b) 2000.

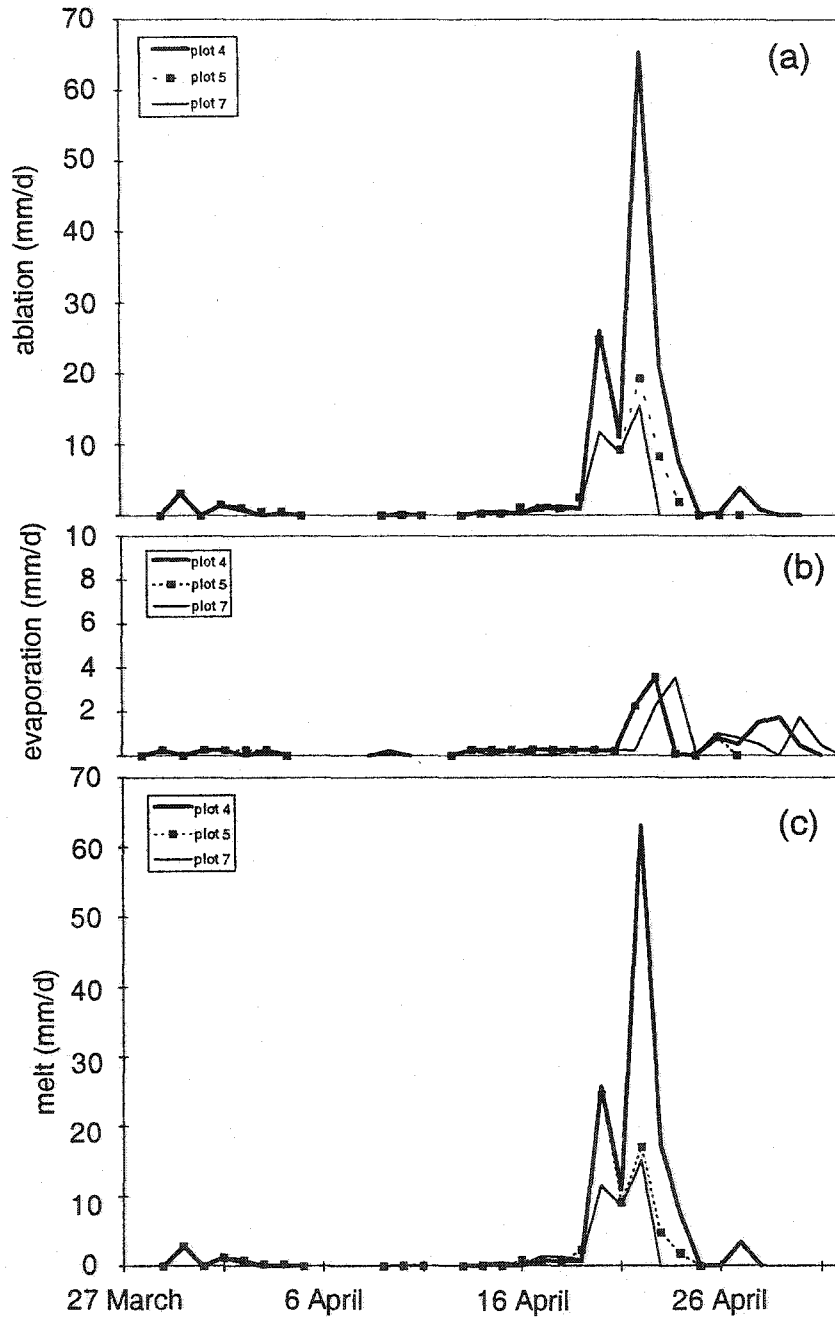


Figure 11: Spring of 2000 a) snow ablation, b) evaporation and c) snowmelt for three of the four plots at Pocket Lake. Ablation rates are illustrated at the top, evaporation in the middle and snowmelt at the bottom.

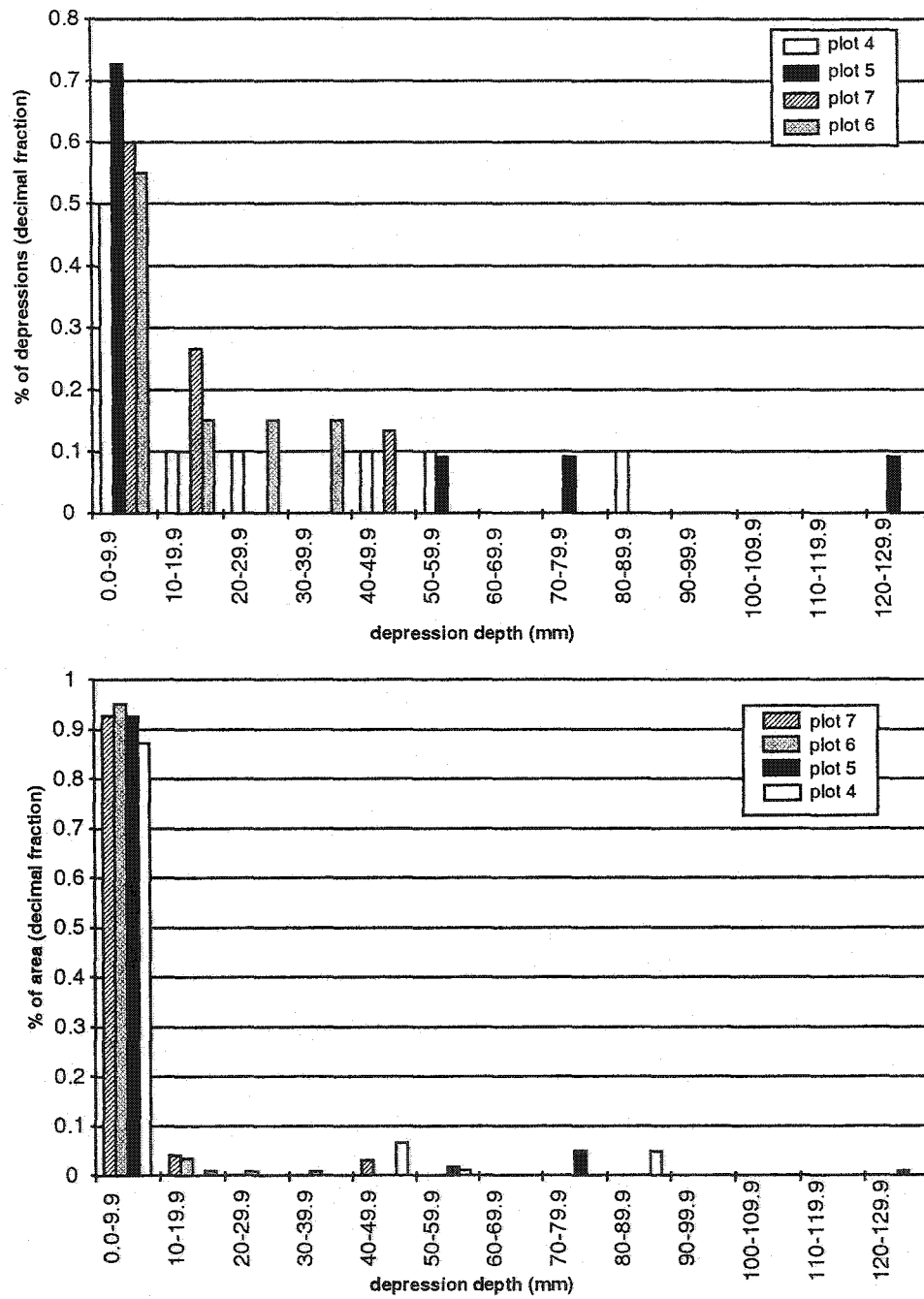


Figure 12: Frequency and areal distributions of depressions in each bedrock runoff plot.

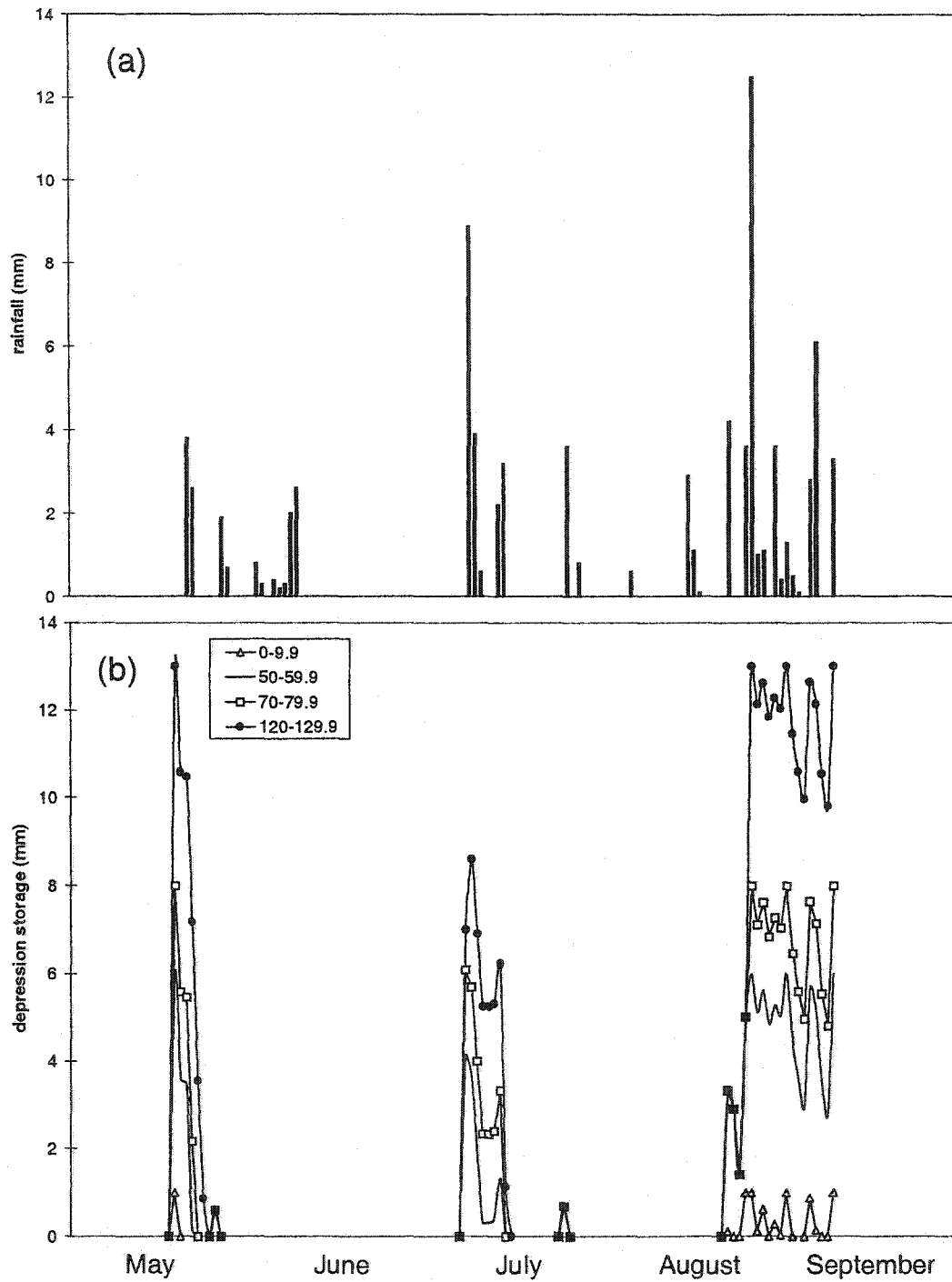


Figure 13: a) 1999 rainfall time series and b) storage in individual depression class sizes in plot 5.

5.1.4 Evaporation

Monthly mean evaporation calculated from the soil-filled lysimeters is listed in Table 5. Average daily evaporation rates can be high due to advection of sensible heat from dry exposed granitic bedrock.

Table 5: Monthly mean evaporation from lysimeters

Month	E_t (mm/day)
August 1999	0.9
September 1999	1.6
May 2000	1.6
June 2000	1.0
July 2000	2.0
August 2000	1.7
September 2000	1.0

The low storage capacity of the bedrock face permits most rainfall to run off so that the bedrock face dries quickly after rainfall ends, or during a break in the rain event, leaving only a thin film of water to evaporate. As many rainfall events were gentle and started and stopped for several hours, a large proportion of rainfall was evaporated from the water film. Evaporation was sustained over several days after rainfall by water in deeper depressions. Despite higher evaporation from the deeper depressions, it is the prevalence and larger areal coverage of the shallow depressions that controlled the overall plot evaporation (Figure 14). Evaporation ceased when storage dropped to zero in the deep depressions. Evaporation is limited by the availability of water on the rock, as is shown by plot 7 in 1999 (Figure 14) where 35% of seasonal evaporation occurred

in August and September despite lower evaporative demand at the end of the summer.

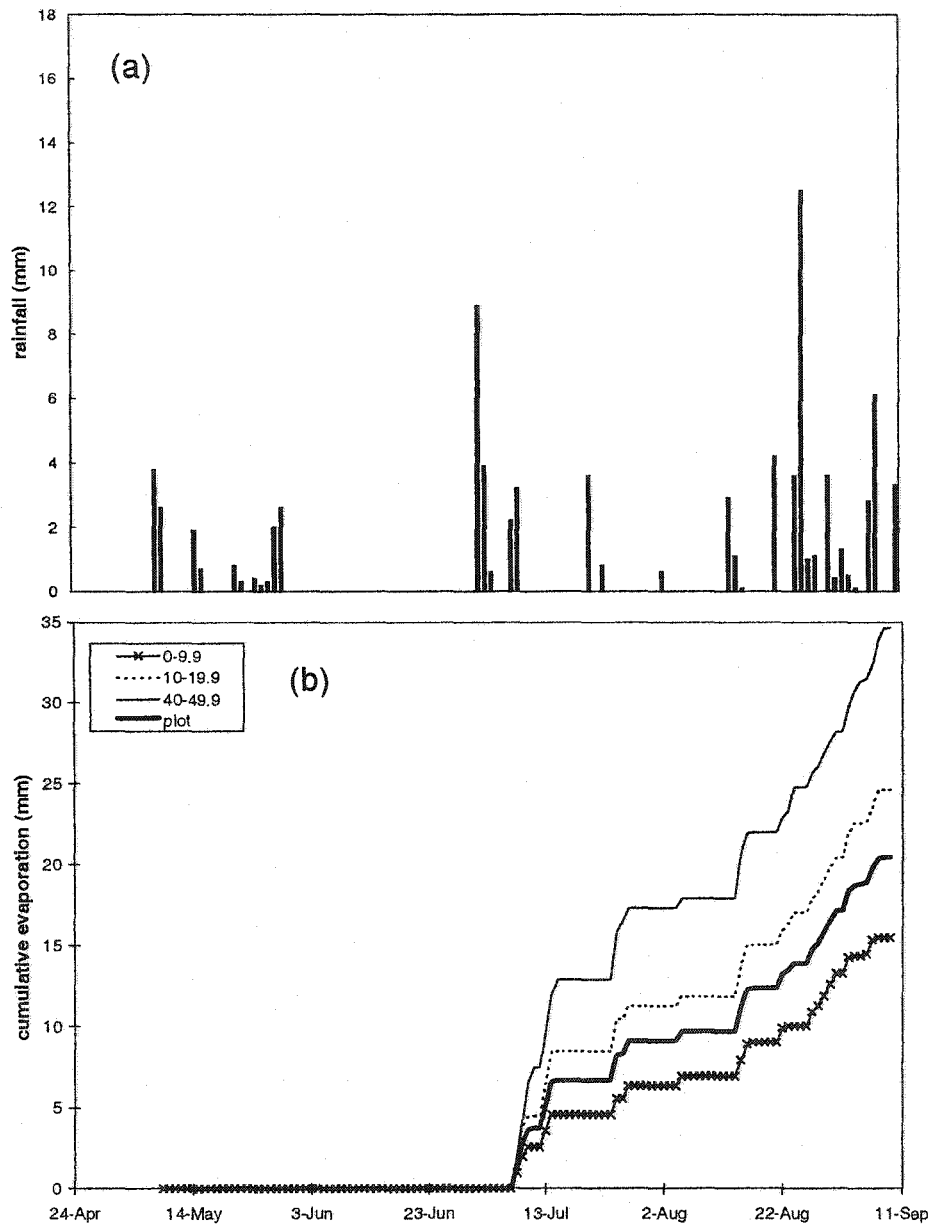


Figure 14: a) 1999 rainfall and b) 1999 cumulative evaporation from plot 7 and individual depression class sizes within plot 7.

5.1.5 Infiltration

Plots 6 and 7 had similar average infiltration ratios (22% and 23%, respectively) for the 1999 summer but very different fracture densities (Table 2). This implies fracture width is more important than fracture density in controlling infiltration. Figure 15 and Table 6 illustrate the rainfall and runoff patterns of two storms with contrasting rainfall intensities as measured at Plot 5. The infiltration ratio of the more intense storm was 30% smaller than that of less intense storm. This supports Thorne et al.'s (1999) theory that more intense storms experience less infiltration because rainfall intensities exceed the constant maximum fracture infiltration rates that are controlled by fracture width.

The bedrock was frozen at 0.3 m depth on 20 April 2000 and frost free on 30 August 2000 (Figure 16). The same measured infiltration rates on both days of 20 mm/h entering 3 mm wide fractures suggest that the frozen conditions in April did not inhibit infiltration. This corroborates the findings of Thorne et al. (1994) who observed a water table rise in frozen Precambrian bedrock in southeastern Manitoba during snowmelt. A negative relationship between snowmelt period infiltration ratios and average daily melt rates in 2000 (Figure 17) suggests that, as in the summer, the input rate of water to the bedrock surface dictates the proportion of infiltration.

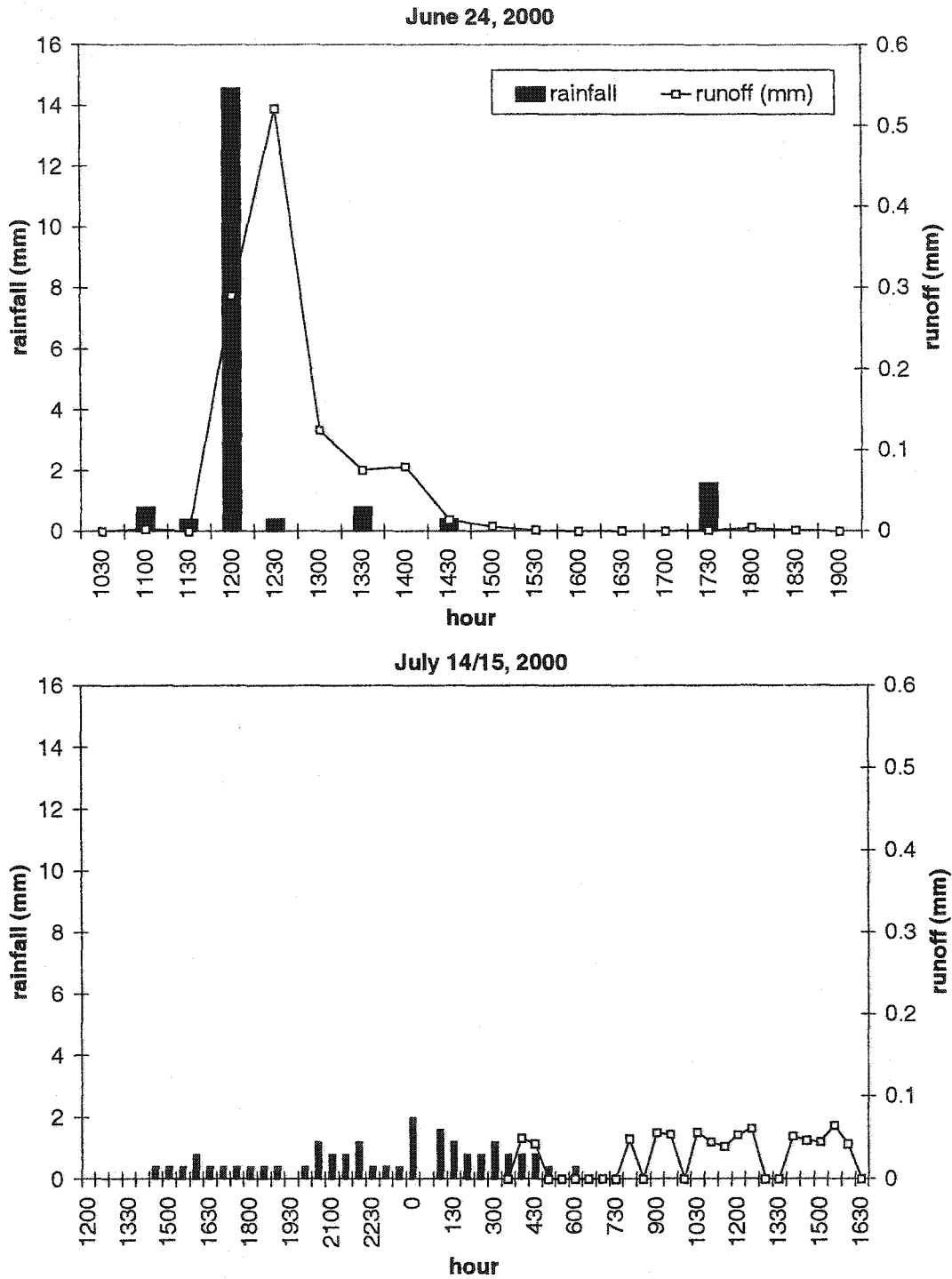


Figure 15: Hyetographs and hydrographs from two storms as measured in Plot 5 during the summer of 2000.

Table 6: Water budget measurements of two rainfall runoff events at Plot 5. Water budget terms are expressed in millimeters. E/P is the evaporation ratio and I/P the infiltration ratio.

Event	P	Peak intensity (mm/hr)	Duration (hr)	R_b	R_b/P	E	E/P	I	I/P
24 June 2000	18.9	29.2	7.5	1.1	.06	11.3	.60	6.4	.36
14 July 2000	22.0	3.6	16	0.8	.04	10.0	.45	11.2	.51

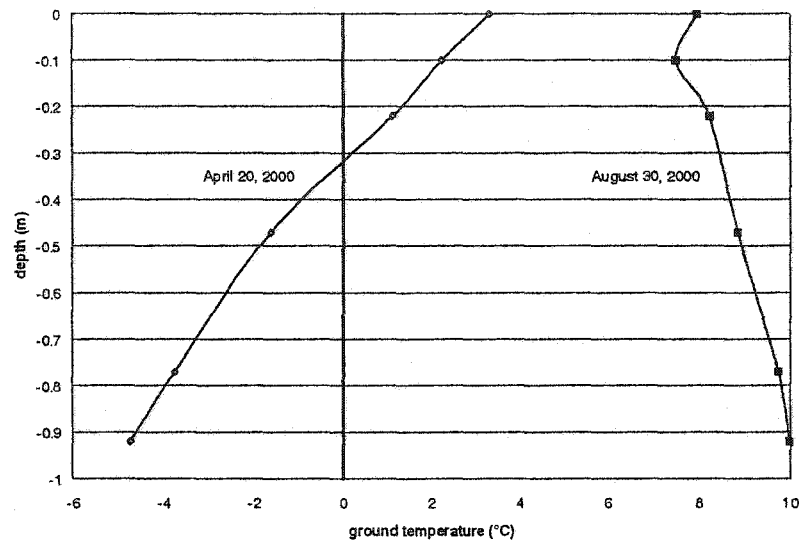


Figure 16: Ground temperatures adjacent to plot 6 in April and August 2000.

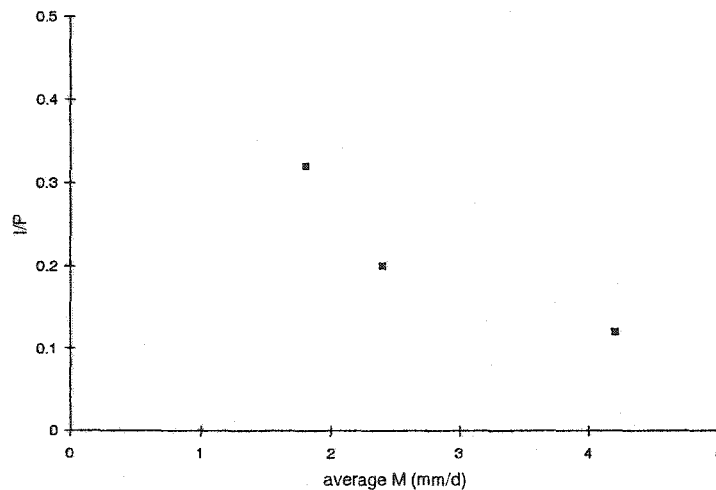


Figure 17: Infiltration – melt ratios versus average daily melt rates at three bedrock runoff plots

5.1.6 Runoff

Evaporation can affect runoff magnitude in two ways. Higher evaporative rates reduce water available for runoff (i.e., the storms of 9 July 1999 and 25 August 1999; Table 7). As well, higher total evaporation associated with longer events can reduce runoff (i.e., the storms of 15 August 1999 and 22 August 1999; Table 7). In the instance of 22 August 1999, the reduction in runoff was negligible (1%) for Plot 7 but for Plots 5 and 6, runoff was halved.

Table 7: Characteristics of selected events showing rainfall (P), plot evaporation (E) and runoff ratio (R_e/P)

Event	P (mm)	Peak intensity (mm/hr)	Duration (days)	Mean E (mm/day)	Plot R_e/P			
					4	5	6	7
9 July 1999	13.4	4.3	3	2.2	0.02	0.04	----	0.23
15 Aug. 1999	4.1	1.3	3	1.0	0	0.02	0.29	0.52
22 Aug. 1999	4.2	0.6	1	0.9	0	0.06	0.63	0.53
25 Aug. 1999	18.2	0.6	4	0.7	0.05	0.1	0.57	0.68

Figure 15 and Table 6 show that increased rainfall intensity has little effect on runoff magnitude. Surface storage was zero in Plot 5 prior to both the 24 June 2000 and 14 July 2000 storms so that an equal amount of water was taken up by storage. High rainfall intensity allowed storage capacity to be met more quickly, which generated runoff quickly, but the magnitude of runoff was controlled by the available storage.

Soil patches often have the most available storage on exposed bedrock slopes. An interpretation of Figure 18 shows that the presence of the available

storage in soil on a bedrock slope significantly reduces runoff. The average runoff ratio for the exposed bedrock plots (6 and 7) was 52% while the average runoff ratio from the two plots with soil (4 and 5) was 8%. The higher minimum threshold required to generate runoff from Plot 4 (Figure 18), where the soil patch was at the bottom of the plot, shows that the distribution of available storage in bedrock plots influences runoff generation. Allan and Roulet (1994) note that at the small basin scale, the soil covered zones downslope of exposed bedrock can delay, reduce or even nullify runoff from some events. This applies also at the small plot scale.

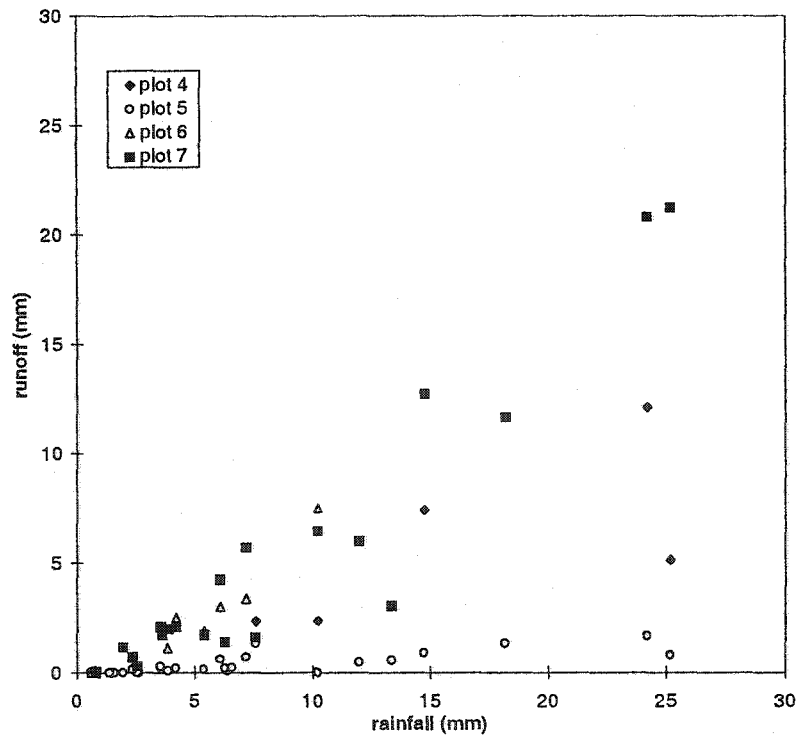


Figure 18: Individual rainfall and runoff measurements for each plot for the period of study

5.2 Seasonal water balance

Daily water budget terms for the four study plots are given in eq. 13:

$$\Delta S = P + M - E - R - I \quad (13)$$

Table 8 shows the differences in the water balance between plots. High available storage in the soil-covered plots retained water longer to encourage infiltration at the expense of runoff. Summer rainfall totals were larger in 2000, permitting higher evaporation than in 1999, but the evaporation ratios for the two summers remained similar. Averaged over the two years, runoff ratios were 52% for Plot 6 and 7 and 8% for Plots 4 and 5. The ratio for the bare plots is comparable to other studies, but the result from the soil covered plots is substantially lower (Allan and Roulet, 1994; Thorne et al., 1999).

Table 8: Water balance totals and ratios. The 1999 summer measurements from Plot 6 began on July 13 and from Plot 7 on July 8.

Summer 1999 (May 19 - September 9)								
Plot	<i>P</i> (mm)	<i>E</i> (mm)	<i>R_s</i> (mm)	<i>I</i> (mm)	ΔS (mm)	<i>E/P</i>	<i>R_s/P</i>	<i>I/P</i>
4	84	36	2.2	88	-42	0.29	0.02	0.69
5	84	33	4.1	54	-7	0.36	0.05	0.59
6 ¹	55	17	26	12	0	0.31	0.47	0.22
7 ²	69	20	34	16	1	0.29	0.48	0.23
Summer 2000 (May 9 - September 26)								
4	142	54	34	82	-28	0.32	0.20	0.48
5	142	71	8	72	-9	0.47	0.05	0.48
6	n/a							
7	142	45	85	12	0	0.32	0.60	0.08
Snowmelt 2000 (March 30 - May 2)								
Plot	<i>M</i> (mm)	<i>E</i> (mm)	<i>R_s</i> (mm)	<i>I</i> (mm)	ΔS (mm)	<i>E/M</i>	<i>R_s/M</i>	<i>I/M</i>
4	143	14	130	17	-15	0.10	0.91	0.12
5	73	10	37	15	10	0.14	0.50	0.20
6	n/a							
7	55	13	24	18	0	0.24	0.44	0.32

¹1999 summer measurements began July 8

²1999 summer measurements began July 13

The soil-covered plots were at storage capacity at the beginning of the study. By 9 September 1999 there was a loss of 42 and 7 mm in the soil covered plots as much of this water had been removed. Rainfall in early October 1999 filled the storage in Plot 4 to capacity (S. Kokelj, personal communication). This storage was depleted by 15 mm during the 2000 melt period and a further drop of 28 mm occurred during the summer. Although Plot 5 did not reach storage capacity in October 1999 low snowmelt runoff allowed storage to increase to capacity at the beginning of the 2000 summer season. Higher losses than precipitation inputs during the summer of 2000 resulted in a net loss of 9 mm.

During the snowmelt period (Table 8) a large amount of water was released within five weeks to produce considerably more runoff from the plots than during the summer. Plots 4 and 5 experienced a large increase in the runoff ratio over summer values as storage requirements were easily met by the large meltwater release. The runoff ratio of Plot 7 remained similar to its summer values as the small storage demands on the bare rock are met just as easily in the summer as during snowmelt. Plot infiltration and ratios decreased in Plots 4 and 5 because snowmelt rates were higher than most rainfall intensities and exceeded infiltration rates of smaller fractures.

5.3 Rainfall-runoff curves

The field results permit the conceptualization of the runoff generation process from exposed bedrock surfaces. The pattern of measurements expressed in Figure 18 suggests that there may be a family of rainfall-runoff curves for bedrock surfaces. Bedrock in the Canadian Shield is often assumed to be impervious and have no storage capacity so that it can generate runoff ratios near 1.0. This study suggests departures from this simplification and the runoff ratio can be reduced by several physiographic and climatic factors. To obtain the 1.0 runoff ratio envelope curve there must be a sufficient amount of rain or snowmelt over a short duration so as to restrict infiltration and evaporation losses and available storage must be zero. Regarding physiographic influences, infiltration increases and runoff decreases with mean plot fracture width. The influence of higher available storage on runoff reduction is reflected in the significant difference in runoff ratios between soil covered and bare plots. The lower this available storage in the plot, the further runoff can be reduced (Figure 19a). In terms of climatic influences, rainfall or snowmelt intensity is positively related and duration is negatively related to the runoff ratio. Increasing evaporative demand decreases runoff (Figure 19b).

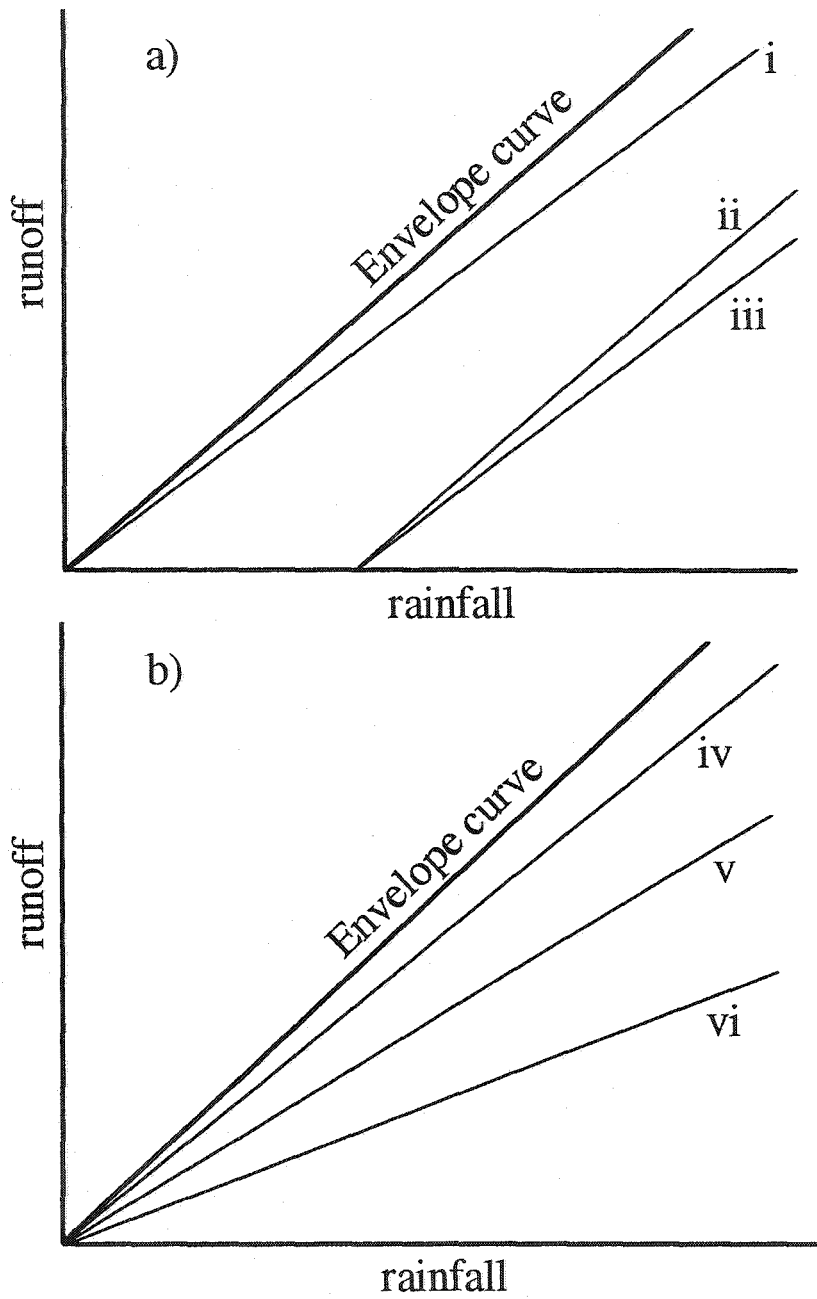


Figure 19: Conceptual rainfall runoff curves illustrating the effects of a) physiographic and b) climatic factors on runoff at the bedrock plot scale. The factors are i) increasing fracture width at the bedrock plot scale, ii) increasing storage capacity, iii) storage capacity further downslope, iv) decreasing precipitation intensity, v) increasing event duration and vi) increasing evaporative demand.

CHAPTER 6

HYDROLOGICAL PROCESSES IN A SOIL FILLED VALLEY

6.1 Hydrological Processes

The following section described hydrological processes observed in the Pocket Lake soil filled valley from 15 March 2000 to 16 May 2001.

6.1.1 Ground frost

The soil-filled valley has only seasonal frost. Ground thaw proceeded evenly during the spring and early summer of 2000, with rates that varied within the accuracy of the frost probe measurements. Thaw rates between 29 March and 1 June 2000 averaged 5 mm/d and increased to 15 mm/d after 1 June. The frozen layer disappeared between mid and late June. Surface soil temperature reached a maximum in June and July, but the entire column was the warmest when it became isothermal at the end of August. The soil was frozen to approximately 1 m depth by the spring of 2001. Periodic measurements indicated that ground thaw was negligible during the snowmelt period.

6.1.2 Snowmelt

A snow survey on 1 April 2001 measured 160 mm of snow water equivalent in the valley. Ablation rates between 2 April and 19 April 2001 averaged 2.8 mm/d. Latent heat flux estimated from tower measurements suggested that an average of 0.6 mm/d of the ablation during this period was evaporation and sublimation. Meltwater produced in these two weeks was refrozen within the snowpack as a cold snap ensued until 23 April. After 24 April above-freezing air temperatures ripened the entire snow cover and snowmelt increased to a peak of 16.7 mm on 5 May 2001. The rate of evaporation and sublimation increased to an average of 1.9 mm/d after 23 April. The entire snowpack in the valley was gone by 10 May. Total valley snowmelt equaled 112 mm while the remainder, 47 mm, evaporated or sublimated.

6.1.3 Rainfall

Rainfall, assumed to be uniform over the entire basin, in the summer of 2000 totaled 155 mm (Figure 20), almost half of which fell between 14 August and 29 August. Much of the remaining amount came from three thunderstorms on 20 and 23 June and 14 July. While May, July and September were drier than normal, wet conditions dominated June and August. With an average May to September rainfall of 141 mm, Yellowknife is drier than most other Canadian Shield locales where hydrological studies were undertaken (e.g., 321 mm at Thompson, 360 mm at the Experimental Lakes Area, 358 mm at Schefferville and 444 mm at Muskoka)

(Metcalf and Buttle, 2001; Wright, 1979; Thorne et al., 1994; McDonnell and Taylor, 1987).

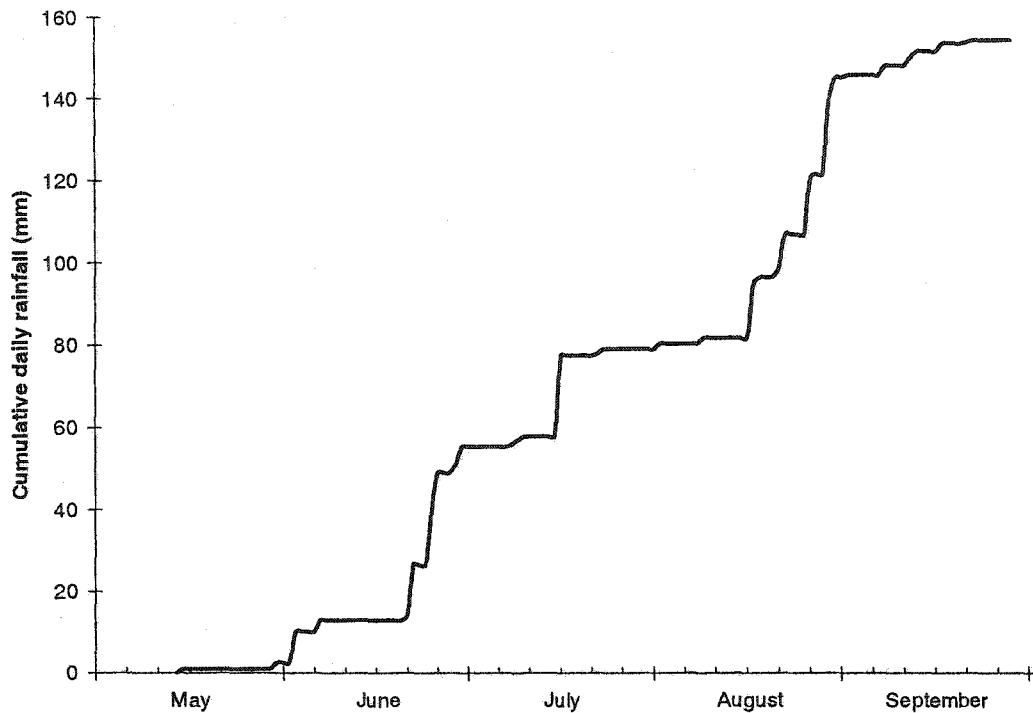


Figure 20: Cumulative rainfall measured at Pocket Lake from 10 May to 25 September 2000.

6.1.4 Infiltration

Double-ring infiltrometer measurements yielded infiltration rates of about 1 m/d regardless of whether the soil was frozen or otherwise. This is attributed to the frozen but unsaturated conditions of the porous soils prior to spring melt. Such non-limiting infiltration capacities for frozen soil (Gray et al., 2001) allowed snowmelt and lateral inflow to percolate through the frozen layer. Shallow soil moisture measurements showed that despite the ability of the soil to accept

infiltration, a large fraction of rainfall (~ 0.6) was intercepted by the ground vegetation mat of lichen and moss because of its dryness during much of the summer, findings similar to those of Bello and Arama (1989). A lack of soil moisture response after small (< 12 mm) rainfall events at 0.3 m depth implies that this intercepted water evapotranspired.

6.1.5 Inflow from exposed bedrock upland

Summer inflow from the bedrock upland was intermittent (Figure 21). All inflow entered the valley along the soil-bedrock interface, in agreement with Peters et al.'s (1995) observation near Muskoka that most lateral inflow from upslope exposed bedrock enters Canadian Shield soil zones along the bedrock surface. In the spring, inflow also traveled along the bedrock surface as the frozen soil did not have much ice to seal its pores. Spring inflow at the contact plot began on 28 April 2001. A lag time between peak bedrock upland snowmelt on 18 April and peak lateral inflow to the valley on 3 May was mostly due to two periods of sub-freezing temperatures during which the meltwater was refrozen in the snow or in shallow depressions on the bedrock surface.

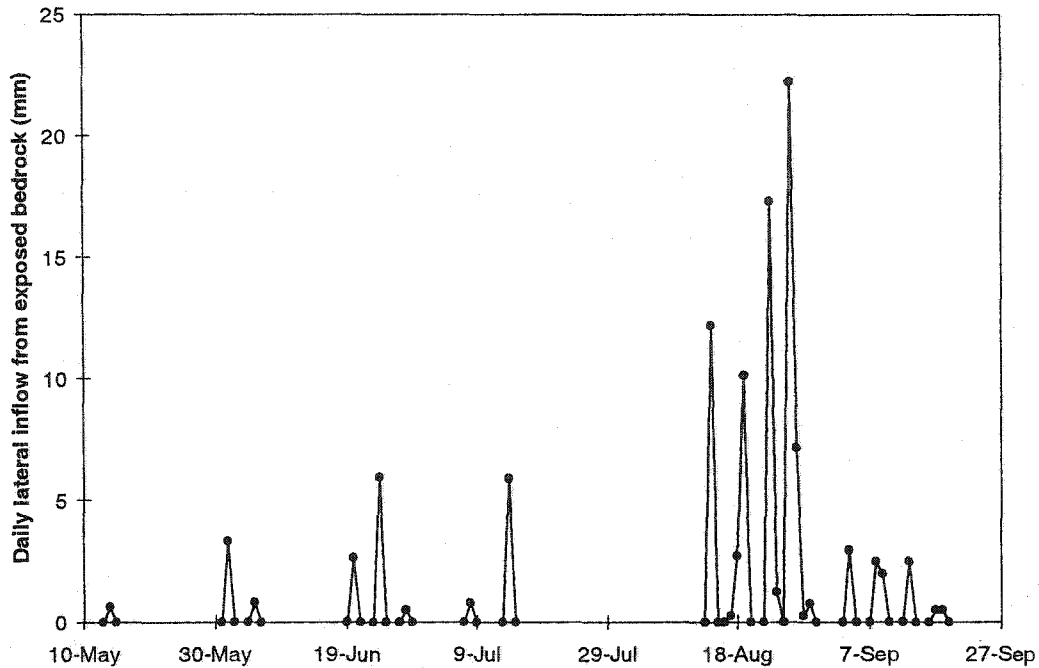


Figure 21: Daily lateral inflow from exposed bedrock to the soil filled valley.

6.1.6 Evapotranspiration

Between May and July 2000, evapotranspiration from the soil-filled valley averaged 1.8 mm/d. Evapotranspiration exceeded rainfall in May, July and September and almost equaled the June precipitation. August was the only month when rainfall exceeded evapotranspiration, as cool and wet conditions reduced the evapotranspiration rate to 0.8 mm/d. The similarity in calculated evapotranspiration and change in storage during the dry period between 6 June and 17 June 2001 shows that, in the absence of rainfall input, evapotranspiration was sustained by moisture storage in the soil (Figure 22). This is in agreement with observations from the Skeeter Lake site described in chapter 4.

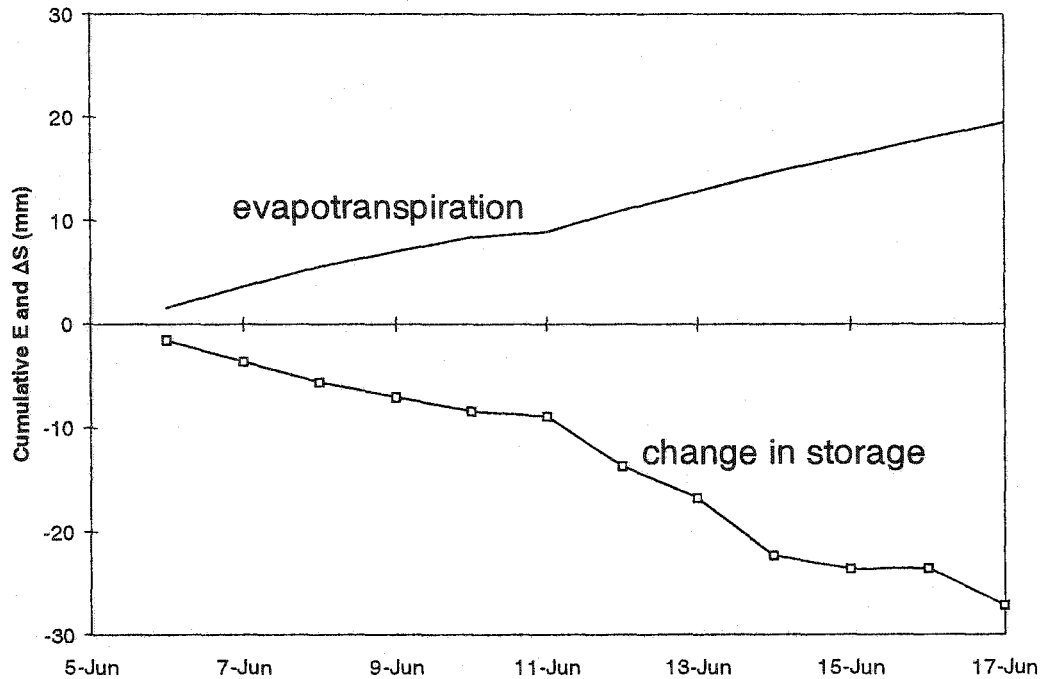


Figure 22: Cumulative daily evapotranspiration and change in storage during a dry period in the middle of the 2000 growing season.

6.1.7 Storage

Soil moisture in the unsaturated zone at the valley edge responded more readily to rainfall events than at the center (Figure 23). Valley edge soil moisture always increased more than observed rainfall because it was augmented by lateral inflow. In contrast, soil moisture at 0.05 m at the valley centre averaged only 60% of rainfall during events. At 0.3 m depth in the centre of the valley, the soil moisture content increased only with the largest rainfall events (>12 mm).

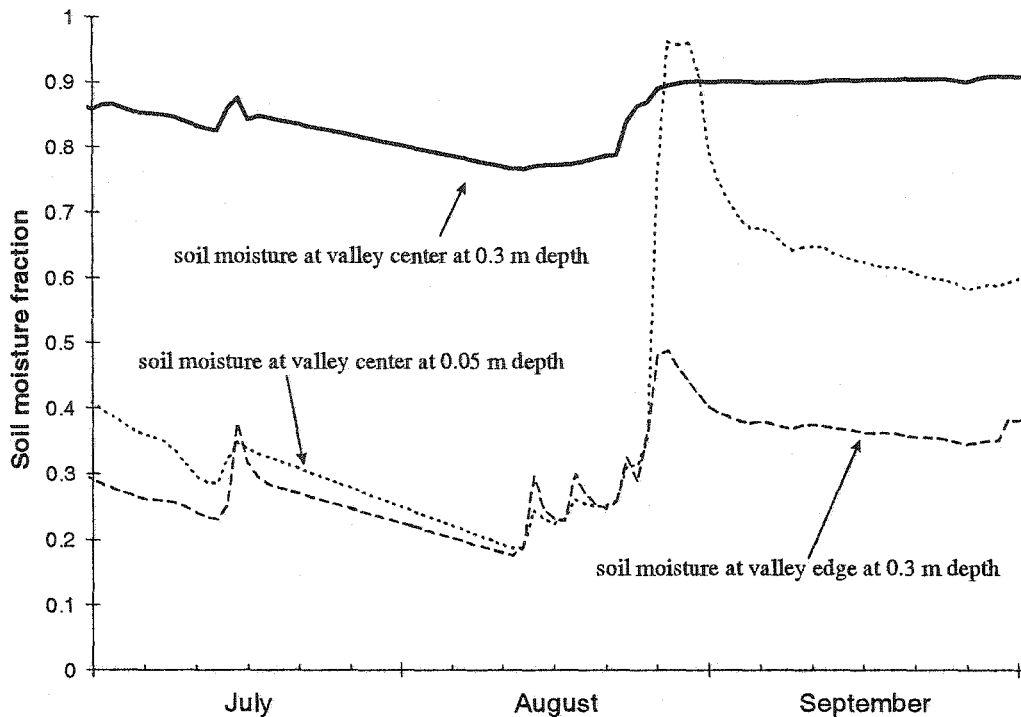


Figure 23: Daily soil moisture measurements at different locations and depths in the soil filled valley, summer 2000.

As the summer of 2000 progressed, evapotranspiration loss exceeded rainfall and lateral inflow, leading to a depletion of soil moisture storage. During dry conditions the water table was uniform across the valley (Figure 24). Large rainfall inputs generated large lateral inflow from the bedrock upland and caused distinct spatial differences in valley water table response. The water table rose higher and more rapidly at the sides of the valley because lateral inflow was larger and quicker than rainfall percolation (Figure 25). Large lateral inflows also caused uneven rises in the water table along the valley. During a late August 2000 event higher lateral inflow inputs close to transect H raised the water table at transect H an average of 0.3 m but only 0.1 m at transect G.

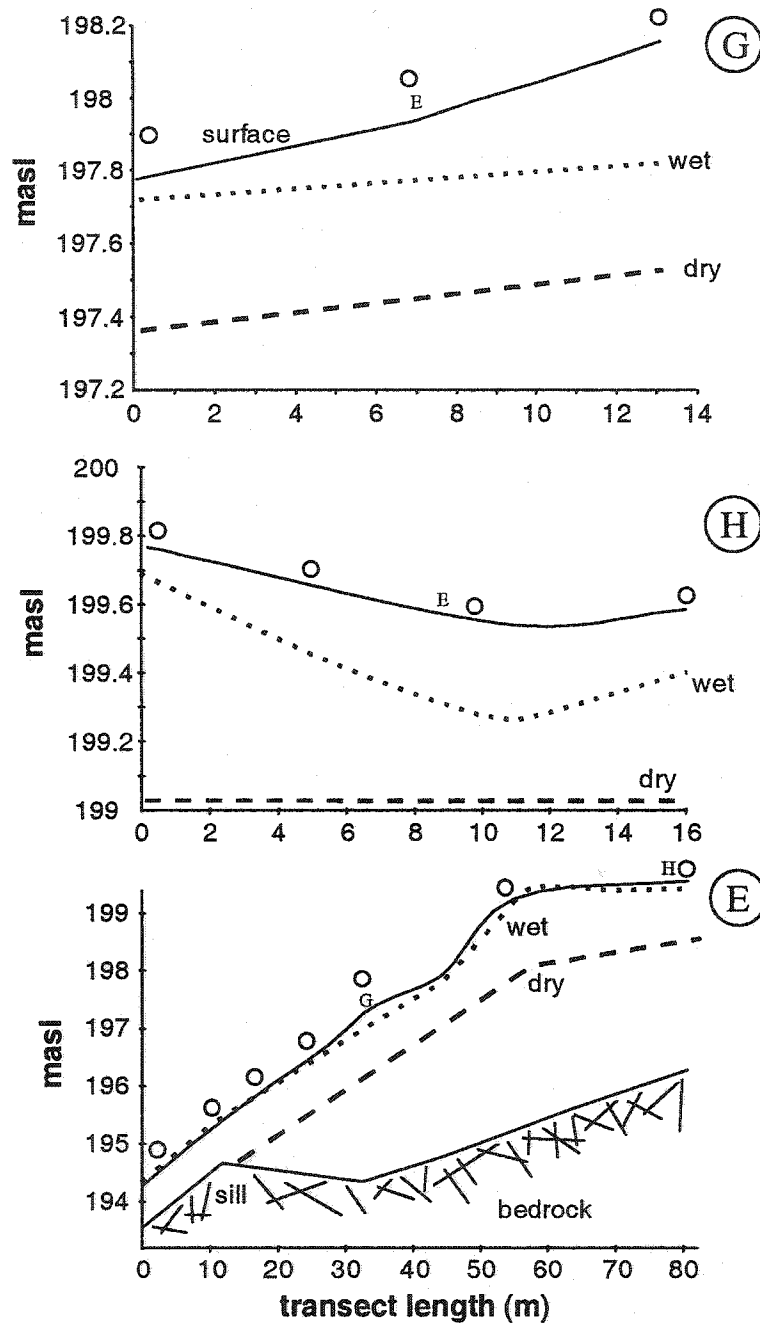


Figure 24: The water table across and along the soil filled valley during wet (27 August 2000) and dry (16 August 2000) conditions. The locations of other transects are referenced on each cross section. Information on transect H only covers the western 16 m of its length. The white circles denote locations of piezometers or wells. Refer to Figure 1 for locations of transects.

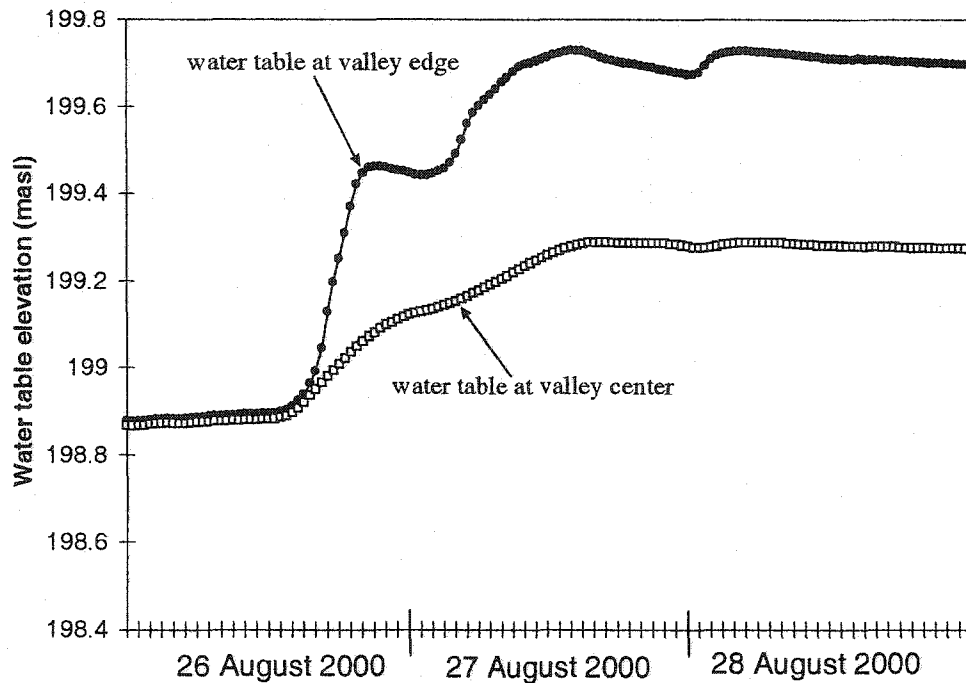


Figure 25: Half hourly measurements of soil moisture storage at the soil edge and the water table at transect H.

After 29 August, the water table declined, first at the sides, then in the middle. Throughout the winter of 2000-01, groundwater probably drained through the fractures of the bedrock underneath the soil-filled valley. Immediately before snowmelt (end of March), the water table profile across the valley was of uniform elevation and appeared similar to the dry summer condition. The first rise of the water table (0.6 m) occurred on 18 April in the middle of the valley, indicating that the water source was from snowmelt in the valley and the meltwater was able to infiltrate the frozen soil. The water table at the sides of the valley did not rise until 28 April when lateral flow began in earnest. Before 28 April, 70% of the input (snowmelt, rainfall and lateral inflow) entered valley storage and the

remainder evaporated or sublimated. The water table reached the topographic surface on April 29 and remained there until the end of the study period.

6.1.8 Subsurface runoff

Pumping tests and direct measurement of flow at the trenches indicate a hydraulic conductivity of approximately 1 m/d for the soil, whether frozen or thawed. Piezometric measurements across transects G and H showed that water from the bedrock upland consistently drained towards the center of the valley and then down the valley. The presence of a bedrock sill in the lower valley (Figure 24) restricted subsurface runoff for much of the summer, a situation similar to that reported by Allan and Roulet (1994) at another Canadian Shield watershed in Ontario. Subsurface runoff was first observed at the lower trench when the water table rose above the sill on 26 August 2000 in response to 40 mm of rainfall, and continued until 25 September when the water table dropped below the elevation of the sill.

6.1.9 Surface runoff

Surface runoff in the summer of 2000 began on 27 August (Figure 26) after 58 mm and 66 mm of rainfall and lateral inflow, respectively, which began and peaked on 14 August and 27 August, respectively. Saturation overland flow was initiated at 0800 27 August as the water table rose above ground at the western valley edge at transect H. Surface runoff followed the valley thalweg. A

rapid rise in near surface soil moisture near transect G indicated that this flow reached that position between 0900 and 0930 27 August. The piezometric heads along and adjacent to the flow path showed that part of the surface runoff infiltrated the soil as it travelled downstream, suggesting the influent nature of this intermittent stream. The cessation of rainfall and a reduction of inflow from the bedrock upland caused the water table to recede on 29 August, but the loss to stream influence continued. The streamflow segment retreated upstream until surface flow ceased altogether. The overall effect of the surface flow process is therefore the formation of an intermittent stream that expanded from and contracted to the source of saturation overland flow near transect H. The eastern arm of the valley did not yield surface runoff during this storm because lateral inputs from exposed bedrock were not large enough to overcome local saturation thresholds.

Runoff in the spring of 2001 followed two phases. Despite 93 mm of precipitation, snowmelt and inflow, only 8 mm of surface runoff was generated by 1 May. The remainder of these inputs percolated the dry frozen soil and replenished storage. Most of the spring runoff (396 mm) was produced after the cold spells in early May and was fed by 377 mm of inflow from the bedrock upland (Figure 27). Valley margins close to the bedrock inflows were the only sections of the valley that produced surface runoff. Initial saturation overland flow from these sites then followed water tracks along the valley but it was subject to infiltration

losses, and there was not enough sustained flow to reach the valley outlet. Both the eastern and southern portions of the valley eventually contributed to outflow, but as inflows from the upland decreased, these intermittent streams receded back to the up-valley areas.

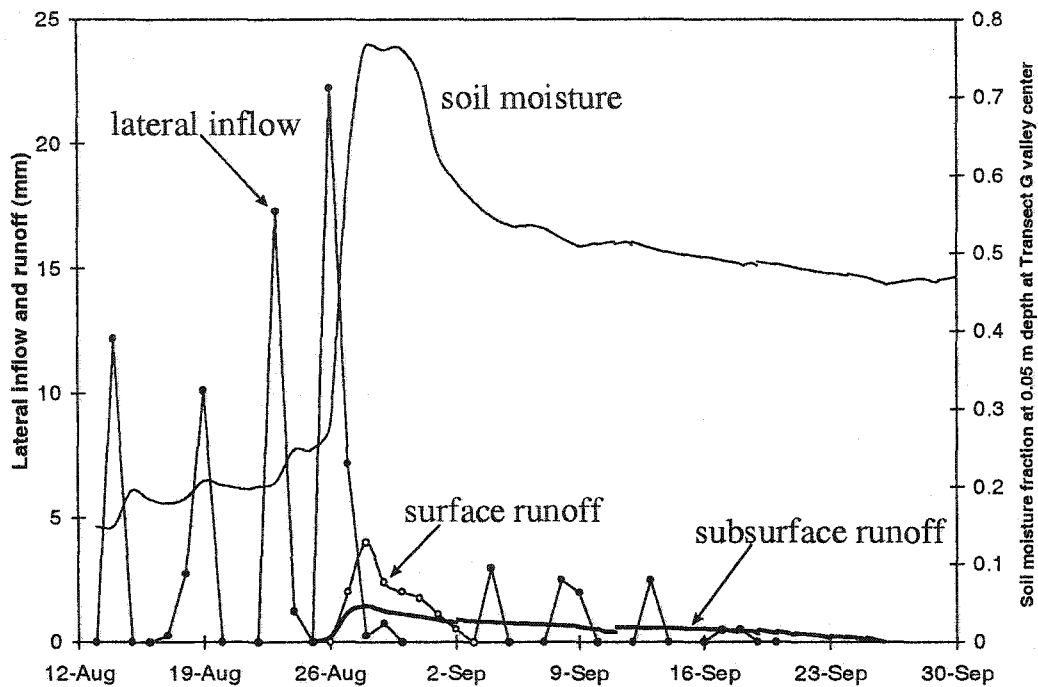


Figure 26: Inflow from exposed bedrock, the response of soil moisture at the center of the soil filled valley at Transect G and runoff during the 23 August rainfall event.

The concordance of daily flow rates between the surface inflows and surface runoff may imply that the soil-filled valley served mainly as a conduit for runoff without significantly altering the flows through soil storage. However, as the frozen ground had little effect on infiltration and soil hydraulic conductivity, inflow from the upland could enter the saturated soil-filled valley after 29 April, to

mix with the water already residing in the valley soils. An analysis of water collected during previous spring melt events at Pocket Lake [from a study by and using analytical methods described in Gibson et al. (1998)] revealed that surface runoff was a chemical mixture of snowmelt event water and pre-event groundwater. Table 9 shows that ground ice and groundwater from the soil-filled valley were relatively enriched with oxygen-18 (^{18}O) and deuterium (2H) and had significantly higher electrical conductivity (C) when compared to snow. Surface runoff had chemical values between those of the snow and ground ice and groundwater, and this suggests that at least a part of the valley contributed its pre-event water to the spring runoff.

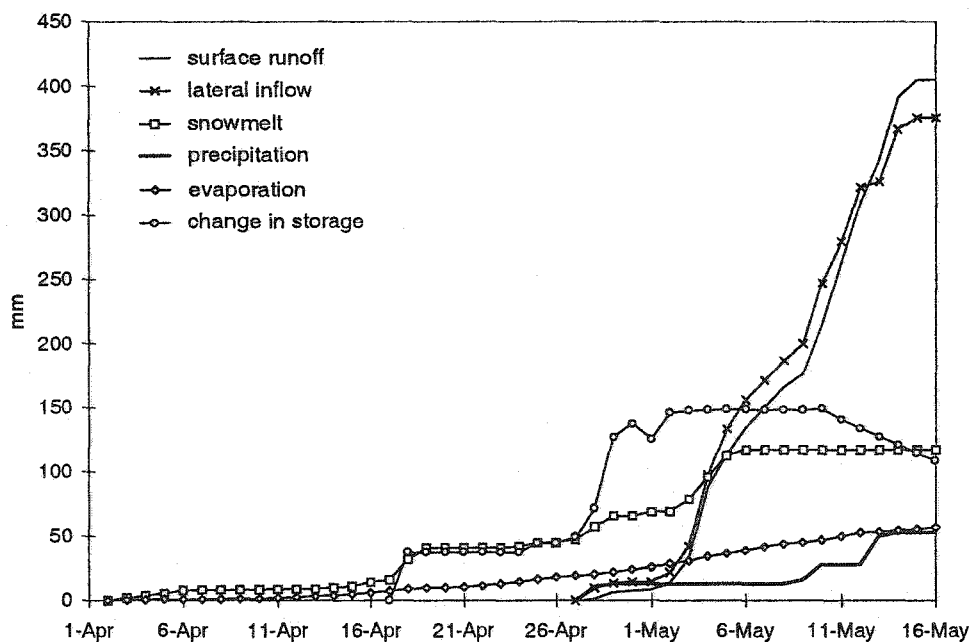


Figure 27: Cumulative water budget in a soil filled valley in the spring of 2001.

Table 9: Average values of selected chemical characteristics of water from the Pocket basin site from 1995 to 2000. Stable isotope values are presented in standard δ notation as deviations per mille from Vienna-SMOW (standard mean ocean water) such that $\delta_{\text{sample}} = 1000\{(R_{\text{sample}}/R_{\text{SMOW}})-1\}$ where R is $^2\text{H}/^1\text{H}$ and $^{18}\text{O}/^{16}\text{O}$.

	^{18}O	^2H	C (mS/cm)
Snow	-28±2.8	-215±16	7±3.5
Snowmelt runoff	-24±1.8	-191±15	106±5
Ground ice / groundwater	-20±1.6	-162±13	330±17

The sources that dictated the timing and volume of runoff differed even though similar runoff generation processes occurred in the spring and summer events. In the spring, over half the valley snowpack was directed to soil moisture storage and evaporation, so the timing and magnitude of inflow from the bedrock upland controlled the outflow hydrograph of the soil-filled valley. In contrast, the lateral sources and not the vertical inputs replenished the summer storage deficit. This resulted in a significant delay between lateral inflow and valley outflow, a phenomenon not exhibited during the spring melt.

6.2 Hydrological linkages between upland and valley

The hydrological importance of the bedrock uplands to the soil-filled valley is demonstrated by the water balance during snowmelt and the summer periods. Summer values show that upland lateral inflows constitute a significant portion of total inputs to the valley and are important for maintaining evapotranspiration and storage (Figure 28). Without lateral inflows, there would not have been excess water to produce valley runoff in August 2000. Spring melt values show instances when valley runoff is also directly influenced by lateral inflows.

Table 10: Water budgets of the growing season in 2000 and spring melt in 2001. All units are in mm. N/A denotes not available because of flooding in the trenches.

Month	R_s	R_g	M	P	ET	I_b	ΔS	ΔS (calc.)
May 2000	0	0		2.5	29	1	-11	-26
June 2000	0	0		52	50	14	19	16
July 2000	0	0		25	40	7	-52	-8
Aug. 2000	12	6.2		66	26	74	163	96
Sept. 2000	1.6	14		8.6	19	11	-45	-15
2000 summer	13.6	20.2		154	164	106	74	64
2001 spring	404	N/A	117	53	50	390	108	106

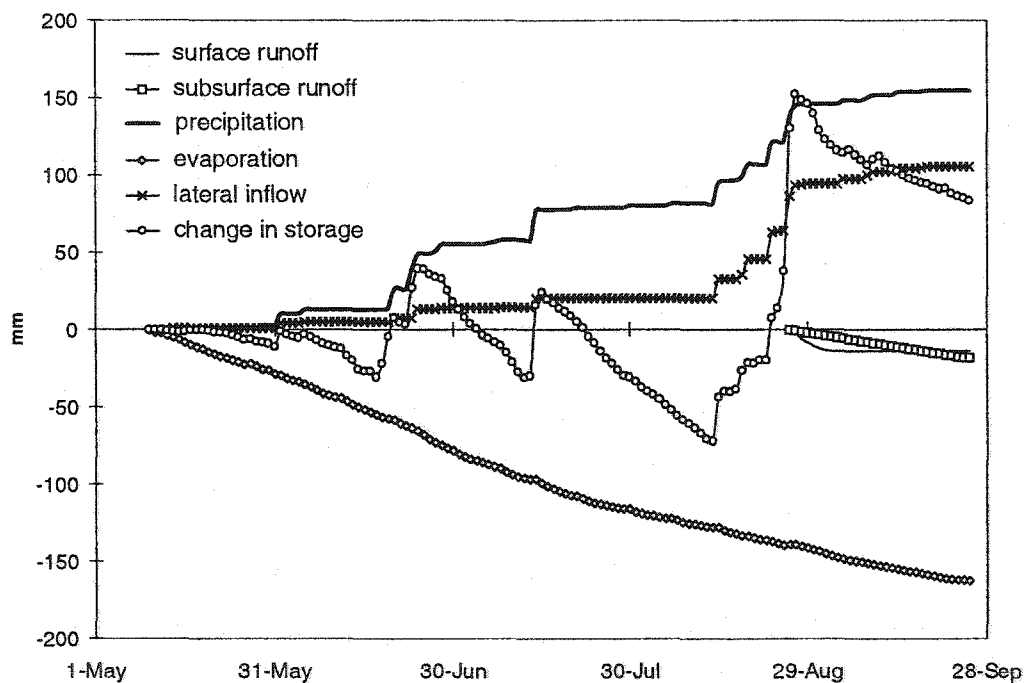


Figure 28: Cumulative water budget in a soil filled valley in the summer of 2000.

6.3 The fill and spill flow mechanism

Buttle et al. (2000) state that saturation overland flow is the dominant surface runoff mechanism in Shield valleys. Saturation overland flow at the Pocket Lake valley

site is dependent on the spatially and temporally variable valley storage that needs to be satisfied before water spills to generate flow. Storage capacity in the valley is spatially variable owing to topographical diversity, soil heterogeneity and uneven thickness, and the seasonal presence of ground frost. Available storage, a function of antecedent moisture, vertical and lateral inputs, and evapotranspiration loss, is temporally dynamic and determines the minimum input required to exceed the thresholds for subsurface and surface flow generation. Variable soil depths caused by bedrock topography generally indicate that the valley edges have a shallow soil that has a lower saturation threshold than the middle of the valley. The proximity of the edge zones to the bedrock slopes increases the opportunity for large lateral inflow and greater likelihood to reach storage capacity than the other parts of the valley. As a result, saturation overland flow tends to begin in upper and edge locations in subarctic Shield soil-filled valleys. There is also a feedback between valley surface flow and valley soil recharge. Runoff from an upper valley segment may encounter a non-saturated lower segment and the water will infiltrate along the flow path until the lower valley storage is satisfied or until all surface flow is lost to seepage. In the latter case, the stream becomes intermittent. Such processes are an example of what the author terms the fill and spill flow mechanism of saturation overland flow.

The fill-and-spill flow system differs from the normal modes of flow in a humid climate where the channel flow in the valleys is permitted to leave the catchments with little significant interruption. The importance of lateral inflows and variable storage

present a system that departs greatly from typical saturation overland flow processes in humid areas such that contributing areas do not necessarily grow upslope from the stream channel. The Shield valley represents a series of storage reservoirs with the flow cascading down the valley, filling individual segments to satisfy their deficits until the thresholds are reached; then spillage resumes to continue the flow downstream (Figure 29).

The fill-and-spill flow system can also be applied to the large catchments of the Canadian Shield. For ephemerally and perennially draining wetlands, Buttle and Sami (1992) and Branfireun and Roulet (1998) noted a progression of water table rise down valley during runoff events, indicating that each segment is first filled by lateral inflows before saturation overland flow can continue downstream. During the summer in a southern Ontario swamp, Devito et al. (1996) observed that lateral surface inflows exceeded surface outflow, suggesting that some of the surface flow seeped underground to address storage demands. Of particular importance is the frequent presence of lakes in the Shield, which through their well known role in flow regulation, exaggerate the storage and release functions of the hydrologic system as has been reported by Fitzgibbon and Dume (1981) and Spence (2000).

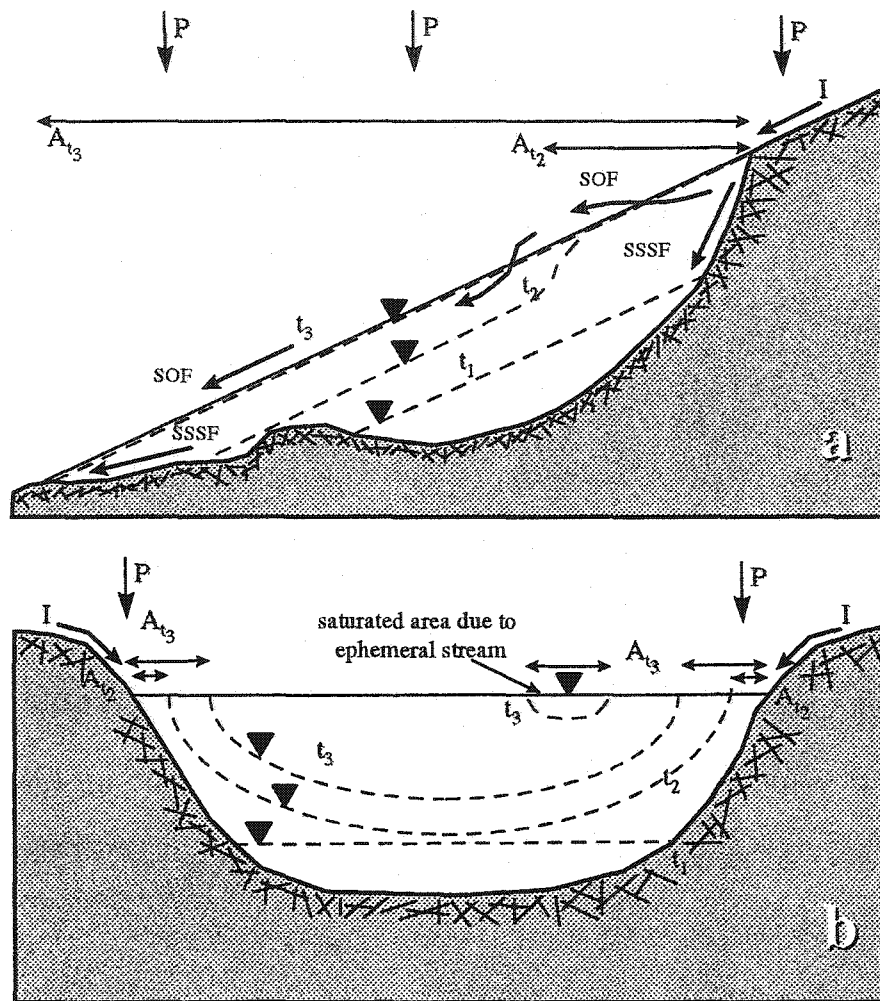


Figure 29: An illustration of conceptualized fill-and-spill runoff generation. a is a longitudinal profile of the valley and b is a cross section. P is precipitation, t is time at step 1, 2 or 3. $SSSF$ is subsurface stormflow and SOF is saturation overland flow. A is the contributing area at t_2 or t_3 .

CHAPTER 7

HYDROLOGICAL PROCESSES IN HEADWATER BASINS

This chapter examines three distinctly different but typical events from the Pocket Lake site in order to discern how hydrological processes on different land cover types interact in order to produce a basin runoff response. These events include a summer event with dry antecedent conditions and low rainfall input, a summer event with dry antecedent conditions but large rainfall input, and a spring melt event with dry antecedent conditions and high snowmelt and rainfall input. Basin responses to these events provide evidence for developing an integrated framework of runoff generation from subarctic Canadian Shield headwater basins. This framework will attempt to account for basin heterogeneity, which is a function of landscape geometry and topology. Landscape geometry outlines the spatial extent and border of each land cover unit and the variable contributing areas within it and allows relative size and shape to be discerned. Landscape topology defines the arrangement of land cover units and their contributing areas in relation to one another on the landscape. Lateral inflow and storage terms are presented as volumes (m^3) in this chapter to permit easier comparison of fluxes within the basin, between land cover types and from the basin.

7.1 Runoff events

7.1.1. Summer season with dry conditions and low rainfall

Low precipitation and high evapotranspirative demand created arid conditions with little water in storage immediately prior to 23 June 2000 (Table 11). Event rainfall totaled 28.8 mm (Figure 30), evenly distributed across the small study basin. The high relative storage demands of bedrock areas with soil patches permitted only 167 m³ of surface runoff from these areas and only allowed for a small contributing area focused in the bedrock outcrops. Nevertheless, lateral inflow from bedrock, and not direct rainfall, was the primary water source to the valley because of rainfall interception by arboreal and ground vegetation. These spatial differences in inputs to the valley resulted in a larger water table response at the valley edge than at the valley centre. Since valley storage did not overcome soil saturation thresholds, there was no runoff response from the basin during this event.

Table 11: Cumulative change in storage from May 10, 2000 until the occurrence of three events in the study basin. All units are in m³.

Cover type and location	23 June 2000	23 August 2000	2001 melt
bedrock with soil patches (plot 5)	-0.27	-0.27	-0.27
bedrock outcrop (plot 7)	0	0	0
valley edge	-250	-120	-109
valley centre	-98	-2930	-1570

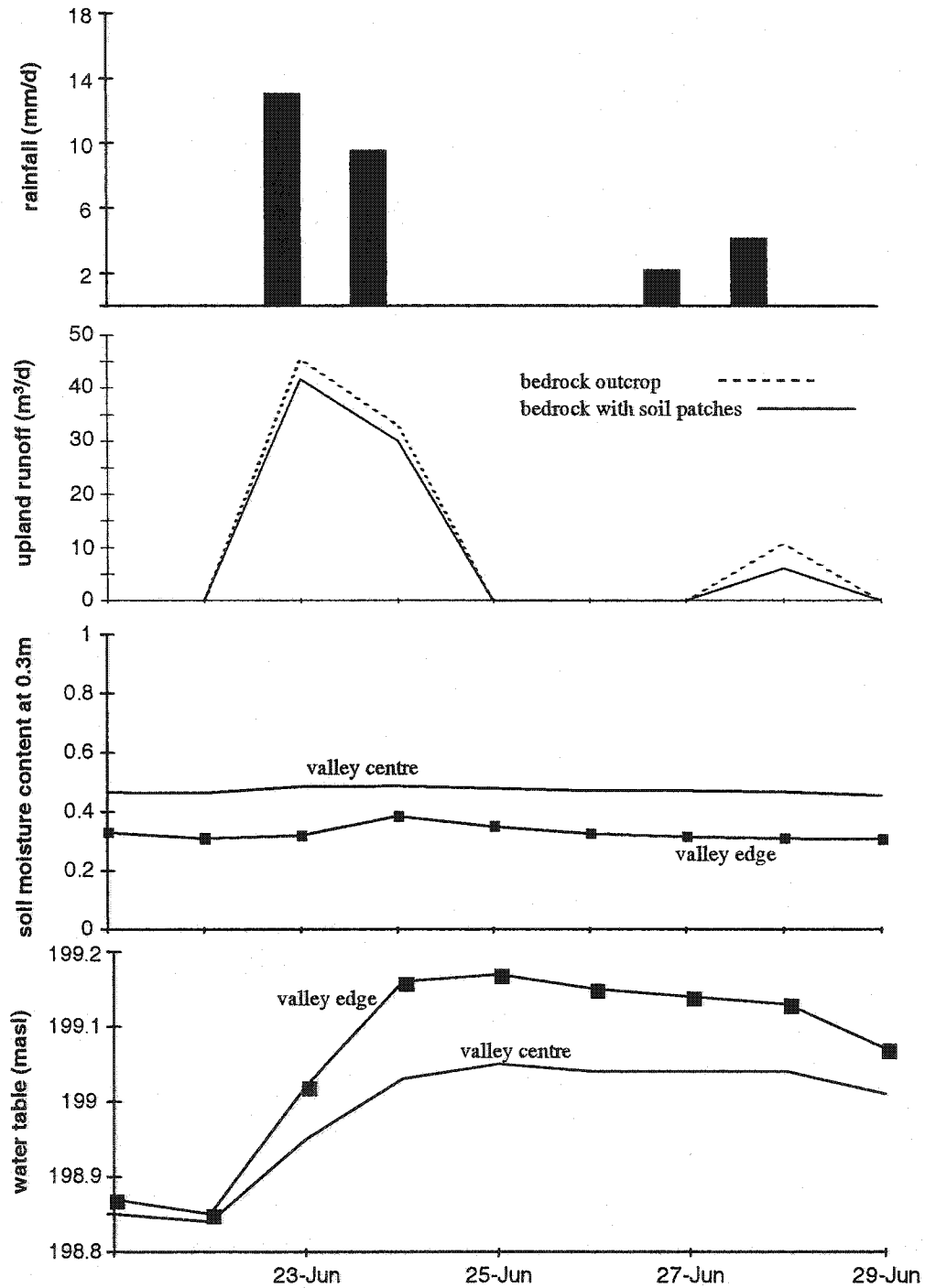


Figure 30: Characteristics of the 23 June 2000 rainfall-runoff event at the Pocket Lake site.

7.1.2 Summer season with dry conditions and high rainfall

On 22 August 2000, antecedent moisture storage status of the bedrock upland was similar to that of the June event but storage in the valley was further depleted by evapotranspiration (Table 11). The basin received 48 mm of rain between 23 August and 18 September (Figure 31), which readily overcame the storage demands of the bedrock slopes with soil patches. The bedrock upland contributing area, runoff volume and runoff ratio grew disproportionately with the increase in rainfall because bedrock slopes with soil patches occupy most of the upland (Table 12 and Figure 31). Table 13 shows that soil patches extended lag times and flow recession through storage processes identified in Chapter 5. With the higher precipitation, bedrock runoff was provided to the valley for longer periods of time.

Much of the initial inputs to the valley were directed to storage. The initial water table increase was at the valley edge at transect H because most of the lateral inflows entered at the upper valley. Groundwater flow proceeded down valley to raise the lower valley water table above the bedrock sill, allowing subsurface flow to be observed at the lower trench between 26 August and 25 September. Only the valley edge water table declined after major rainfall inputs ceased. This, and similar recession coefficients of 0.98 and 0.94 from the valley

edge water table and subsurface runoff, respectively, imply that subsurface flow was maintained by storage at the valley edge.

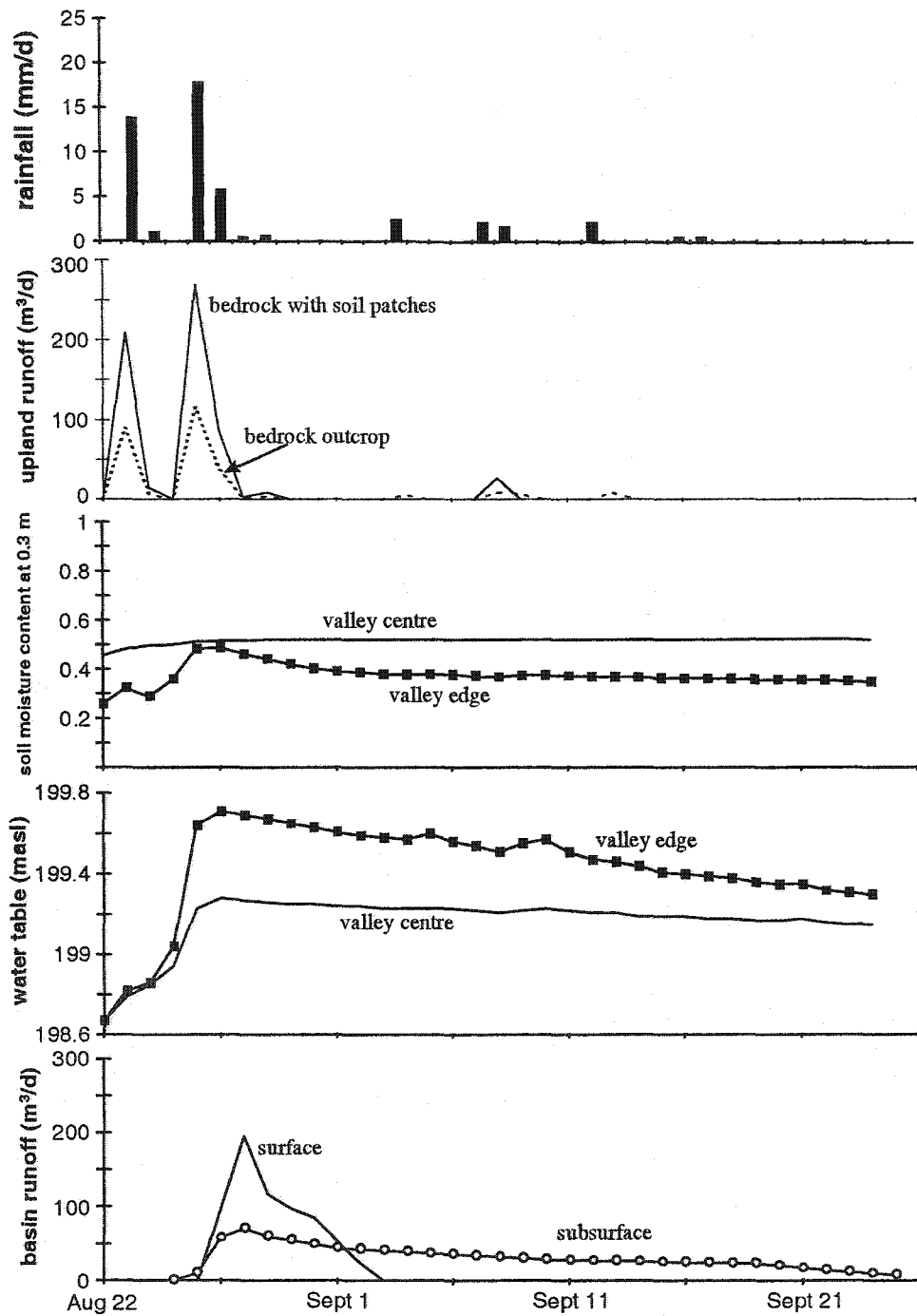


Figure 31: Characteristics of the 23 August 2000 rainfall-runoff event at the Pocket Lake site.

Table 12: Runoff ratios for the three events at different scales

	Area (m ²)	23 June 2000	23 August 2000	2001 melt		
vertical inputs		28.8 mm	47.6 mm	81 mm	103 mm	140 mm
plot 7	6.5	0.41	0.78	0.78		
plot 4	38	0.09	0.42		0.70	
basin	48,823	0	0.16			0.57

Table 13: Characteristics of several runoff events at Pocket Lake catchment. L_p is the lag time between peak rainfall and peak runoff. t^* is the recession coefficient defined by Carey and Woo (2001). f_{ca} is the fraction of the basin contributing to surface runoff.

Date	P or M (mm)	basin R/P	L_p (days)	t^* (days)	f_{ca}
22 August 1999	4.2	0 (runoff only from bedrock outcrops)	0.02	0.37	0.18
23 June 2000	29	0 (runoff expanded to bedrock with soil patches)	0.15	0.70	0.45
23 August 2000	48	0.16 (runoff across and from basin)	2	0.77	0.55
2000 melt	104	0.38 (runoff across and from basin)	5	n/a	0.69
2001 melt	140	0.57 (runoff across and from basin)	11	n/a	0.72

When storage in the valley peaked on 27 August, there had been only 20 m³ of surface runoff generated in the valley, despite 828 m³ of lateral inflow from the bedrock and 415 m³ of valley precipitation. After 28 August, much of the rain had stopped and bedrock contributions were an intermittent 75 m³. The 69 m³ of surface runoff after 27 August was fed largely by bedrock runoff temporarily stored at the sides of the upper valley, just as with subsurface runoff. Widely different inputs and storages created spatial and temporal variation in surface runoff. This was characterized early in the event by surface runoff only on the bedrock upland. Later there was a limited expansion into the upper valley and along an ephemeral stream of saturation overland flow controlled by the fill and spill runoff mechanism (Figure 32).

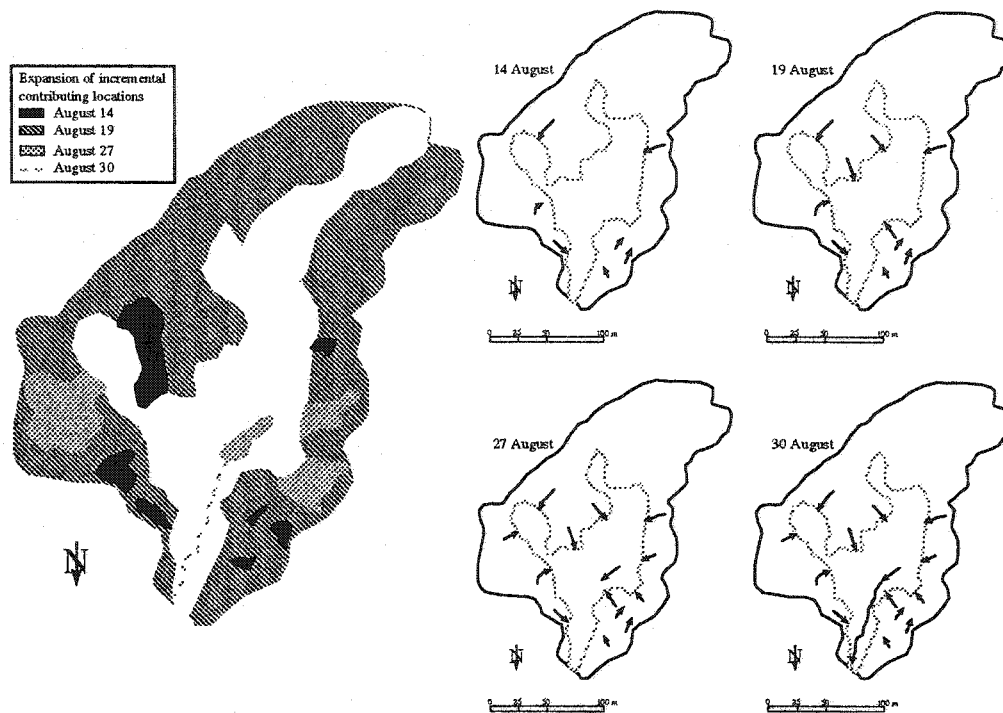


Figure 32: Contributing areas (left) and surface runoff linkages (right) during the August 2000 event. The shading represents a cumulative expansion of the contributing area.

7.1.3 Spring melt with dry conditions and high rainfall and melt

163 cm of snow accumulated over the winter of 2000/2001. There was much redistribution of snow, especially on the bedrock upland (Figure 33). Snow depth in the valley exhibited less variability because of less micro-relief and more sheltered conditions than on the bedrock ridge. The resulting snowmelt pattern was one where snow on south facing slopes and ridge tops contributed meltwater first followed by areas with average snow depth (Figure 34). The valley snowpack began to melt as early as 3 April but factors allowed the snow cover to remain continuous as late as 1 May. The valley received less radiation input because it

faces north, includes tree shadows (Giesbrecht and Woo, 2000) and the even depth of the valley snowpack prevented bare patches from appearing until 2 May.

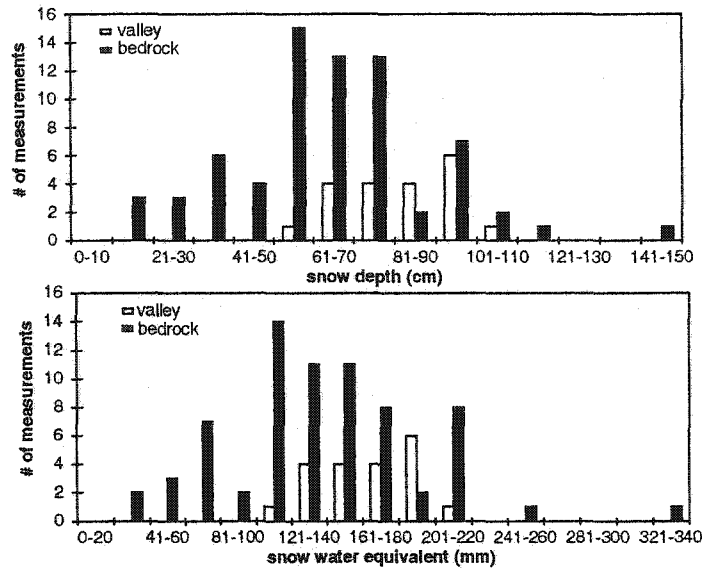


Figure 33: Frequency distributions of snow depth and snow water equivalent from the 2001 spring snow survey.

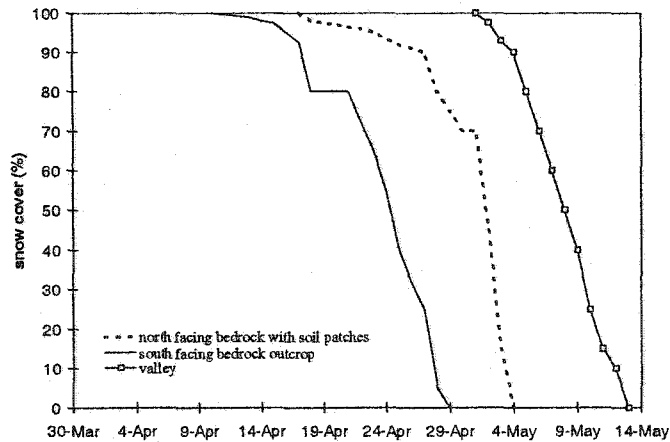


Figure 34: Snow depletion curves for three ablation lines.

Differences in available storage between the upland and valley were similar to the August 2000 event. There was no measured change in unsaturated soil moisture storage as increases were attributed to thawing of pore ice. The water

table initially rose in the valley centre (Figure 35) in response to meltwater contribution from the valley. There was no water table response at the valley edge until the bedrock runoff began in earnest on 28 April. This lateral inflow entered the soil-filled valley along the bedrock surface unimpeded by the frozen ground because of its low ice content.

As noted in Chapter 5, the spring melt runoff ratios do not increase from bare bedrock areas over those observed during summer rainfall events, but can significantly increase for bedrock areas with soil patches. A high runoff ratio and an expansion of the runoff contributing area into a large bedrock area to the south of the valley (Figure 36) tripled the peak lateral inflow to the valley from the August 2000 storm.

Surface flow in the valley began only after local meltwater and early runoff from bedrock slopes raised the storage in the valley to its saturation threshold. Before 27 April, 1,109 m³ of rainfall, meltwater and lateral inflow reached the valley but it was not until 28 April that 11 m³ of surface runoff was observed. After 4 May there was no residual snow in the valley nor runoff entering from the valley-side bedrock slopes. All the water entered from the bedrock contributing areas to the south or east where the bedrock is covered by soil patches that sustained surface flow to the valley until runoff was generated from within the valley itself (Figure 36). The basin hydrograph shows (Figure 35) that this was the

only event in the entire study that both basin components of bedrock ridge and soil filled valley were connected by surface runoff. A preliminary saturation of the soil by gradual snowmelt followed by rapid meltwater production in the uplands led to a more continuous and connected contributing area than was afforded by the rainstorm events. For the snowmelt event studied, access to a large runoff generation area (72% of the basin) produced the largest runoff response of the study period.

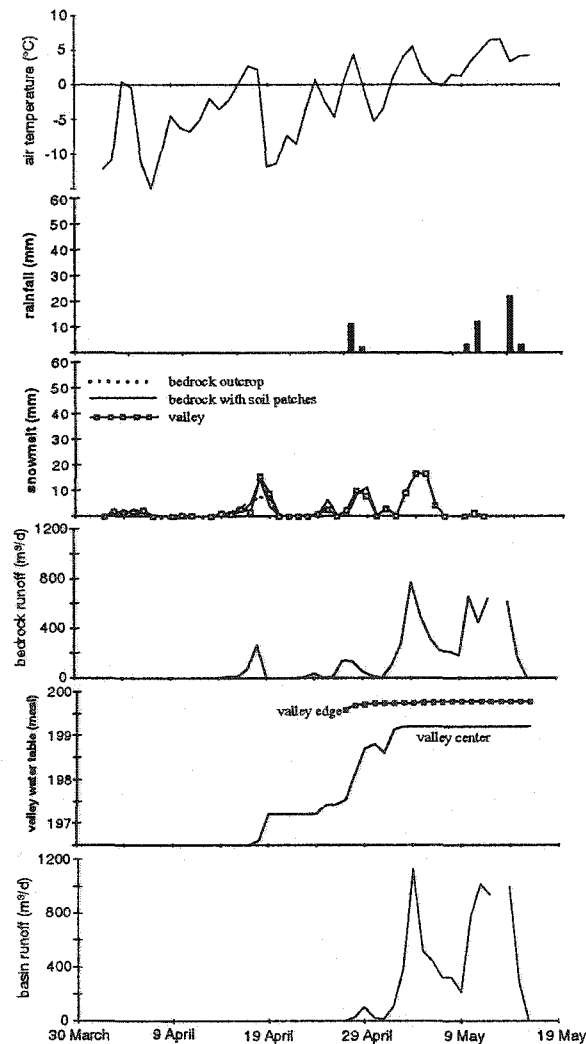


Figure 35: Characteristics of the 2001 spring melt runoff event

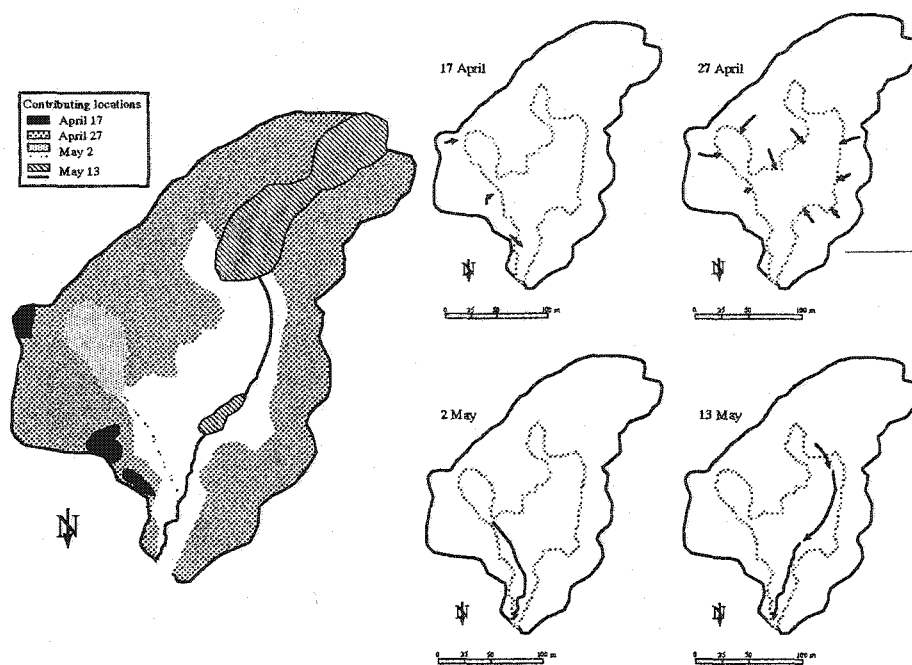


Figure 36: Contributing areas (left) and surface runoff linkages (right) during the 2001 spring melt. Unlike Figure 32, the shading represents the contributing locations only on those particular days.

7.2 Contributing areas

Basin runoff is not an additive function of runoff from each of the land cover types. This is exemplified by larger bedrock upland runoff yield than basin yield during summer (Table 14). Bedrock runoff did not directly contribute to basin runoff during the summer of 2000 because of its location. However, a large upland contributing area relative to the valley can produce sufficient runoff to meet and exceed valley storage thresholds and force runoff from the valley and basin. The first non-zero basin runoff ratio corresponded to a basin contributing area fraction of 0.45 (Figure 37). Much of this contributing area was composed of the minimum area across the upland needed to produce enough runoff to exceed valley

storage capacities. The role of each land cover type in producing basin runoff depends on the landscape geometry and topology. The high vertical inputs of snowmelt events permitted saturation thresholds in the valley to be met prior to the arrival of significant lateral inflows from the upland. These conditions lead to a more efficient coupling of runoff from both land cover types and increases in runoff volume and ratio relative to inputs. Such responses emphasize the importance of land cover unit function in addition to geometry and topology for runoff generation.

Table 14: Contributions to the basin water budget during the 2000 growing season and 2001 spring melt. All units are in m^3 .

Summer 2000	<i>P+M</i>	<i>ET</i>	<i>F</i>	<i>R</i>	ΔS	ΔS (calc.)
upland	5,882	2,163	2,087	1,684	0	-35
valley	1,686	1,783	---	199	1,127	941
basin	7,568	3,946	---	199	1,127	---
Spring 2001						
upland	5,085	569	645	4,212	-607	-341
valley	1,794	685	---	4,393	598	928
basin	6,879	1,254	---	4,393	-9	---

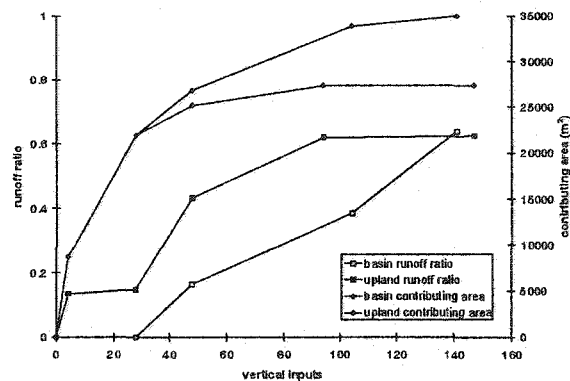


Figure 37: Variation in land cover, fraction of the basin wide contributing area and runoff ratio at the Pocket Lake catchment. The upland runoff includes that measured at the valley inflow weir sites plus that estimated using eq. 9.

7.3 Hydrological elements and the Element Threshold Concept

The highly heterogeneous landscape within Canadian Shield headwater basins exaggerates the effects of landscape geometry and topology on basin runoff response. Hydrologically homogenous land cover units within a heterogeneous headwater basin can be defined simply as those with a spatially consistent one-dimensional (vertical) water budget. For practical purposes, their extents may be estimated using topography, soil and vegetation (i.e., physiography).

An hydrologically homogenous land cover unit can serve three functions: storing, linking and contributing. Dynamic hydrological processes acting within the unit determine which function that unit plays at a given time. Inputs are predominantly directed to storage during the driest conditions. Linking functions control the delivery of runoff through elements via processes such as fill-and-spill or lake attenuation. Contributing functions provide surface runoff. Linking and contributing functions remain predominant as long as there is enough water for sub-basin and basin storage thresholds to be exceeded. On the landscape, the geometric, topologic and hydrological characteristics are all expressed as hydrological elements which are defined as hydrologically homogenous land cover units with similar lateral inputs from adjacent elements such that their functions will be similar over time.

Dunne (1978) defined the variable source area concept based on work by Hewlett and Hibbert (1967) who explained that the portion of a watershed yielding surface flow shrinks and expands as subsurface flow from upslope exceeds the capacity of the soil to transmit it, the magnitude of which is controlled by rainfall and antecedent moisture. Field studies on which the variable source area concept is based consistently show that downslope areas contribute to runoff first via saturation overland flow, and expand upwards (Dunne, 1978). This study and others (Allan and Roulet, 1994; Buttle and Sami, 1992) clearly show that on the Canadian Shield, contributing areas appear upslope and expand downwards until runoff cannot satisfy moisture deficits downslope. The variable source area concept suggests that different portions of a small basin, rather than having distinctly different reactions to rainfall, contribute to runoff by the same process, but with differing frequencies (Dunne, 1978). The heterogeneous physiography of small Canadian Shield basins leads to the occurrence of several runoff processes within the same headwater basin (Allan and Roulet, 1994). Runoff generation within each hydrological element on the Canadian Shield may exhibit properties of the variable source area concept (e.g., yielding portion shrinks and expands seasonally and throughout a storm depending on rainfall and antecedent moisture). However, the physical manifestation of runoff at the larger scale of the heterogeneous headwater basin is significantly different enough that another process must be present. The element threshold concept explains how runoff

cascades through headwater basins and how contributions from a number of hydrological elements integrate to produce runoff from a heterogeneous landscape.

The Skeeter Lake upland may be subdivided into five hydrological elements (Figure 38). Both bedrock outcrops can be considered one element as they have similar water budgets and their hydrological functions are not dependent upon adjacent upslope or downslope areas. The two forested areas and two wetlands require four hydrological elements because different inputs from adjacent upslope elements affect the function for a similar volume of precipitation. The difference in the relative sizes of the two wetlands and differences in contributing functions of their upslope elements requires them to be defined as separate elements.

One particular elemental characteristic, the saturation threshold or storage capacity, varies significantly among elements because of physiography and affects the frequency and magnitude of contributing functions. Antecedent conditions influence available storage, which also promotes storage dissimilarities over space and time. The result is a very disjointed contributing area pattern. This is the key difference between the variable source area and element threshold runoff concepts (Table 15). The prevalence of contributing functions in downslope elements may depend on the functional state of upslope elements because relative geometrical and physiographical differences control the size of upslope runoff volume relative to downslope saturation thresholds. Topology describes where elements with low

saturation thresholds are located relative to other elements. Such elements can be at high locations within a basin. As a result, runoff from upslope elements may be independent of downslope elements, creating the possibility of multiple combinations of contributing element patterns over space and time in a single basin. Dunne and Black (1971) note this type of variability during spring snowmelt even in basins where the variable source area concept is usually applicable. The nonuniform nature of snow accumulation, ground frost, and soil saturation causes runoff to be spatially and temporally dynamic at these locations.

Small basins where element threshold processes predominate exhibit similar or larger runoff ratios than where variable source processes predominate (Table 16). Lag times between peak rainfall and peak runoff in element contribution basins show a great deal of variability. Short lag times are due to the presence of elements that exhibit high runoff ratios and low available storage close to the stream channel. Recession coefficients in element threshold basins are similar to or exceed those from variable source basins. This may be because of the predominance of subsurface stormflow with its longer recession constants in certain landscape elements (Peters et al., 1995) if bedrock topography allows it (Allan and Roulet, 1994).

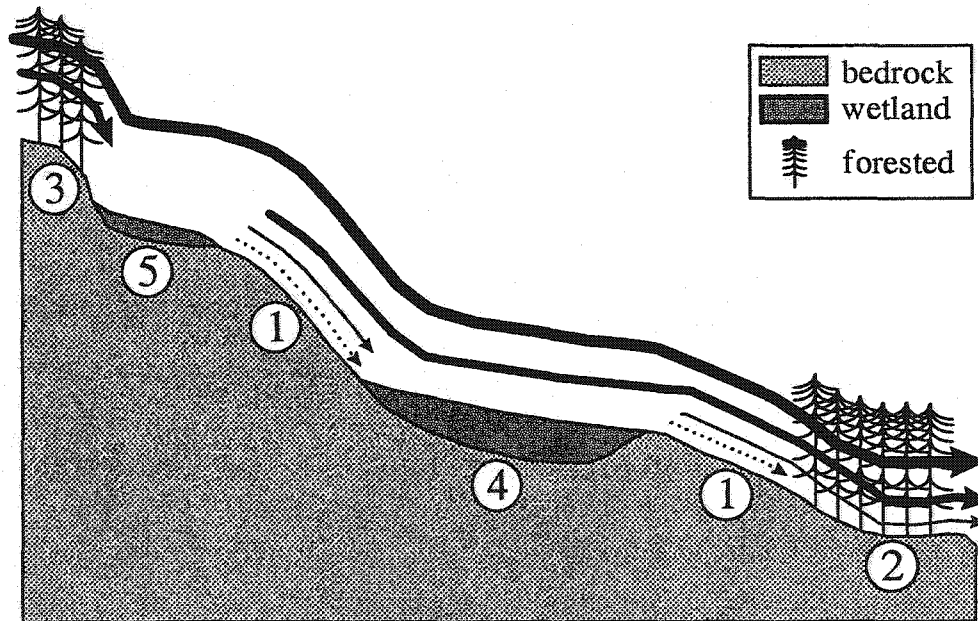
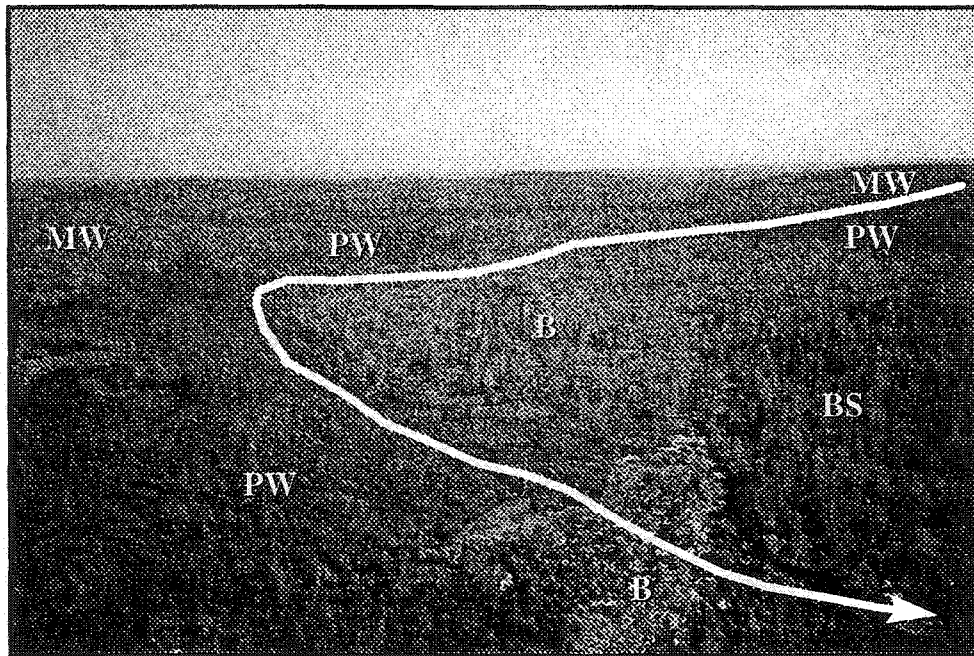


Figure 38: Skeeter Lake upland with one longitudinal drainage profile. Initials in the photograph denote land cover types shown in Figure 1. Numbers in the bottom frame denote hydrological elements. Arrows denote surface runoff and those elements with active contributing functions. Sequentially wider arrows imply surface runoff under wetter conditions.

Table 15: Features of the variable source concept and element threshold concept

Similarities	
Contributing areas are dynamic, varying between seasons and within storm events	
Antecedent moisture and input magnitude and duration affect contributing area behaviour	
The extent of contributing areas strongly affects basin discharge	
Differences	
<i>Variable source area</i>	<i>Element threshold concept</i>
Applies to small mainly uniform areas	Applies to larger strongly heterogeneous areas
Different areas of the basin contribute to runoff by the same hydrological process	Different areas of the basin contribute to runoff by different hydrological processes
Saturation thresholds are similar throughout the basin	Saturation thresholds vary extensively across the basin
Similar thresholds allow contributing area patterns to be more continuous	Different thresholds exhibit strong control on contributing areas so the pattern tends to be disjointed
Contributing areas expand and contract at different rates which depend on slope	Contributing areas expand and contract at different rates which depend on all physiographic parameters (i.e., slope, soil depth, vegetation cover) as well as landscape topology
Contributing areas expand upslope	Contributing areas expand downslope and runoff cascades through basin
Upper slopes depend on storage capacities of lower slopes for runoff generation	Upslope runoff is generated independent of lower slopes

Table 16: Characteristics of Canadian Shield headwater basin and slope hydrographs indicative of the element threshold concept compared with small basins exhibiting the variable source concept.

Reference	runoff ratio	lag time	basin size (m²)	recession coefficient
Allan and Roulet (1994)	0.35	7 hours	1×10^3	0.8
Buttle and Sami (1992)	0.15	6 days	3.1×10^4	n/a
Pocket Lake (this study)	0 - 0.71	2 - 11 days	4.8×10^4	0.77
Skeeter Lake (this study)	0 - 0.58	2 - 19 days	5.6×10^5	0.79
Peters et al. (1995)	0.4	10 hours	3.2×10^4	n/a
Branfireun and Roulet (1998)	0.02 - 0.59	4 - 16.5 hours	1.3×10^5	n/a
Dunne (1978)	0 - 0.58	< 1 hour	$10^3 - 10^5$	0.001 - 0.76

The element threshold concept is derived from Canadian Shield headwater basins at the scale of < 10 hectares. Canadian Shield and southern Canadian arctic headwater watersheds 10 to 100 hectares in size with similar intermittent outflow patterns described by Spence (2000) and Woo et al. (1981) may also adhere to the element threshold concept because the location of specific hydrological elements

controls runoff linkages within the basins and at the basin outlets. This study has not determined if and how the concept upscales to basins 1 square kilometer in size and larger. Verification at larger scales would be a useful future contribution to improved understanding of the impact of environmental changes to streamflow in larger order rivers.

CHAPTER 8

CONCLUSIONS

The Canadian Shield landscape has unique hydrological conditions that range from those occurring on exposed Precambrian bedrock to those observed in the lakes, wetlands and soil-filled valleys with ample storage capacity to dampen runoff. These heterogeneous conditions combine to render Shield basins distinctly different from the predominantly soil-covered, temperate latitude catchments where most basin hydrological studies are undertaken. This research, carried out in a subarctic headwater basin, reveals several hydrological processes common to the Canadian Shield environment.

The spring and summer energy budgets are strongly influenced by the magnitude of spring snowmelt, when many water filled shallow basins on the exposed bedrock provide freely evaporating surfaces. During a dry year, the exposed bedrock remains dry and latent heat fluxes are diminished in favour of sensible and ground heat fluxes. Under these conditions, the surface energy balance indicates greater aridity than most other subarctic surfaces reported in the literature. Large latent heat fluxes and low soil water storage consistently create a

moisture deficit that controls headwater basin runoff response during the summer and the autumn.

Conventional thinking says that there is diminished storage and vertical losses during runoff generation from exposed bedrock. This research shows that the hydrological processes involved in runoff generation from exposed bedrock are much more complicated. While soil cover and fractures control the rates of infiltration, ground frost has no demonstrable effect. Rainfall, snowmelt and evaporation characteristics during individual events influence runoff by influencing infiltration and the magnitude of soil storage. The distribution and location of available storage in thin soil patches in exposed bedrock uplands influence the amount and the location of runoff generation.

High lateral inflow from uplands relative to available storage in valleys is needed to maintain hydrological linkages between valleys and adjacent uplands. Within the valleys, saturation overland flow is the major runoff generation process but storage exerts a strong influence on the runoff process.. Surface runoff is usually generated at the valley edges where inputs from adjacent slopes are the highest and most likely to exceed the threshold of saturation. Surface runoff is not necessarily transferred quickly to the basin outlet but may be interrupted by storage demands in between. The fill-and-spill concept explains this transfer

system and represents a significant departure from the saturation overland flow concept derived from humid region, non-Shield studies.

The element threshold concept is introduced to reflect the dynamism of contributing elements and the variable connectivity among these elements that dictate runoff response from headwater basins in the Canadian Shield. It represents a new conceptualization of Canadian Shield runoff processes. In general, the concept states the following.

- 1) Canadian Shield catchments consist of a number of hydrological elements.
- 2) Differences in element physiography result in differences in storage capacity across catchments.
- 3) Differences in available storage status within and among elements are a result of hydrological processes within individual elements as well as connections with adjacent elements.
- 4) The importance of hydrological connectivity among adjacent elements means that the geometry and topology of elements are important factors in determining elemental functions, and where, when and how runoff is generated.
- 5) Runoff is only permitted to continue downslope where an element's saturation threshold is exceeded. The spatial and temporal differences

in storage requirements result in a cascading runoff pattern through Canadian Shield headwater basins.

The element threshold concept is applicable to small heterogeneous headwater basins where individual elements control the transfer of runoff downstream. The concept is likely widely applicable where runoff is periodically interrupted, as in ephemeral or intermittently draining basins. Previous studies suggest that the element threshold concept applies at least those basins in the Canadian Shield and the southern Canadian arctic smaller than 1 km². Basins of such size would certainly include small ephemeral draining lakes. Such lakes likely constitute well defined elements within headwater basins, as their storage functions are dependent upon evaporation and their linking and contributing functions depend on lateral inflows. The scale at which the element threshold concept becomes less important may occur when lake, or river, discharge becomes less a function of lateral inputs and more a function of routing processes. This may coincide with the scale at which perennially draining basins begin to occur. Verification of this idea through future research is recommended. Such work would complement this research and provide a strong foundation for the development of a hydrological model that accounts for the pertinent hydrological processes operating at a range of scales on the subarctic Canadian Shield. Such a tool would be useful in predicting impacts from development and climatic change in this ecozone.

REFERENCES

- Allan, C. and N. Roulet, 1994. Runoff generation in zero order Precambrian Shield catchments: the stormflow response of a heterogenous landscape. *Hydrological Processes* 8: 369 – 388.
- Amiro, B. and E. Wushcke, 1987. Evapotranspiration from a boreal forest drainage basin using an energy balance / eddy correlation technique. *Boundary Layer Meteorology* 38: 125 – 139.
- Baldocchi, D., C. Vogel and B. Hall, 1997. Seasonal variation of energy and water vapor exchange rates above and below a boreal jack pine forest canopy. *Journal of Geophysical Research* 102: 28939 - 28951.
- Bello, R. and A. Arama, 1989. Rainfall interception in lichen canopies. *Climatological Bulletin* 23: 74 – 78.
- Blanford, J. and L. Gay, 1992. Tests of a robust eddy correlation system for sensible heat flux. *Theoretical and Applied Climatology* 46: 53 – 60.
- Branfireun, B. and N. Roulet, 1998. The baseflow and storm flow hydrology of a Precambrian Shield headwater peatland. *Hydrological Processes* 12: 57 – 72.
- Brown, R.J.E., 1978. Permafrost. Plate 32. *Hydrological Atlas of Canada*. Department of Fisheries and Environment, map.
- Buttle, J. and D. Peters, 1997. Inferring hydrological processes in a temperate basin using isotopic and geochemical hydrograph separation: a re-evaluation. *Hydrological Processes* 11: 557 – 573.
- Buttle, J. and K. Sami, 1992. Testing the groundwater ridging hypothesis of streamflow generation during snowmelt in a forested catchment. *Journal of Hydrology* 135: 53 – 72.
- Buttle, J.M., I.F. Creed and J.W. Pomeroy, 2000. Advances in Canadian forest hydrology, 1995 - 1998. *Hydrological Processes* 14: 1551 - 1578.

- Carey, S.K. and M.K. Woo, 2001. Slope runoff processes and flow generation in a subarctic, subalpine catchment. *Journal of Hydrology* 253: 110 - 129.
- Church, M., 1974. Hydrology and permafrost with reference to North America. In: *Permafrost Hydrology, Proceedings of Workshop Seminar 1974*, Canadian National Committee for the International Hydrological Decade, Ottawa, Ontario, 7 - 20.
- Davison, C., 1984. Hydrogeological characterization at the site of Canada's Underground Research Laboratory. in: *Proceedings of an International Groundwater Symposium on Groundwater Resources Utilization and Contaminant Hydrogeology*, Montreal, International Association of Hydrogeologists, 310-355.
- Devito, K., A.R. Hill and N. Roulet, 1996. Groundwater-surface water interactions in headwater forested wetlands of the Canadian Shield. *Journal of Hydrology* 181: 127 - 147.
- Domenico, P.A. and F.W. Schwartz, 1998. *Physical and Chemical Hydrogeology*, Wiley and Sons, Toronto.
- Drury, M. and T. Lewis, 1981. Thermal studies in the Lac du Bonnet Batholith at Pinawa, Manitoba, Report TR-163, SDDO, Atomic Energy of Canada Limited, Chalk River.
- Dunne, T., 1978. Field studies of hillslope flow processes. In Kirkby, M.J. (ed.) *Hillslope Hydrology*. Wiley, Toronto. 227 - 293.
- Dunne, T. and R.D. Black, 1971. Runoff processes during snowmelt. *Water Resources Research* 7: 1160 - 1172.
- Farouki, O., 1981. *Thermal Properties of Soils*, CRREL Monograph, #81-1.
- Fitzgibbon, J. and Dunne, T. 1981. Land surface and lake storage during snowmelt runoff in a subarctic drainage system. *Arctic and Alpine Research* 13: 277 - 285.
- Fitzjarrald, D. and K. Moore, 1994. Growing season boundary layer climate and surface exchanges in a subarctic lichen woodland. *Journal of Geophysical Research* 99: 1899 - 1917.
- Freeze, R.A. and J.A. Cherry, 1979. *Groundwater*. Prentice Hall, Englewood Cliffs.

- Fyson, W.K. and W.A. Padgham, 1993. *Geology of the Slave Structural Province*. Indian and Northern Affairs Canada, Yellowknife.
- Gale, J., 1982. Assessing the permeability characteristics of fractured rock. *Recent Trends in Hydrogeology*, Narasimhan, T. (ed.), Boulder, Geological Society of America, 163-181.
- Garratt, J., 1975. Limitation of the eddy correlation technique for the determination of turbulent fluxes near the surface *Boundary Layer Meteorology* 8: 255 – 259.
- Gibson, J.J., R. Reid and C. Spence, 1998. A six year isotopic record of lake evaporation at a mine site in the Canadian subarctic: results and validation, *Hydrological Processes* 12: 1779 – 1792.
- Giesbrecht, M.A. and M.K. Woo, 2000. Simulation of snowmelt in a subarctic spruce woodland: 2. Open woodland model. *Water Resources Research* 36: 2287 - 2295.
- Gray, D.M., Toth, B., Zhao, L., Pomeroy, J.W. and Granger, R.J. 2001. Estimating areal snowmelt infiltration into frozen soils. *Hydrological Processes* 15: 3095-3111.
- Heron, R. and Woo, M.K. 1978. Snowmelt computation for a High Arctic site. Proceedings 35th Eastern Snow Conference, Hanover, New Hampshire, 162-172.
- Hewlett, J. and A. Hibbert, 1965. Factors affecting the response of small watersheds to precipitation in humid areas. *International Symposium on Forest Hydrology*, Sopper, W. and H. Lull (eds.), 275 – 290.
- Jarvis, P. and K. McNaughton, 1986. Stomatal control of transpiration. *Advances in Ecological Research* 15: 1-49.
- Jarvis, P.G., Massheder, J., Hale, S., Moncrieff, J., Rayment, M. and S. Scott, 1997. Seasonal variation of carbon dioxide, water vapour and energy exchanges of a boreal black spruce forest. *Journal of Geophysical Research* 102: 28953 – 28966.
- Kershaw, K. and W. Rouse, 1971. Studies on lichen dominated systems. I. The water relations of *Cladonia alpestris* in spruce lichen woodland in northern Ontario. *Canadian Journal of Botany* 49: 1389 – 1399.

- Lafleur, P. and C. Schreuder, 1994. Water loss from the floor of a subarctic forest. *Arctic and Alpine Research* 26: 152 – 158.
- Lafleur, P. and P. Adams, 1986. The radiation budget of a subarctic woodland canopy. *Arctic* 39: 172 - 176.
- Lafleur, P., 1992. Energy balance and evapotranspiration from a subarctic forest. *Agricultural and Forest Meteorology* 58: 163 – 175.
- Lafleur, P., J. McCaughey, D. Joiner, P. Bartlett D. Jelinsky, 1997. Seasonal trends in energy, water and carbon dioxide at a northern boreal wetland. *Journal of Geophysical Research* 102: 29009 - 29020.
- Lafleur, P., W. Rouse and D. Carlson, 1992. Energy balance differences and hydrologic impacts across the northern treeline. *International Journal of Climatology* 12: 193 – 203.
- Landals, A. and Gill, D. 1972. Differences in volume of surface runoff during the snowmelt period: Yellowknife, NWT. In: *The Role of Snow and Ice in Hydrology*, IAHS Publication #107. 927 – 942.
- Maxwell, B., 1997. *Responding to Global Climate Change in Canada's Arctic, Volume II of The Canada Country Study: Climate Impacts and Adaptation*. Environment Canada, No. En 56-119/5-1997E.
- McCaughey, J.H., P.M. Lafleur, D.W. Joiner, P.A. Bartlett, A.M. Costello, D.E. Jelinski and M.G. Ryan, 1997. Magnitudes and seasonal patterns of energy, water and carbon exchanges at a boreal young jack pine forest in the BOREAS northern study area. *Journal of Geophysical Research* 102: 28997 - 29007.
- McDonnell, J. and C. Taylor, 1987. Surface and subsurface water contributions during snowmelt in a small precambrian Shield watershed, Muskoka, Ontario. *Atmosphere Ocean* 25: 251 – 266.
- McNamara, J.P., Kane, D.L., Hinzman, L.D., 1998. An analysis of streamflow hydrology in the Kuparuk River Basin, Arctic Alaska: a nested watershed approach. *Journal of Hydrology* 206: 39 - 57.
- Metcalf, R.A. and J.M. Buttle, 2001. Soil partitioning and surface store controls on spring runoff from a boreal forest peatland basin in north-central Manitoba. *Hydrological Processes* 15: 2305 - 2324.

- Moore, C., 1986. Frequency response corrections for eddy correlation systems. *Boundary Layer Meteorology* 37: 17 – 35.
- Moore, K.E., Fitzjarrald, D., S. Wofsy, B. Daube, J.W. Munger, P. Bakwin and P. Crill, 1994. A season of heat, water vapor, total hydrocarbon, and ozone fluxes at a subarctic fen. *Journal of Geophysical Research* 99: 1937 – 1952.
- Moore, K.E., D.R. Fitzjarrald, R.K. Sakai and J.M. Freedman, 2000. Growing season water balance at a boreal jack pine forest. *Water Resources Research* 36: 483 - 493.
- Moore, R.D. 1989. Tracing runoff sources with deuterium and oxygen-18 during spring melt in a headwater catchment, southern Laurentians, Quebec. *Journal of Hydrology* 112: 135 - 148.
- Peters, D., J. Buttle, C. Taylor and B. Lazerte, 1995. Runoff production in a forested shallow soil Canadian Shield basin. *Water Resources Research* 31: 1291 – 1304.
- Petrone, R., W.R. Rouse and P. Marsh, 2000. Comparative surface energy budgets in western and central subarctic regions of Canada. *International Journal of Climatology* 20: 1131 - 1148.
- Phillips, D., 1990. *The climates of Canada*, Minister of Supply and Services, Canada.
- Pietroniro, A. et al., 1998. Hydrology for cold regions: GEWEX sub basin working group (ad hoc), paper presented at the Fourth Scientific Workshop for the Mackenzie GEWEX Study, Montreal, November 16 - 18, 1998.
- Pomeroy, J. and D. Gray, 1995. *Snowcover: Accumulation, Relocation and Management*. NHRI Science Report #7, Saskatoon, Saskatchewan.
- Price, A.G. and L.K. Hendrie, 1983. Water motion in a deciduous forest during snowmelt. *Journal of Hydrology* 64: 339 - 356.
- Priestley, C.H.S. and R.J. Taylor, 1972. "On the assessment of surface heat flux and evaporation using large scale parameters", *Monthly Weather Review* 100: 81- 92.

- Raven, K., Smedley, J., R. Swezey and K. Novalowski, 1985. Field investigations of a small groundwater flow system in fractured monzonitic gneiss. In: *Hydrogeology of Rocks of Low Permeability*. Proceedings of the International Association of Hydrogeologists 17th International Congress, January 7 - 12, 1985. Tucson, 72 - 85.
- Reid, R. 1997. Evaporation studies at mine tailings ponds in the Northwest Territories. In: Milburn, D., (ed.) *Proceedings of the Hydro-ecology Workshop on the Arctic Environmental Strategy – Action on Water*: May 1996, Banff, National Hydrology Research Institute Symposium #16. National Hydrology Research Institute, Saskatoon, Canada. 115 – 133.
- Roulet, N., 1990. The hydrological role of peat covered wetlands. *Canadian Geographer* 34: 82-83.
- Rouse, W., Mills, P. and R. Stewart. 1977. Evaporation in high latitudes. *Water Resources Research* 13: 909-914.
- Rouse, W.R. and R.L. Bello, 1985. The potential for climatic modification in the Hudson Bay Lowlands through the influence of the ocean on the energy balance. *Atmosphere Ocean* 23: 375 - 392
- Rouse, W.R., R.L. Bello and P.M. Lafleur, 1997: The low arctic and subarctic. *The Surface Climates of Canada*, Bailey, W., T. Oke, and W. R. Rouse, Eds., McGill Queen's University Press, 198-221.
- Schuepp, P., Leclerc, M., Macpherson, J. and R. Desjardins, 1990: Footprint prediction of scalar fluxes from analytical solutions of the diffusion equation. *Boundary Layer Meteorology* 50: 355 – 373.
- Sellers, P. *et al.*, 1997. BOREAS in 1997: Experiment overview, scientific results and future directions. *Journal of Geophysical Research* 102: 28731 – 28769.
- Singh, B. and R. Taillifer, 1986: The effect of synoptic scale advection on the performance of the Priestley Taylor evaporation formula. *Boundary Layer Meteorology* 36: 367 – 382.
- Spence, C. and G. Stephens, 1997. "Measurement of the shallow groundwater regime of a northern lake", in: *Proceedings of the Hydro-Ecology Workshop on the Arctic Environmental Strategy: Action on Water*, Milburn, D. (ed.), NHRI Symposium #16, May, 1996, Banff, Alberta p. 135 – 152.

- Spence, C., 1996. "Ground Penetrating Radar as a Tool in an Investigation of Shallow Groundwater Flow Near Yellowknife, NWT", internal report, Water Resources Division, Indian and Northern Affairs Canada.
- Spence, C., 2000. The effect of storage on runoff from a headwater subarctic Shield basin, *Arctic* 53: 237 - 247.
- Spence, C., 2001. Sub grid runoff processes and hydrological modeling in the subarctic Canadian Shield. *Soil-Vegetation-Atmosphere Transfer Schemes and Large Scale Hydrological Models* (Proceedings of a symposium held during the 6th IAHS Scientific Assembly at Maastricht, The Netherlands, July 2001, IAHS Publ. No. 270, 113 - 116.
- Szeto, K. 1998: Low level inversions, precipitation recycling and air-land interactions over the Mackenzie Basin, Proceedings of the 4th Scientific Workshop for the Mackenzie GEWEX Study (MAGS). Strong, G.S. and Y.M.L. Wilkinson, Eds., Environment Canada, 27 - 28.
- Thorne, G., J. Laporte, and D. Clarke, 1994. Infiltration and recharge in granitic terrains of the Canadian Shield during winter periods. In: *Proceedings, 10th International Northern Research Basins Symposium and Workshop*, Spitsbergen, Norway, 449-466.
- Thorne, G., J. Laporte, D. Clarke and C. Davison, 1999. Water budget of an upland outcrop recharge area in granitic rock terrane of southeastern Manitoba, Canada. In: *Proceedings, 12th International Northern Research Basins Symposium and Workshop*, Reykjavik, Iceland, 317 – 330.
- Wedel, J.H., A. Smart and P. Squires, 1990. *An overview study of the Yellowknife River Basin, NWT*. Inland Waters Directorate, Environment Canada.
- Wight, J., 1973. Aspects of evaporation and evapotranspiration in the water balance of Baker Creek, near Yellowknife, NWT, unpubl. M.Sc. thesis, University of Alberta.
- Witherspoon, P., Wang, J., Iwai, K. and J. Gale, 1980. Validity of cubic law for fluid flow in a deformable rock fracture. *Water Resources Research* 16: 1016-1024.
- Woo, M.K., R. Heron and P. Steer, 1981. Catchment hydrology of a high arctic lake. *Cold Regions Science and Technology* 5: 29 - 41.

Wright, R. 1981. *The Water Balance of a Lichen Tundra Underlain by Permafrost*. McGill SubArctic Research Paper #33.

Wright, R., 1979. Preliminary results of a study on active layer hydrology in the discontinuous zone at Schefferville, Nouveau-Quebec. *Geographie Physique et Quaternarie* 33: 359 – 368.